NAVAL POSTGRADUATE SCHOOL

Monterey, California

THESIS

AN ANTENNA DESIGN FOR PANSAT USING NEC

by

Daniel A. Ellrick

June, 1991

Thesis Advisor: Richard W. Adler

Approved for public release; distribution is unlimited

REPORT DOCUMENTATION PAGE

1a REPORT SECURITY CLASSIFICATION Unclassified	1b RESTRICTIVE MARKINGS
2a SECURITY CLASSIFICATION AUTHORITY	3 DISTRIBUTION/AVAILABILITY OF REPORT Approved for public release; distribution is unlimited.
2b DECLASSIFICATION/DOWNGRADING SCHEDULE	
4 PERFORMING ORGANIZATION REPORT NUMBER(S)	5 MONITORING ORGANIZATION REPORT NUMBER(S)
6a NAME OF PERFORMING ORGANIZATION Naval Postgraduate School 6b OFFICE SYMBOL *(If applicable)* EC	7a NAME OF MONITORING ORGANIZATION Naval Postgraduate School
6c ADDRESS (*City, State, and ZIP Code*) Monterey, CA 93943-5000	7b ADDRESS (*City, State, and ZIP Code*) Monterey, CA 93943-5000
8a NAME OF FUNDING/SPONSORING ORGANIZATION 8b OFFICE SYMBOL *(If applicable)*	9 PROCUREMENT INSTRUMENT IDENTIFICATION NUMBER
8c ADDRESS (*City, State, and ZIP Code*)	10 SOURCE OF FUNDING NUMBERS Program Element No / Project No / Task No / Work Unit Accession Number
11 TITLE (*Include Security Classification*) An Antenna Design for PANSAT Using NEC	
12 PERSONAL AUTHOR(S) Ellrick, Daniel A.	
13a TYPE OF REPORT Master's Thesis 13b TIME COVERED From To	14 DATE OF REPORT (*year, month, day*) June 1991 15 PAGE COUNT 108
16 SUPPLEMENTARY NOTATION The views expressed in this thesis are those of the author and do not reflect the official policy or position of the Department of Defense or the U.S. Government.	
17 COSATI CODES FIELD / GROUP / SUBGROUP	18 SUBJECT TERMS (*continue on reverse if necessary and identify by block number*) Antenna, Design, Satellite, Tangential Turnstile, Numerical Modeling, NEC, PANSAT,

19 ABSTRACT (*continue on reverse if necessary and identify by block number*)

In this thesis the Numerical Electromagnetics Code (NEC) is used to design an omnidirectional antenna for the Petite Amateur Navy Satellite (PANSAT). The completed antenna design uses a tangential turnstile antenna to achieve a circularly polarized radiation pattern with predicted worst nulls of approximately -10 dBi. The use of NEC-3, recently ported to 80386 personal computers, demonstrates the potential of personal computers for performing this type of design work. A simple antenna feed system was also designed. Performance predictions were made through the application of simple statistical functions to the NEC output.

20 DISTRIBUTION/AVAILABILITY OF ABSTRACT ☒ UNCLASSIFIED/UNLIMITED ☐ SAME AS REPORT ☐ DTIC USERS	21 ABSTRACT SECURITY CLASSIFICATION Unclassified
22a NAME OF RESPONSIBLE INDIVIDUAL Adler, Richard W.	22b TELEPHONE (*Include Area code*) 408-646-2352 22c OFFICE SYMBOL EC/AB

Approved for public release; distribution is unlimited.

AN ANTENNA DESIGN FOR PANSAT USING NEC

by

Daniel A. Ellrick
Captain, United States Marine Corps
B.S.E.E., Purdue University, 1984

Submitted in partial fulfillment
of the requirements for the degree of

MASTER OF SCIENCE IN ELECTRICAL ENGINEERING

from the

NAVAL POSTGRADUATE SCHOOL
June 1991

Author: Daniel A. Ellrick
Daniel A. Ellrick

Approved by:
Richard W. Adler, Thesis Advisor

Rudolf Panholzer, Second Reader

Michael A. Morgan, Chairman
Department of Electrical and Computer Engineering

ABSTRACT

In this thesis the Numerical Electromagnetics Code (NEC) is used to design an omnidirectional antenna for the Petite Amateur Navy Satellite (PANSAT). The completed antenna design uses a tangential turnstile antenna to achieve a circularly polarized radiation pattern with predicted worst nulls of approximately -3.0 dBi. The use of NEC-3, recently ported to 80386 personal computers, demonstrates the potential of personal computers for performing this type of design work. A simple antenna feed system was also designed. Performance predictions for the completed antenna system were made through the application of simple statistical functions to the NEC output.

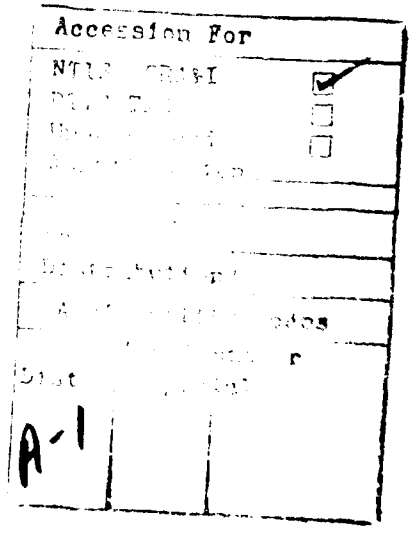

TABLE OF CONTENTS

LIST OF TABLES

LIST OF FIGURES

ACKNOWLEDGEMENT

Numerous individuals assisted me in completing this thesis through their advice, encouragement, technical expertise, and proofreading skills. Many thanks to each of you. Of those who helped, a few individuals stand out as having played key roles. Professor Adler's technical expertise, clear explanations and advice were invaluable. Professor Panholzer provided direction, support, and a sense of humor when I needed these things. Engineer Walt Gregorwich took time out of his busy schedule at Lockheed to share insights and ideas from his own antenna designs. The PANSAT antenna design is essentially an adaptation of the tangential turnstile he designed for the Synchronous Meteorological Satellite (SMS). Engineer Jack Jakstys of Space Systems/LORAL was also extremely helpful; he took the time to dig through all of his own old notes and then mailed a great deal of helpful material on omnidirectional antenna designs to me. Last, but far from least, my wife Karen, who is also an electrical engineer, provided tremendous assistance through encouragement, proofreading, and her own considerable engineering insight. Many thanks, and may God bless each of you.

I. INTRODUCTION

A. OBJECTIVES

The primary objective of this thesis is to design, model, and document an omnidirectional, Ultra High Frequency (UHF) antenna system for use on the Petite Amateur Navy Satellite (PANSAT). This objective is accomplished by modeling candidate designs using the Numerical Electromagnetics Code (NEC) and then refining the most promising design using a detailed NEC model. The process of refinement is continued until the design meets all required performance specifications. The scope of this thesis is limited to designing the antenna system and predicting its performance through the use of numerical modeling. Additionally, a simple antenna feed system is designed. The completed antenna and feed system design is summarized in Appendix D for easy reference during construction of the satellite. After the antenna system is built its performance should be tested tc confirm the accuracy of the numerical modeling performed in this thesis.

A secondary thesis objective is to provide additional validation and performance information for the recently developed 32-bit, personal computer version of NEC-3. This version of NEC-3 ("386 NEC") runs on IBM compatible 80386 personal computers under the Microsoft Disk Operating System

(MS-DOS) with the aid of a DOS extender. The 386 NEC code used for this thesis was compiled with the Lahey compiler and linked using the Ergo OS 386 DOS Extender. The work on this objective is of limited scope and consists mainly of using the 386 NEC software to perform the PANSAT antenna design, recording any difficulties encountered, and verifying that the mainframe NEC software predicts the same antenna performance characteristics for the finished antenna design as 386 NEC. Additionally, the Central Processing Unit (CPU) time required for the code to run on the personal computer is compared to the time required on the mainframe.

B. BACKGROUND

1. PANSAT

In order to facilitate research and to broaden educational opportunities for students, the Space Systems Academic Group at the Naval Postgraduate School (NPS) has initiated a Small Satellite Design Studies research program. The PANSAT project is being conducted as a part of this program and is designated as experiment number 901 (NPS-901).

Historically the Department of Defense (DoD) has relied on complex, capable, and expensive satellites to fulfill its communication requirements. In contrast, the amateur radio community has had significant successes with small, single mission satellites that have been built and

launched by the Amateur Radio Satellite Corporation (AMSAT). Similar small, inexpensive satellites could play a significant role in meeting the global communication needs of DoD. Such satellites could supplement the larger and more complex communication satellites by filling important niches in the DoD communications requirements. One such niche is the need to transmit long messages that tend to interrupt the normal flow of information over existing command and control circuits. The use of small packet communications satellites for long messages would reduce the burden such long messages place on existing heavily used circuits. From this example it may be inferred that small, relatively simple satellites might be capable of augmenting existing complex communication satellites in a cost efficient manner. This is not, however, the strongest argument in favor of developing such small, low-cost, communication satellites.

A more important advantage of small satellites is that they could provide the capability to quickly replace satellite communications that have been lost as a result of hostile action, unusual solar activity[1], or other events. The immediate launch of a single, small, Low Earth Orbit (LEO) satellite would provide packet communications to the theater affected by the outage. The launch of a number of these

---

[1] Unusual solar activity, e.g. solar flares, has resulted in the temporary or permanent functional loss of a number of satellites.

"light-sats" could provide real time, wide area, over-the-horizon communications through the use of an inter-satellite network which would forward messages between satellites before retransmission to the desired ground station. Such satellites could use spread spectrum channels to enhance survivability by making detection more difficult. The use of spread spectrum technology also provides excellent resistance to noise jamming.

The PANSAT project provides a stepping stone for the development of the "light sats" envisioned in the preceding scenario. This project combines the educational mission of NPS with the objectives of the Defense Advanced Research Project Agency (DARPA) Advanced Space Technology Program which seeks to develop ways of augmenting DoD communication capabilities through the application of existing technology.

The objectives of the PANSAT experiment (Sakoda, 1989, pp. 1-2) include enhancing the educational experience of NPS students, demonstrating a small, low-cost, quick-reaction, spread spectrum, packet communications satellite, providing a space-based platform for small experiments, and supporting the amateur radio community by providing access to a spread-spectrum satellite platform.

Opportunities for valuable educational experiences for NPS students will span the entire life cycle of the satellite project. Thesis opportunities will be present throughout the process of satellite and subsystem design, and will include

integration of satellite systems, construction and testing of the satellite and subsystems, planning and monitoring the launch, and evaluation of on-orbit performance. Additional work may be available in the development and design of small experiments that can ride aboard the satellite. Educational opportunities will not end when the satellite is launched but will continue through use of the satellite as an in-orbit laboratory asset for satellite communications instruction.

The satellite communications package will implement a direct sequence spread spectrum packet communications channel with a center frequency of 437.25 MHz (Paluszek, 1990). A Binary Phase Shift Keyed (BPSK), 1200 bit-per-second signal with a bandwidth of 960 kHz will be used. Communications will be done in the half duplex mode using the AX.25 message protocol. This communications channel will perform all required Telemetry, Tracking, and Control (TT&C) functions as well as acting as the message conduit for packet communications. The packet communications function of the satellite will be available for use by the amateur radio community. This will result in a larger number of sample usages which will facilitate development of a statistical description of satellite performance. Opening the satellite to amateur use also simplified the process for obtaining the 437.25 MHz frequency assignment which lies within the amateur band.

Since the satellite is intended as a baseline demonstration design, no attitude control or propulsion system is being included. As a result the satellite antenna system must be as nearly omnidirectional as possible. The antenna design problem is further complicated by the size of the satellite, which is approximately 19 inches in diameter. At the design frequency of 437.25 MHz, this is approximately 7/10ths of a wavelength. Therefore the satellite body cannot be considered either large or small in terms of wavelength and must instead be treated as an integral part of the antenna system. This thesis does precisely this by modeling the satellite body and antenna system using a method of moments numerical code (NEC) in order to achieve an appropriate antenna system design.

Additional information about PANSAT and its various subsystems is included in Appendix A for reference purposes.

2. NEC

Antenna design and analysis using analytical methods is practical in only a few simple cases involving well-behaved geometry and boundary conditions. Due to this limitation, the traditional approach to antenna design has relied heavily on construction of models and measurement of the resulting radiation patterns and feed impedances. The models are then modified until acceptable performance is obtained. This approach is very time consuming and can be prohibitively

expensive if the required models are complex, or if highly accurate measurements are required.

In recent years this approach has been supplemented more and more by numerical modeling. In some cases physical modeling may be skipped altogether if the design requirements are not too stringent and the risk is low enough. Computer codes used for numerical modeling generally rely on either the Method of Moments (MoM), ray optics, or the Geometric Theory of Diffraction (GTD) as their underlying theoretical basis. Codes intended for modeling large structures (in terms of wavelength) use either ray optics or the GTD approach, while codes for modeling structures of less than two or three wavelengths use the MoM approach.

The PANSAT satellite body is a 26 sided polyhedron which may be approximated by a sphere 19 inches in diameter. As discussed previously this gives the satellite body a diameter of approximately 7/10ths of a wavelength at 437.25 MHz. For this reason a MoM code was required for the antenna design work.

There are a number of MoM electromagnetic modeling codes in existence, but the bulk of these are proprietary. The exception is NEC, which is available in the public domain[2].

[2] Further information concerning NEC is available through Professor Richard W. Adler, Naval Postgraduate School, Code EC/AB, Monterey, California, 93943.

Over the years a number of versions of NEC have been developed since the original NEC-1 version was written at Lawrence Livermore National Laboratory in 1977 under the sponsorship of the Naval Ocean Systems Center (NOSC). Two versions of the code were used for the design work in this thesis. Personal computer based NEC-81 was used for preliminary modeling because it is conveniently bundled into the Numerical Electromagnetic Engineering Design System (NEEDS). This version of NEC, however, can only handle problems with less than 300 unknowns[3]. As the satellite model became more complex, it was necessary to switch to a more capable version of NEC. Therefore the bulk of the design work was done in 386 NEC. This version of NEC consists essentially of NEC-3 ported to IBM compatible 80386 personal computers (Wright, 1990). The version of NEC-3 running on the mainframe is capable of handling up to 1,000 unknowns. This number is exceeded by 386 NEC which has been used to solve problems with as many as 1,588 unknowns (Howard, 1990, pp. C-3) and may have potential for application to even larger problems. All versions of NEC used were obtained through Professor Richard W. Adler. After the PANSAT antenna design was completed, the performance of 386 NEC was validated by running the completed design problem on the Amdahl 5990 mainframe, which also has

[3]The number of unknowns in a numerical modeling problem using MoM is the number of wire segments plus the number of patches. How many "unknowns" a code can handle is a direct measure of how large and detailed a problem can be solved.

NEC-3 available. This validation run was the only use made of the mainframe; all other work was done on a personal computer. This fact demonstrates that numerical modeling of this type can be done effectively using off-the-shelf, high-performance, personal computers. The theory on which the NEC code is based is discussed in Appendix B.

C. DESIGN METHODOLOGY

The approach used in designing the PANSAT antenna system consisted of several steps. The first was to examine the mission requirements of PANSAT and the work already done on PANSAT communications in order to define the desired antenna performance specifications accurately. The second was to identify proven omnidirectional antenna designs for satellites through library research and personal contacts with engineers in industry. The most promising candidate designs were then modeled in NEC and examined in greater detail. A final design configuration was then chosen and a detailed NEC model constructed. Minor adjustments were made in the antenna element positions and sizes in order to optimize the pattern and feed impedances. The final model of the finished antenna design was then run on the mainframe to provide further verification of the accuracy of the 386 NEC code and to compare the performance of the 386 version of the code to the mainframe performance.

II. PANSAT ANTENNA DESIGN REQUIREMENTS

A. ELECTRICAL SPECIFICATIONS

No formal definition of the antenna specifications for PANSAT had been made at the time this thesis was undertaken. However, the parameters used for the link analysis performed by Stephen Paluszek in his thesis on spread spectrum communications for PANSAT provided definitive guidelines for most PANSAT antenna electrical parameters. The requirements taken from his thesis are listed below:

- Approximately omnidirectional pattern with no nulls exceeding -10 dBi[4] (Paluszek, 1990, pp. 12-13).
- Power handling capability of at least 5 watts (Paluszek, 1990, pp. 17).
- Operational bandwidth of 960 kHz with a center frequency of 437.25 MHz (Paluszek, 1990, pp. 18-19).
- Maximum antenna noise temperature of 161.9°K (Paluszek, 1990, pp.20).
- Maximum gain to null ratio (amplitude ripple) of 11 dB (Paluszek, 1990, pp. 29).

These requirements provide a starting place for specifying the antenna characteristics, but they are incomplete. Additional parameters to be specified include the desired

---

[4] The term dBi refers to decibels of gain in comparison with an isotropic radiator. Use of the term dBi when referring to antenna gains is more exact than use of the term dB which indicates gain without specifying any reference point. Nonetheless, use of dB when dBi is meant is common in the literature. Additionally, all references to antenna gain in this thesis refer to directive gain rather than power gain.

input impedance and maximum acceptable Voltage Standing Wave Ratio (VSWR) for the feed lines, and the desired radiation pattern polarization. Specifications for these parameters were chosen to conform to the PANSAT mission requirements after consideration of the engineering feasibility of the alternatives.

The antenna system input impedance specification was chosen to be $Z_{in}=50\Omega$ since this is a very common transmitter output impedance. This choice should be easy to incorporate in follow-on work on the communications system design since 50Ω components are readily available. Additionally, 1.4 was chosen as the maximum input line VSWR. Note that these choices are rather arbitrary since no restrictions were placed on these choices in the communication system design developed by Paluszek since he designed only to the block diagram level.

The PANSAT requirement to act as a packet radio carrier for amateurs makes it desirable that ground stations be able to effectively utilize simple, linearly polarized antennas. This leads to the conclusion that the omnidirectional[5] pattern radiated by the satellite should be circularly polarized to the greatest extent possible. This avoids the large cross polarization losses which would occur between linearly

---

[5]Note that although antennas such as dipoles are often referred to as "omnidirectional" this is not strictly accurate. These antennas are "omnidirectional" in only two dimensions. In this thesis "omnidirectional" is always used in the three dimensional sense because PANSAT is not stabilized in any axis.

polarized ground antennas and linearly polarized signals arriving from the satellite at arbitrary orientation angles. It follows that with the satellite using circular polarization the ground antennas should always be linearly polarized in order to prevent mismatches between left and right hand sense circular polarizations. This approach will make it possible to limit the polarization mismatch loss to about three decibels. The need to accept this small mismatch is clear since the alternative risks having a polarization mismatch of 30 dB or more[6]. Note that the sense of the circular polarization of the satellite antenna must be treated as arbitrary since it will vary between left handed and right handed on opposite sides of the satellite, thus precluding any attempt to use circular polarization at both antennas.

The requirements specified for bandwidth and power handling are omitted from further discussion because they will be easily met by any antenna system which is viable in other respects. Additionally, since the antenna noise temperature does not depend on the physical antenna arrangement but only on the antenna gain pattern and the environment, it is also omitted from further discussion.

---

[6]Theoretically a 90° mismatch between linearly polarized antennas or a left handed-right handed sense mismatch between circularly polarized antennas would result in zero antenna coupling, but in practice the loss is on the order of 30-40 dB.

B. MECHANICAL SPECIFICATIONS

The primary physical constraints on the antenna design involve mounting, deployability, weight, and suitability for the space environment. The mounting requirement is that the antenna system may only occupy the triangular portions of the satellite body because the rectangular portions will be covered with solar cells. Figure 1 displays the satellite body and indicates the permissible mounting surfaces. Any or all of the indicated triangular areas may be used, although it is clear that as few as possible should be used so that weight is minimized. Additionally, unused sections may prove useful for mounting more solar cells or additional experiments as the design is finalized.

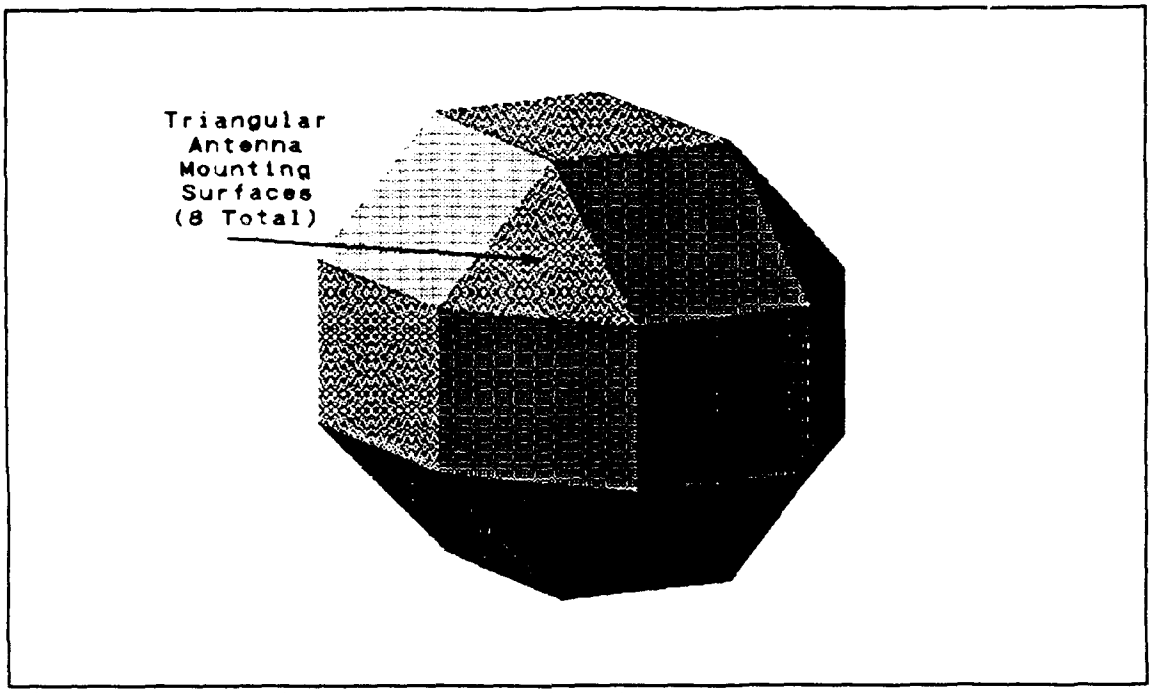

Figure 1 Mounting Spaces Available for PANSAT Antennas.

The primary launch vehicle for PANSAT is considered to be the space shuttle; the satellite would be carried as a Complex Self-Contained Payload (CSCP). Payloads of this type must fit in a shuttle Get Away Special canister (GAS can) and have specific size requirements that cannot be varied. This must be considered in the antenna design since the antenna must either be sufficiently small to fit while extended, or it must be stowed and then deployed. Any deployment scheme would have to be simple, lightweight and reliable. The requirement of suitability for the space environment is best met by using materials that have already been space tested in the past since PANSAT is not sufficiently well funded to undertake the expensive process of space qualifying new materials. For the

same reason caution should be used in considering any design configuration that departs radically from past designs.

Table I summarizes the PANSAT antenna design specifications used for comparison of alternative antenna configurations.

TABLE I. PANSAT ANTENNA DESIGN SPECIFICATIONS

PARAMETER	SPECIFICATION
Antenna Pattern	Omnidirectional, with no nulls below -10 dBi, pattern amplitude ripple less than 11 dB, circularly[7] polarized.
Antenna Feed System Constraints	Input impedance of Z_{in}=50 + j0 Ω, maximum VSWR of 1.4.
Physical Constraints	Minimum weight design, easily deployed, space proven, must mount on triangular surfaces.

[7] The term "circular" polarization is used loosely here to describe any radiation with a rotating electric field vector ("E vector"). Strictly speaking, only in cases where the E vector remains at a constant amplitude as it rotates is the radiation circularly polarized. Otherwise the polarization is elliptical rather than circular. The term "aspect ratio" refers to the ratio of the minimum of the E vector to its maximum and is a measure of polarization ellipticity. The aspect ratio is equal to one for circular polarization.

III. OMNIDIRECTIONAL ANTENNA DESIGN

A. ALTERNATIVE OMNIDIRECTIONAL ANTENNA DESIGNS

1. Low Gain Antennas

Omnidirectional antenna designs are generally based on extensions of low gain antenna designs. For this reason it is worthwhile to review certain characteristics of low gain antennas before proceeding to the discussion of antennas which are fully omnidirectional. The most common of these low gain antennas may be broadly characterized as dipoles, loops, and slots. Most omnidirectional antenna designs use two or more of these low gain antennas in an array configuration. In some cases a single low gain antenna mounted on the conductive skin of a satellite body may provide fairly good omnidirectional coverage.

Dipole antennas may be either low or high gain depending on their length in terms of wavelengths at the frequency of interest. Dipoles which are short in this sense have a directive gain of 1.76 dBi and a capacitive input impedance. As the length of the dipole antenna increases, the gain also increases. Dipoles less than a half wavelength long have single lobe, doughnut shaped, electric field radiation patterns. If a dipole antenna is longer than a half wavelength the radiation pattern splits into multiple higher gain lobes.

The most common configuration is the resonant half-wave dipole[8] which has a directive gain of 2.15 dBi and a doughnut shaped electric field radiation pattern. The resonant input impedance of a very thin half-wave dipole is 73Ω. High gain antenna arrays may be formed by placing multiple half-wave dipoles side by side or end to end. On the other hand, near omnidirectional patterns may be achieved by crossing two or more half-wave dipoles in order to "fill the doughnut hole" in the radiation pattern of a single dipole.

Loop antennas that are small in terms of wavelength have the same directive gain as a short dipole antenna and a magnetic field radiation pattern shaped like a doughnut. The pattern nulls of loop antennas are less severe than those of dipole antennas and significant radiation occurs in all directions. These antennas are equivalent to short magnetic dipoles and are the dual of short electric dipoles. Small loop antennas are rarely used for transmitter applications because they have a low radiation resistance and are, as a result, very inefficient antennas. The efficiency of small loops may be increased by using multiple turns and by adding ferrite (or other) cores to the center of the loop. Small loop antennas have high input impedances with an inductive component and may be difficult to match. The input impedance of loop antennas

---

[8] The most common antenna of all is undoubtedly the quarter-wave monopole. It may, however, be viewed as a variation of the half-wave dipole with a conductive ground plane forming the bottom half of the antenna.

decreases as the loop becomes larger and is approximately 50Ω for thin wire circular loops with a circumference of one wave length.

Small slot antennas may also be used as low gain radiators. These antennas have hemispherical radiation patterns and are usually fed with waveguides. Since waveguide feeds are usually impractical at frequencies below the microwave band, slot antennas and derivative designs are not considered further.

2. Omnidirectional Antennas

a. The Hula-Hoop Antenna

Figure 2 is an example of an omnidirectional antenna derived from the low-gain loop antenna discussed earlier. This configuration is called a Hula-Hoop antenna (Burton, 1963). It consists of a quarter-wave, open-ended loop of wire positioned over a conducting back plane. The antenna is fed at one end and positioned so that the distance above the ground plane is much smaller than the radius. The resultant input impedance is close to that of a quarter wave monopole. The radiation pattern is hemispherical with mixed direction linear polarization. For satellite applications, two Hula-Hoop antennas placed opposite one another on the

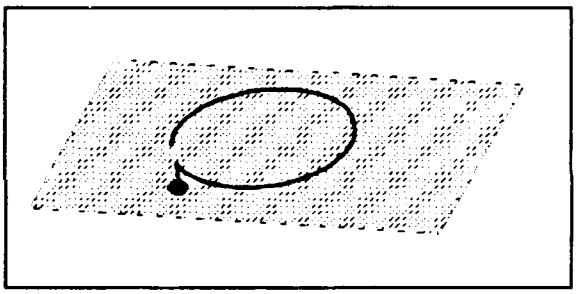

Figure 2 A Hula-Hoop Antenna.

satellite body would be expected to provide a nearly omnidirectional pattern of mixed polarization, although no sample radiation pattern data is available.

b. The Resonant Quadrifilar Helix

One antenna which retains most of the favorable characteristics of the Hula-Hoop antenna and also achieves circular polarization is called a Quadrifilar Helix. This antenna uses four helices arranged 90° apart and fed in phase quadrature. Figure 3 is a sketch of an antenna of this type. This antenna provides excellent hemispherical coverage with circular polarization everywhere (Kilgus, 1968). Additionally, the Quadrifilar Helix is in use on existing satellites and may be considered a proven design for space applications. Two antennas of this design, mounted opposite one another, would be likely to meet all of the electrical requirements for the PANSAT antenna design. It is even possible that one such antenna would be adequate because it would induce significant

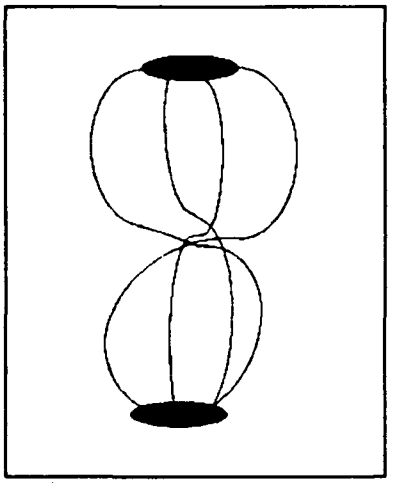

Figure 3 A Quadrifilar Helix Antenna.

currents onto the satellite body[9] thus resulting in approximately omnidirectional coverage.

c. The Turnstile Antenna

The turnstile antenna consists essentially of two crossed dipoles fed in phase quadrature. This configuration results in near omnidirectional coverage with circular polarization in the directions perpendicular to the plane of polarization. The radiation pattern remains linearly polarized in the plane containing the antenna.

In satellite applications, four monopoles mounted at 90° intervals around the satellite body and fed in phase progression achieve the same radiation pattern as crossed dipoles provided that the satellite body is not too large in terms of wavelength.

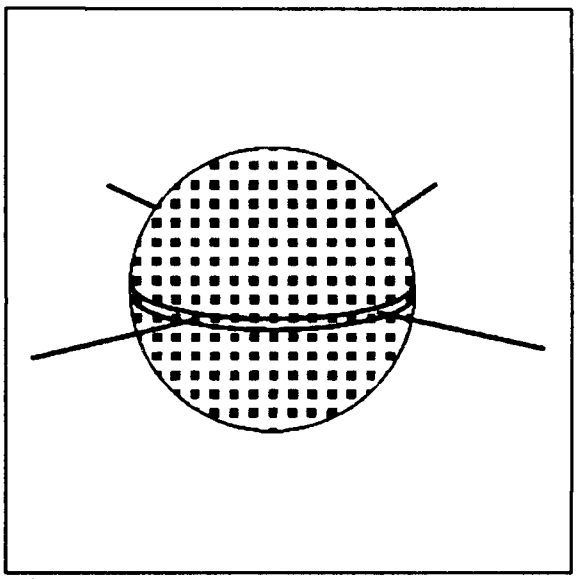

Figure 4 The Currier Satellite and its Turnstile Ant.

Figure 4 shows this configuration as it was used on the Currier satellite (Jakstys, 1991). The theoretical basis of this configuration,

---

[9] In fact, the Hula-Hoop antenna would also induce significant currents onto the satellite body resulting in somewhat omnidirectional coverage even with a single antenna. This is a result of the size of the satellite body and will be true to some extent of any antenna mounted on the satellite.

including field equations, is discussed by S. Nichols (NRL-6907, 1969) in his paper.

d. The Canted Turnstile Antenna

A number of variations to the basic (planar) turnstile antenna design are possible. Figure 5 displays one of these variations as it was used on the Explorer 34 satellite (Figure 5). This antenna configuration has been widely used on satellites, and is called a canted turnstile.

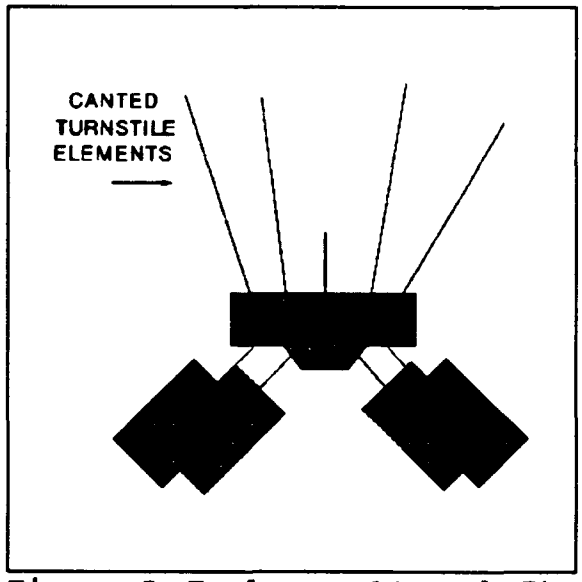

Figure 5 Explorer 34 and Its Canted Turnstile Ant.

The antenna is formed by tilting the four monopoles of the planar turnstile antenna upward. The angle of tilt used varies depending on the size and shape of the satellite body. The use of the canted turnstile has two main advantages over the planar turnstile. The first is that it allows the antenna to be easily mounted on the end of the satellite where the distance from the satellite center can be varied in order to adjust feed impedances. The second is that the antenna may be easier to store during satellite launch since it does not protrude so far to the sides of the satellite. The radiation pattern is not greatly affected by this modification; the

polarization of the antenna radiation pattern remains linear in the plane perpendicular to the satellite body although the polarization vector will no longer lie in the plane (Jackson, 1967)[10].

e. The Tangential Turnstile Antenna

The Tangential Turnstile Antenna is the name given by W. S. Gregorwich (1972) to a novel variation on the canted turnstile that he developed for the Synchronous Meteorological Satellite (SMS). This variation, shown in Figure 6, is formed by rotating all of the elements of the canted turnstile 90° clockwise (or counterclockwise) as seen from above. The advantage of this design is that it results in circular polarization over the entire omnidirectional antenna pattern.

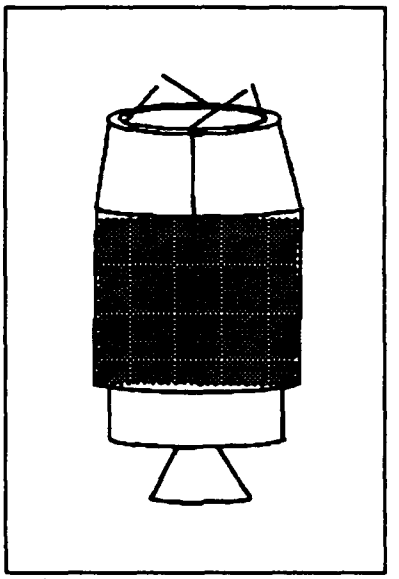

Figure 6 SMS Satellite with Its Tangential Turnstile Ant.

[10] The numerical models of candidate PANSAT antenna configurations do not agree with this statement in that they predicted elliptically polarized fields everywhere for the canted turnstile configuration. Nonetheless, other authors agree with Jackson (Gregorwich, 1972) and the discrepancy may be attributable to radiation from currents induced on the PANSAT body as a result of its size with respect to wavelength.

f. Multiple Monopole Antennas

The original PANSAT design proposal envisioned using eight monopole antennas, one mounted on each of the available triangular surfaces. This was the earliest approach used for satellite antenna design and is known to work well. However, further investigation since that time indicates that there is little or no advantage to using more than four radiators (Philco-Ford). This is particularly true when the satellite body size is on the order of a wavelength as is the case for PANSAT. For these reasons, and because one of the design goals for the PANSAT antenna is to minimize weight, the use of more than four monopoles was not investigated further.

B. SELECTION OF A BASIC ANTENNA CONFIGURATION

The preceding discussion illustrates various approaches to obtaining omnidirectional coverage from a satellite antenna design. The next step in the PANSAT antenna design process was to begin narrowing the design choices. It was decided to pursue designs based on variations of the turnstile antenna by modeling various turnstile configurations on a simple NEC model. The turnstile antenna was chosen because it seemed the most promising approach based on its simplicity and flexibility. The reasons for excluding the other design approaches considered are explained briefly below.

The Hula-Hoop antenna showed potential for meeting most of the PANSAT antenna requirements, but was expected to exhibit

mixed polarization rather than the desired circular polarization. Additionally, the Hula-Hoop and similar designs would have been more difficult to model accurately, thus resulting in a greater risk of getting erroneous data from the model.

The principle difficulties with using a quadrifilar helix antenna design for PANSAT lie in the physical requirements of the PANSAT application. The helix would be comparatively large and would require a complex deployment scheme to position it since it would not fit into a shuttle GAS canister while extended. The antennas complex geometry would also make it very difficult to model accurately.

IV. SIMPLE NEC ANTENNA MODELS

A. CONSTRUCTION OF A SIMPLE MODEL FOR PANSAT

1. NEC Software Installation and Validation

In preparation for testing the various turnstile antenna designs, the NEEDS software was installed on the 386 computer that was to be used for antenna modeling. Verification that the software was operating properly after installation was accomplished by modeling a simple half-wave dipole antenna at a variety of frequencies and then comparing the results with analytical solutions. This process was repeated for several antenna configurations with well known solutions. No problems were encountered other than the necessity of adjusting the path statements in the NEEDS batch files. This verification process was repeated later for 386 NEC when it was installed.

2. Preparation of a Simple NEC Model for PANSAT

The first model of the satellite consisted of a simple cube with the same maximum outside measurements as the satellite body. The cube was formed by a wire grid and tested with a single monopole antenna mounted on it. This model is shown in Figure 7. A second monopole was then added and tested. Finally two more monopoles were added and fed in phase progression at 90° intervals to produce a planar turnstile

model. This process of increasing the model complexity gradually, while checking results at each step instilled a high degree of confidence that the model, when complete, would be accurate. At the same time, it was recognized that the simple cube model was not a very good representation of the satellite body. The cube model served largely to increase skill and confidence in the modeling process and to compare results with those expected from the reading.

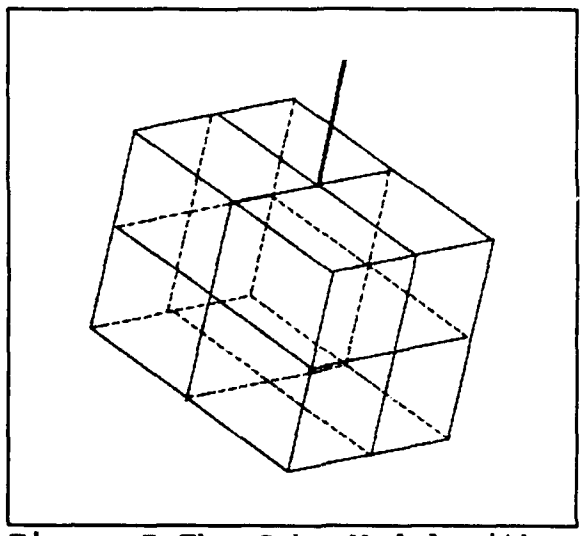

Figure 7 The Cube Model with a Monopole Ant.

The modeling results of interest at this stage were mostly the antenna patterns and polarizations. Input impedances were also generated, but the cube model was not considered detailed enough to provide accurate impedance values. The modeling results for each turnstile configuration are discussed briefly in the following section.

B. TESTING OF VARIOUS TURNSTILE ANTENNAS

1. The Planar Turnstile Antenna

The planar turnstile antenna model is shown in Figure 8. This model produced results in good general agreement with expectations. The wire radius was chosen to comply with the

equal area rule[11]. The number of wires, and the number of segments per wire, were kept at a minimum at this stage since the problem was being run on NEC-81 under NEEDS. The completed model used 52 wires divided into 164 segments. The resulting average gain was rather low, 0.71, but this was considered adequate for the purpose of comparing radiation pattern results with the other turnstile antenna models. The modeling results confirmed that the planar turnstile antenna produced a linearly polarized radiation pattern in the plane containing the antenna. For this reason, the planar turnstile configuration was not considered further for the PANSAT antenna.

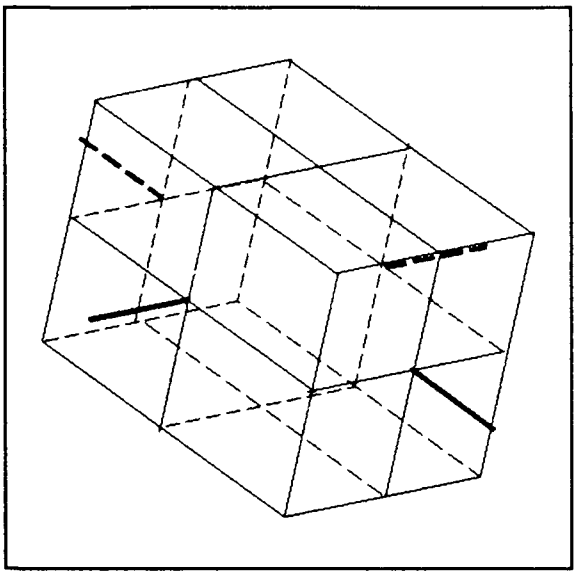

Figure 8 The Planar Turnstile on the Cube Model.

2. The Canted Turnstile Antenna

The model for the planar turnstile was modified by tilting the antenna elements upward by 45° to form a canted

---

[11] The "equal area rule" as applied here refers to choosing the wire radii such that the wires of the completed model have the same total surface area as a solid cube would have. This may be visualized as "unrolling" each wire so that its surface area covers the adjacent gaps between the wires when all of them are "unrolled".

turnstile configuration. Figure 9 illustrates the resulting model. Contrary to expectations from the literature (Jackson, 1967), this resulted in a radiation pattern that was elliptically polarized everywhere, including in the plane perpendicular to the satellite body. Other than this, the radiation pattern and other characteristics were very similar to that obtained from the planar turnstile.

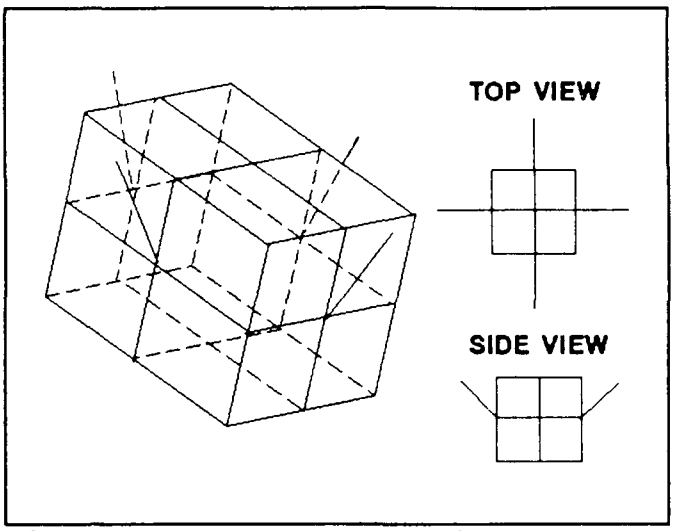

Figure 9 Canted Turnstile on the Cube Model.

3. The Tangential Turnstile

The tangential turnstile configuration was formed by rotating the canted antenna elements 45° counter-clockwise as seen from above. Figure 10 illustrates this configuration. Although this change moved the peaks and nulls of the radiation pattern, only a small change

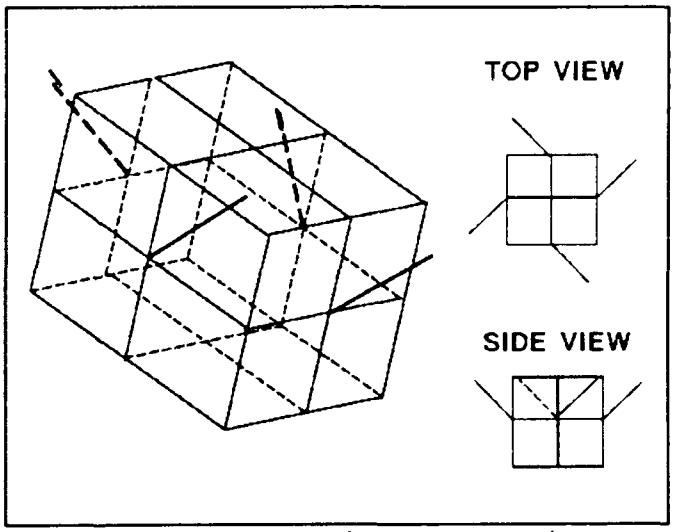

Figure 10 Tangential Turnstile on the Cube Model.

in the amplitudes of these peaks and nulls was observed. This and other differences between the radiation patterns were not sufficient to readily indicate which antenna would perform better on PANSAT. In order to determine which of these configurations would perform best on PANSAT, detailed models of both were built and compared.

V. SELECTION OF THE ANTENNA SYSTEM CONFIGURATION

A. CONSTRUCTION OF A DETAILED PANSAT MODEL

A detailed PANSAT model was constructed in order to provide more precise performance data for comparison of the canted turnstile and tangential turnstile designs. This detailed model was also used for optimization of the final antenna configuration and for predicting the performance of the completed design.

The development of the detailed PANSAT model followed a building block approach using small steps to arrive at the completed model. A large number of intermediate models were developed and discarded. Of these models, only the final version is presented here.

The final detailed model is shown in Figure 11 with the canted turnstile antenna mounted on it. This model accurately portrays the 26-sided polyhedron satellite body shape. The model design assumes that the exterior of the satellite body is conductive and that good electrical conductivity is present between all exterior portions of the satellite body. The effects of the solar cell panels, which will be mounted on the rectangular panels of the satellite body, are neglected. This is reasonable since the bulk of the radiation from the satellite body will occur along the edges of where the

electrical currents will experience a change-of-direction acceleration. Since these edges will not be covered by the solar cell panels, the panels should have little effect on the antenna pattern and impedance characteristics.

The model was optimized by choosing wire radii to follow the equal area rule and by varying the wire segmentation to maximize the average gain. The precise average gain achieved varied with the antenna configuration, but all models used for design decisions had average gains between 0.95 and 1.05. The final PANSAT model consists of 196 wires divided into 772 segments. The average gain diminished if the number of segments was either increased or decreased from this amount. It was observed that the average gain could be improved for individual antenna configurations by varying the wire radii slightly from the sizes calculated under the equal area rule, but this was not done since a single model for all antenna configurations was desired so that they could be directly compared to one another. In any case, the difference in antenna performance parameters for models with wire radii optimized for a particular antenna configuration did not change significantly from those calculated using the standard model. Table 2 compares key characteristics of the final PANSAT model against the guidelines[12] for NEC modeling.

---

[12] All of the guidelines for NEC modeling presented here or elsewhere in this thesis are from either Professor Adler's class notes (Adler, 1990) or from the NEC documentation (Burke, 1981).

TABLE II. THE FINAL PANSAT MODEL VERSUS NEC GUIDELINES[13]

NEC GUIDELINE	PANSAT FINAL MODEL
$L_{segment}$ < 0.1 lambda	$L_{segment}$ < .034 lambda
$L_{segment}$ > 2 x radius[14]	$L_{segment}$ > 3 x radius
Equal Area Rule	Verified
No Overlapping Wires	Verified

B. CONFIGURATION TESTING ON THE DETAILED NEC MODEL

1. The Canted Turnstile

This antenna, shown in Figure 11, exhibited very favorable characteristics when modeled in detail. The detailed model had an average gain of 0.953, an input impedance of Z_{in}= 78.9 -j0.6 Ω, and no radiation pattern nulls below -4.41 dBi. The pattern was elliptically polarized everywhere, although the axial ratio was very low in places. The antenna pattern is shown in Figure 12 as a three dimensional surface above a

---

[13] The numbers indicated in the table for the PANSAT model are those that are "worst case" as compared to the criteria.

[14] The full statement of this guideline indicates that the segment length should be greater than two times the radius for reasonable results and greater than eight times the radius for results with less than 1% error. The PANSAT model lies between these criteria rather than at the high end of the criteria. However, as stated earlier, varying the model to decrease the number of segments (longer segments) or increase the number of segments (shorter segments) both resulted in reduced average gain. For this reason the segment length shown here was retained.

theta versus phi plane. The pattern displays the entire four pi steradian pattern so that the pattern periodicity in phi can be seen easily. The predicted performance of this antenna is discussed in detail in the section comparing its performance to that of the tangential turnstile.

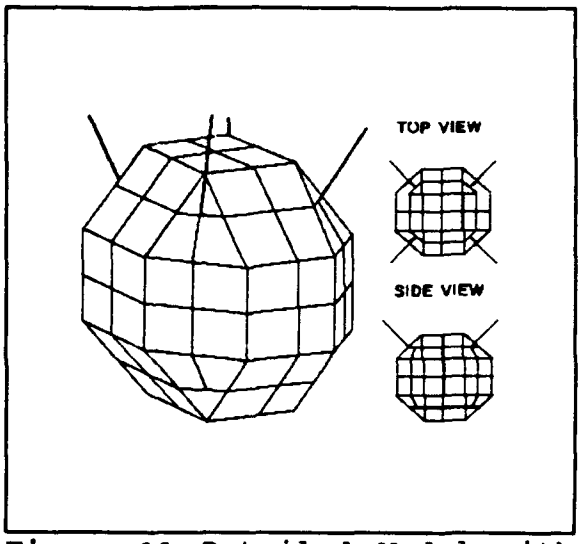

Figure 11 Detailed Model with the Canted Turnstile Ant.

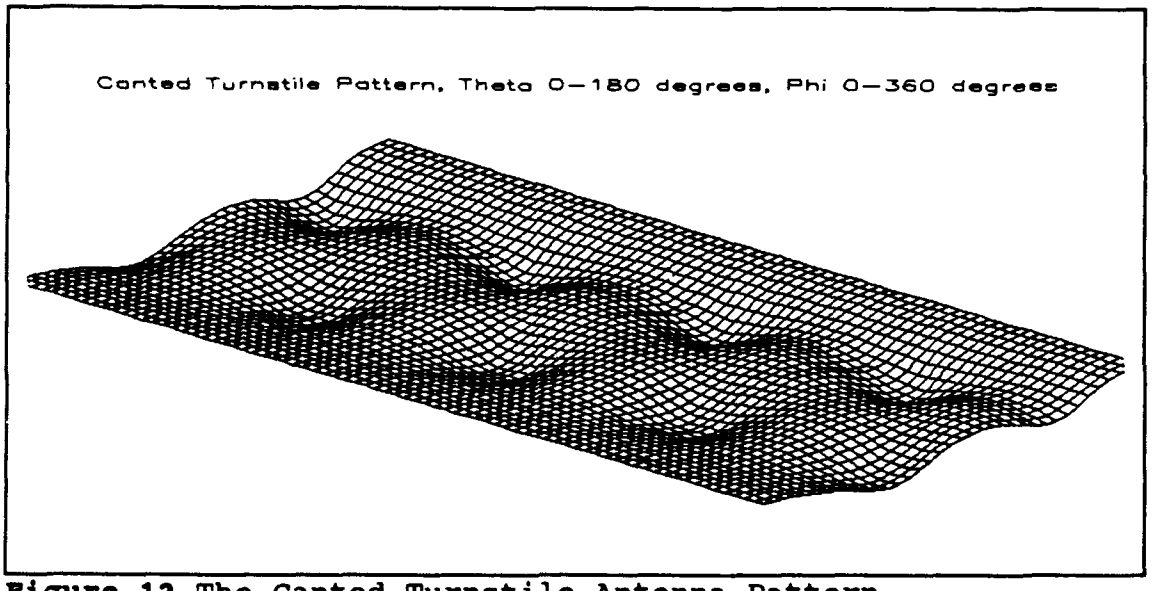

Figure 12 The Canted Turnstile Antenna Pattern.

2. The Tangential Turnstile

Figure 13 displays the detailed model with the tangential turnstile antenna configuration. The resulting antenna pattern is shown in Figure 14. When the tangential turnstile was modeled using the detailed PANSAT model, it was also shown to have very favorable performance characteristics.

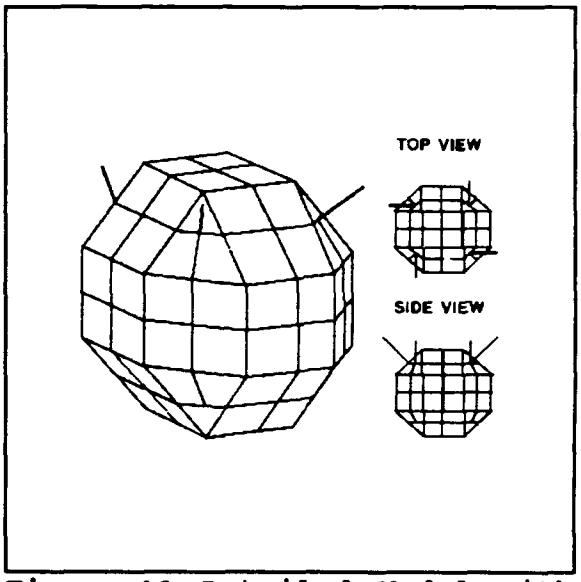

Figure 13 Detailed Model with the Tangential Turnstile.

In fact, the performance characteristics of the two antennas were so similar that a detailed analysis was required to

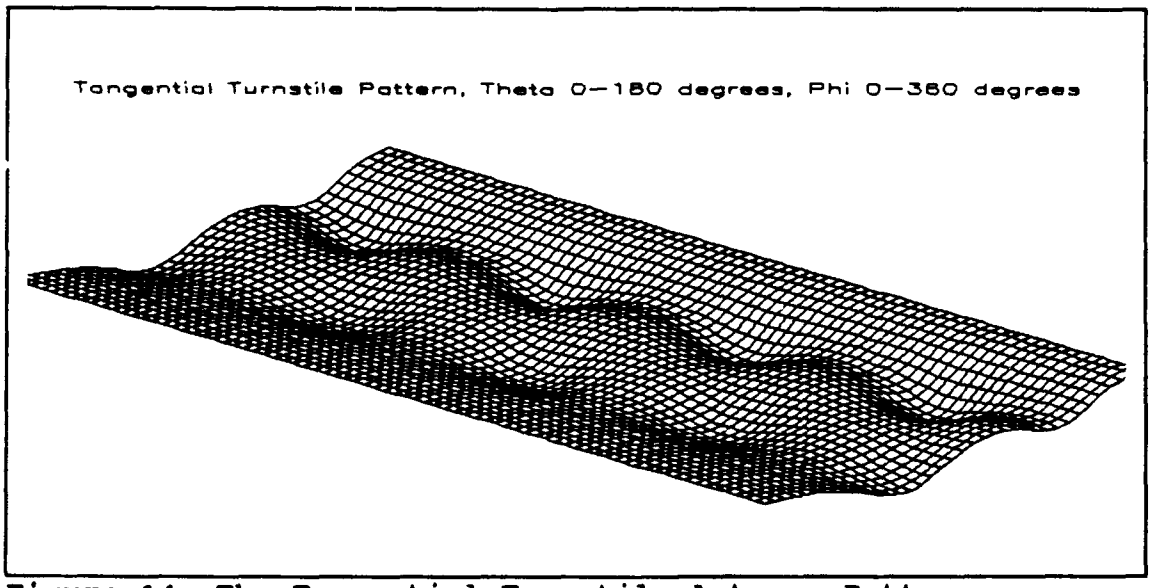

Figure 14 The Tangential Turnstile Antenna Pattern.

choose between the two. This analysis compares key performance parameters of each antenna configuration.

3. Detailed Comparison of the Tangential and Canted Turnstiles Using a Statistical Approach

Since both antenna configurations are capable of meeting the specifications cited in Table I, it was necessary to examine them closely to determine which was actually superior. A meaningful comparison of the performance criteria of the two antenna configurations is made possible by the application of some basic statistics. This approach looks beyond the PANSAT antenna performance specifications to examine the underlying goal of maximizing the likelihood of successful communication with the satellite.

In the case of directional antenna systems, plots of antenna patterns provide meaningful insight into the comparative performance of two systems. However, in the case of omnidirectional antenna systems, a large number of pattern plots at various angles would be required to do a meaningful comparison between two antennas with similar performance. Even three dimensional plots do not provide much insight into the comparative performance between two similar antenna systems as inspection of Figures 12 and 14 demonstrates.

These difficulties are circumvented by plotting histograms of the antenna gain values. By showing pictorially where most antenna gain values are concentrated, it is easy to

see which antenna has the superior omnidirectional pattern characteristics. Histograms of the total antenna gain versus the percentage of sampled antenna field points with this gain are shown in Figures 15 and 16 for the canted and tangential turnstile antennas respectively. Each histogram was constructed by processing field point samples at 5° intervals in theta and phi over the 1 pi steradian area defined by varying theta from 0° to 180° and phi from 0° to 90°. There was no need to process samples from the entire 4 pi steradian spherical surface because of the symmetry in the antenna patterns. Minitab statistical software was used for the tabulation of the histograms and MATLAB was used to plot them. Examination of Figures 15 and 16 indicates that the tangential turnstile antenna has a more omnidirectional pattern because,

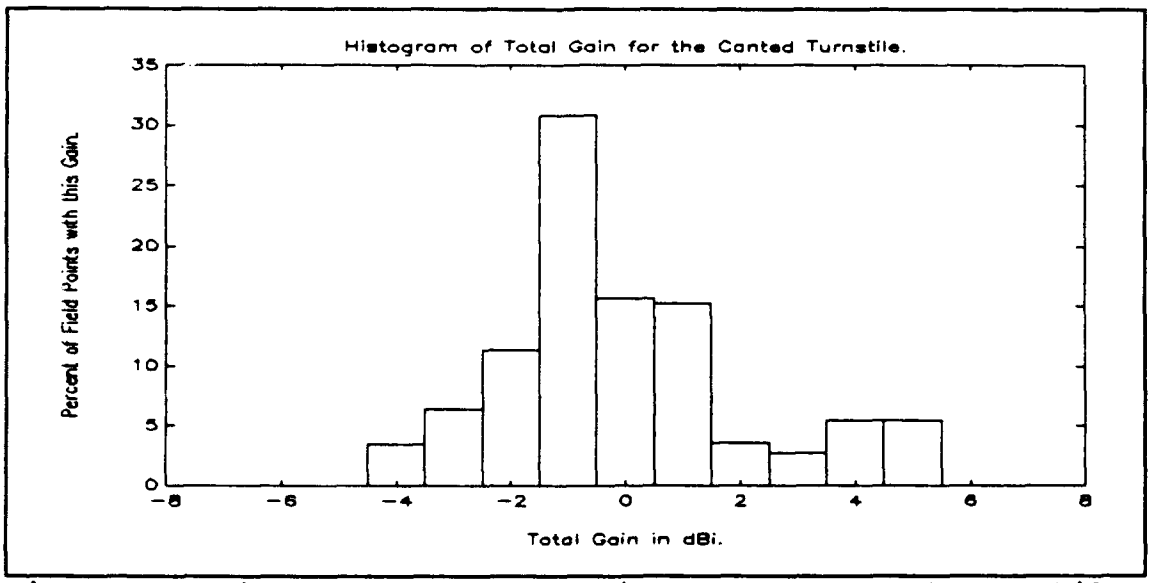

Figure 15 Histogram of Total Gain for the Canted Turnstile.

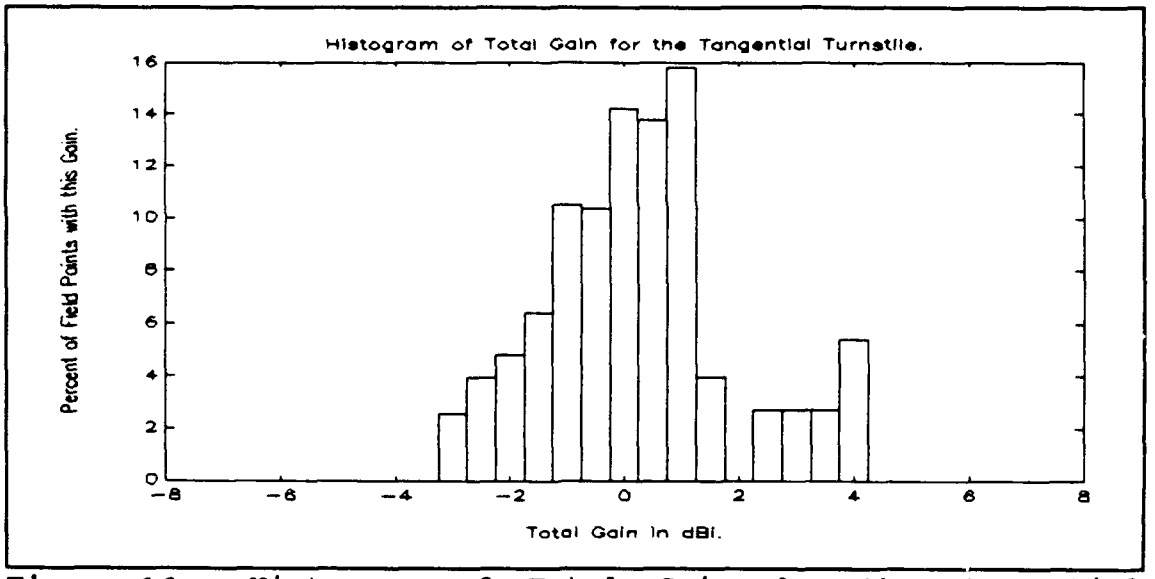

Figure 16 Histogram of Total Gain for the Tangential Turnstile.

in addition to having less severe worst nulls by 1 dB, it also has the smaller percentage of low end gain values.

An additional factor that must be addressed concerns which antenna has the superior polarization characteristics. Since circular polarization is desired, the axial ratio is a useful tool for comparing the polarization performance of the antennas. True circular polarization has an axial ratio of unity and pure linear polarization has an axial ratio of zero[15]. In order to compare the desirability of the polarizations of the canted and tangential turnstile antennas,

[15] For this application, the NEC software was configured to calculate the axial ratios based on the ratio of the minor axis of the elliptical pattern to the major axis of the ellipse. Use of vertical axis versus horizontal axis axial ratios would not have been correct since that would have provided non-zero axial ratios for off-axis linear polarizations.

the maximum, minimum, and mean values of the axial ratios for each were determined. These values are included in Table III, along with other comparisons of the characteristics of the two antenna configurations. As shown in the table, the minimum value of the axial ratio is lower for the tangential turnstile, but the mean value is higher.

Other considerations in choosing between the antenna configurations included physical characteristics and input impedances. With regard to physical characteristics, the two antennas are approximately equal although the tangential configuration might be slightly easier to store for launch since it lies closer to the satellite body. The input impedances are both very reasonable and would result in approximately the same VSWR if fed with 75Ω coaxial transmission line. With these considerations and the axial ratios indicating that the two antenna systems would perform equally well, the antenna pattern gains are the deciding factor. In this respect the tangential turnstile antenna is clearly better and it is chosen as the PANSAT antenna design. The design process is not yet over though, since the design can be optimized with regard to exact antenna placement.

TABLE III. CANTED VERSUS TANGENTIAL TURNSTILES

Parameter (Modeled Value)	Canted Turnstile	Tangential Turnstile
Worst Null	-4.41 dBi	-3.06 dBi
Pattern Ripple	9.13 dB	7.18 dB
Input Impedance	Z_{in}= 78.9-j0.6Ω	Z_{in}=72.3+j0.2Ω
Axial Ratios		
Minimum Value	0.0015	0.0007
Maximum Value	0.9957	0.9957
Mean Value	0.4660	0.4666
Physical Characteristics	Excellent	Excellent

C. OPTIMIZATION OF THE TANGENTIAL TURNSTILE DESIGN

Figure 17 portrays the positions of the monopole antenna elements on the tangential turnstile antenna. The question arises whether the performance of the antenna can be improved by varying the antenna position in theta and phi. In order to answer this question, the numerical analysis was repeated using various values for the angles. In all tested cases, the radiation patterns had nulls worse than those at the original positions. Therefore, surprisingly enough, the original values chosen seem to be the best ones.

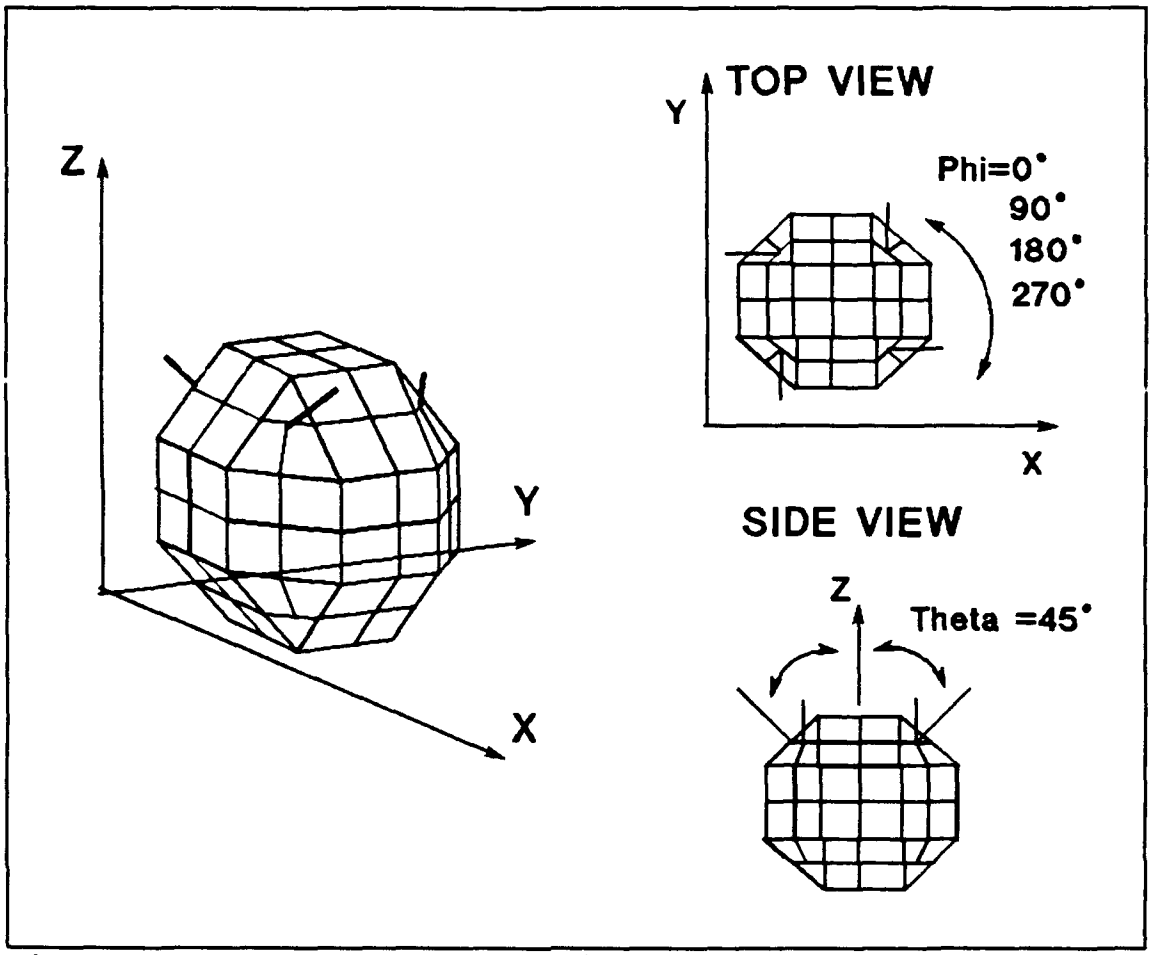

Figure 17 Antenna Element Positions on PANSAT.

Another parameter that could be varied is the lengths of the antenna elements. However, this was already done in the process of developing the detailed NEC models with the criteria being to achieve resonance. The value of the resonance condition is that it results in the antenna feed impedances being real, thus making it comparatively easy to develop an antenna feed system without having excessive VSWR on the feed lines. For this reason, the antenna lengths were not varied to optimize the radiation pattern.

The radius of the antenna elements could also be varied. This was done during the initial development of the detailed NEC model, but resulted in only minor changes in the radiation patterns. The final radius for the antenna model was chosen based on the need for an antenna material that would withstand the space environment without warping. In space, flat or round antenna elements tend to warp due to the large temperature differential which develops between the sun lit side and the shadowed side. Antenna elements should therefore be constructed of resilient materials that retain their shape well and that tend, if deformed, to return to their original shape. One commonly available material that has these characteristics is the slightly concave, spring steel measuring tape used by carpenters. In fact, this material is known informally as "Stanley" tape after one of the leading manufacturers of these tape measures. Stanley tape has been used for satellite antennas before (Batson, 1969) and may be considered space proven. For these reasons, 1/2" Stanley tape was chosen as the antenna material for PANSAT and the model used an equivalent wire radius (Adler, 1990) of one fourth of this width, or one eighth of an inch.

VI. PANSAT ANTENNA FEED SYSTEM DESIGN

A. ANTENNA FEED SYSTEM DESIGN SPECIFICATIONS

The design specifications developed in Chapter I required a 50Ω input impedance and a maximum VSWR of 1.4 for the antenna feed system. The completed PANSAT antenna model predicts an input impedance of $Z_{in}=72.3+j0.2\Omega$ for individual antenna elements, which would result in a VSWR of 1.45 if the elements were fed with 50Ω coaxial cable. Rather than modify the antenna element design or design a complex antenna feed system with impedance transformers, the simplest solution to this conflict is to modify the design specifications. It is acknowledged that this option is not always available in design work; in this case, however, the specifications for VSWR and input impedance were chosen arbitrarily as "good" target numbers because the transmitter and receiver designs have not progressed far enough to specify these parameters. After consultation with Professor Panholzer and other members of the PANSAT design team, it was decided that keeping the VSWR low was more important than retaining a 50Ω input impedance. Therefore, the following antenna feed system design uses 75Ω coaxial cable and a 75Ω antenna system feed impedance in order to minimize the VSWR. Note that 75Ω coaxial cable and

75Ω components are readily available, although less common than their 50Ω counterparts.

B. THE PANSAT ANTENNA FEED SYSTEM

1. Assumptions for the Feed System

In the antenna feed system design, it has been assumed that the PANSAT communications system will consist of a transceiver rather than a dedicated transmitter with a separate receiver. Although this decision has not yet been made, this configuration has significant size and weight advantages. Furthermore, the single feed antenna system has the advantage of flexibility since it can be used with either the transceiver configuration or, by adding a coaxial switch, with a dedicated transmitter and a separate receiver configuration. Therefore, the feed systems considered here use a single connection point to the communications system.

2. Requirements for the Feed System

The requirements imposed on the antenna feed system consist of the modified design specifications discussed earlier plus the requirements imposed by the particular antenna system chosen, the tangential turnstile. These requirements are summarized below:

- Input impedance of 75Ω.
- Maximum VSWR of 1.4.
- Minimum size and weight.

- Provide a single connection point for a transceiver and individual feeds for four antenna elements in 90° phase progression.

3. Design Alternatives for the Feed System

In this section, two simple antenna feed system designs are examined. Either of them would be adequate for the PANSAT application, and a number of variants combining the features of these two designs would also work. The first design considered uses the characteristics of the coaxial cable itself in order to fulfill the design requirements. The second uses power splitter/combiners to achieve similar results.

Figure 18 illustrates the feed system configuration for the first design. This design takes advantage of the phase

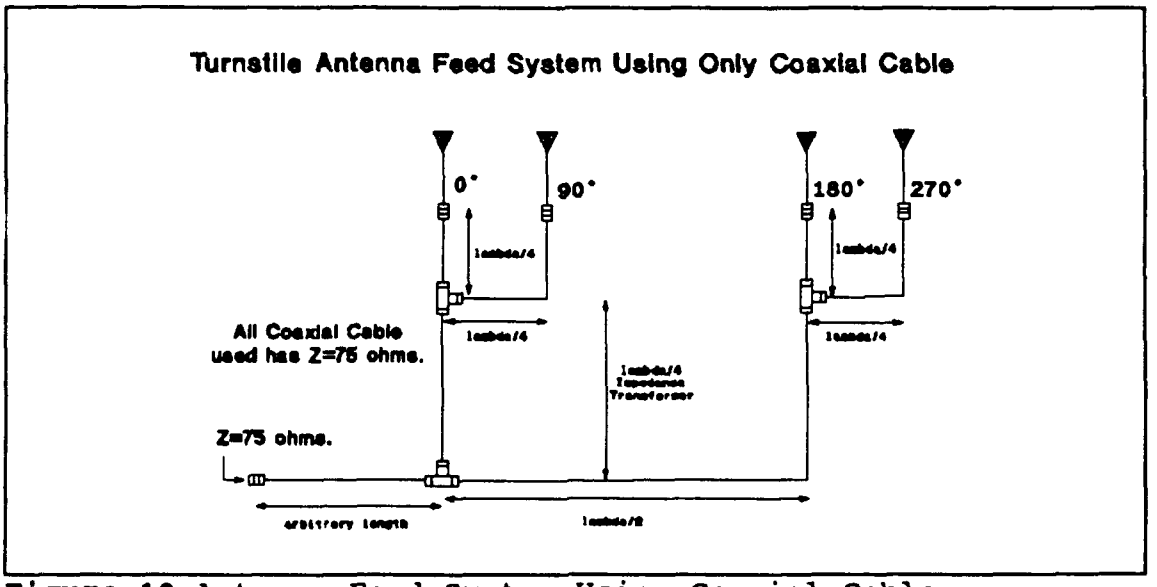

Figure 18 Antenna Feed System Using Coaxial Cable.

shift characteristics of the coaxial cable, ie. a quarter wave length of cable results in a 90° phase shift, etc. The design also uses the impedance transformation characteristic of a quarter wave length transmission line, i.e. $Z_{in}=Z_0^2/Z_{load}$. Note that at the design frequency of 437.25 MHz, a quarter wavelength is 17.1 centimeters or 6 3/4 inches. The advantage of this design is its simplicity; it uses only coaxial cable and coaxial connectors in order to fulfill the requirements. The disadvantages are that this design requires specific coaxial lengths which may not be convenient for physical reasons and, more importantly, this design does not provide any isolation between the antenna elements. This latter consideration could be important in the event that one element was somehow damaged or shorted to the satellite body.

The second design is shown in Figure 19. This design relies on power splitter/combiners to provide the phase shifts and matching between sections. Since inexpensive, reliable, lightweight power splitter/combiners are readily available there is no significant disadvantage to this approach. The advantages are that this approach provides isolation between elements and complete flexibility in choosing coaxial cable lengths based on physical considerations. This design is therefore recommended for use on PANSAT.

4. Predicted Performance of the Feed System

The antenna feed system chosen will provide a 75Ω input impedance for a single point feed transceiver. The use of a transceiver with an output impedance of 75Ω, will result in a very low VSWR on the order of $Z_0/Z_{element}=75/73=1.03$. The coaxial cable lengths L1, L2, and L3 may be selected based on physical convenience.

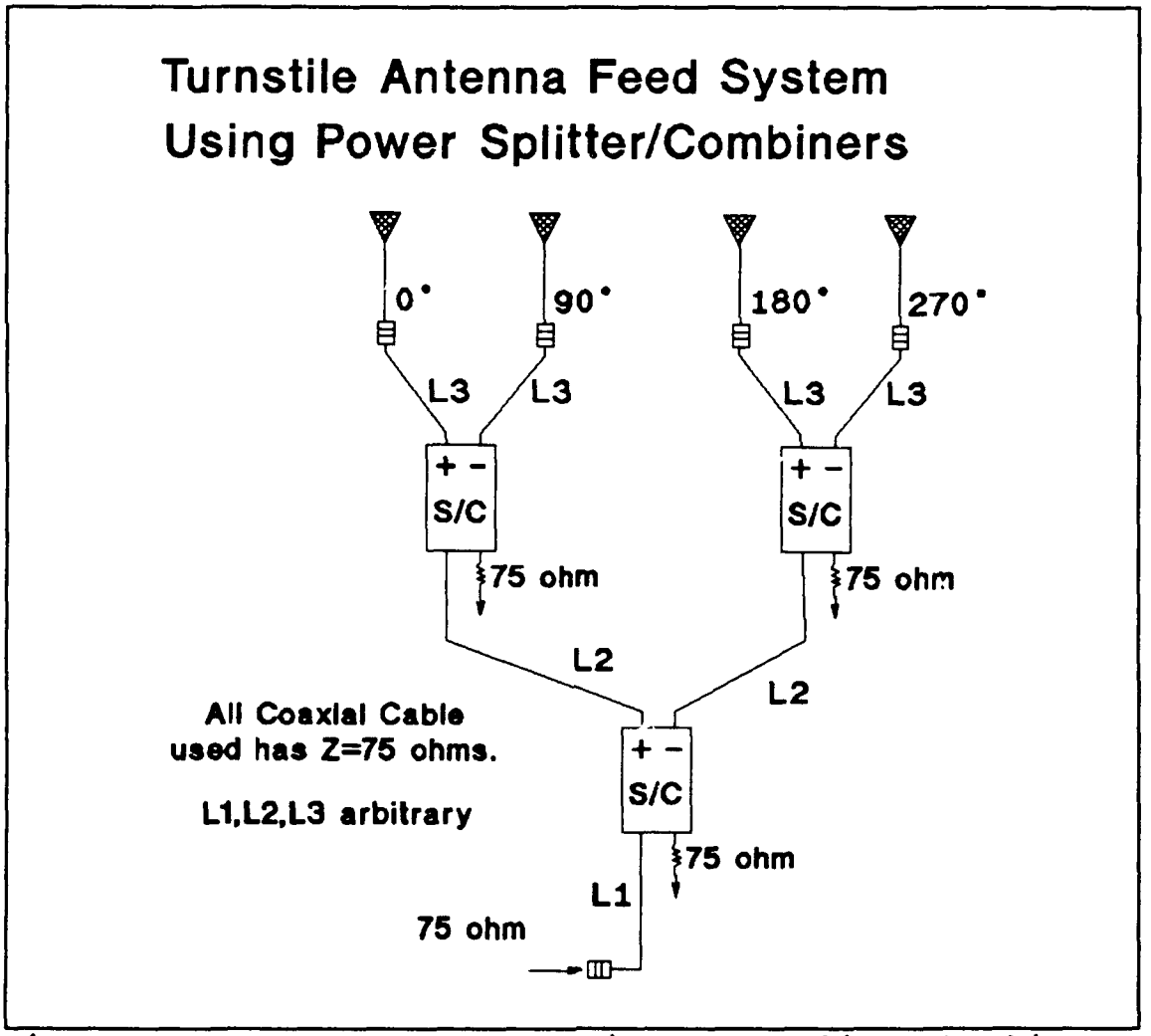

Figure 19 Antenna Feed System Using Power Splitter/Combiners.

VII. PREDICTED PERFORMANCE OF THE COMPLETED DESIGN

A. DESIGN SPECIFICATIONS & PREDICTED PERFORMANCE

Table IV compares the desired performance specifications for the PANSAT antenna system with the performance predicted by the NEC model for the completed tangential turnstile antenna. Examination of the table shows that the tangential turnstile antenna meets all design specifications, as long as the requirement for circular polarization is not interpreted in the strictest sense. Achieving true circular polarization (non-elliptical) everywhere would not have been a realistic goal and the design specification in Chapter II, Table I was footnoted to this effect originally. In conclusion, the predicted performance of the PANSAT antenna fully meets the original specifications. However, the existence of elliptical polarization vice perfect circular polarization does have implications for mission performance and these implications are examined in the following sections.

TABLE IV. DESIGN SPECS. VS. THE TANGENTIAL TURNSTILE

PARAMETER	DESIGN SPECIFICATION	TANGENTIAL TURNSTILE (PREDICTED)
Worst Null	-10 dBi	-3.06 dBi
Pattern Ripple	maximum 11 dB	7.18 dB
Polarization	Circularly polarized everywhere. (loose sense)	Elliptically polarized everywhere, average axial ratio of 0.4666.
Physical Characteristics	Minimum weight design, space proven, mounts on triangular surfaces.	Verified
Antenna Feed Input Impedance	Z_{in}= 75Ω (modified spec.)	Z_{in}=75Ω (system) Z_{in}=72.3+j0.2Ω (individual elements)
Maximum VSWR	VSWR<1.4	VSWR=1.03

B. IMPLICATIONS OF ELLIPTICAL POLARIZATION

1. Polarization Loss

In his thesis, Stephen Paluszek (1990, pp. 19-23) develops a link budget for the satellite which considers atmospheric attenuation, noise, and antenna temperatures. However, his link budget does not consider the effects of polarization loss between PANSAT and its ground stations. This type of loss (Schleher, 1986, pp. 419) occurs whenever the transmitter antenna and the receiving antenna have different polarizations. For linear antennas, polarization loss occurs

when the antennas are not aligned with each other and is theoretically infinite when the antennas lie at 90° angles. For circularly polarized antennas, polarization loss is theoretically infinite when the antennas have different senses, i.e. left-handed polarization at one antenna and right-handed at the other. In the case where one antenna is circularly polarized and the other is linearly polarized, the polarization loss is known to be three decibels.

In the case of PANSAT, the antenna polarization is elliptical, and the axial ratio of the ellipse changes with the orientation of the satellite. Furthermore, even if the satellite where not itself rotating, the axial ratio as measured from the ground would still change as the satellite moved in its orbit. For these reasons, the axial ratio is best described as a random variable. By extension, the polarization loss, which depends on the axial ratio, will also be statistical in nature.

2. The Axial Ratio as a Random Variable

Figure 20 displays a histogram of the axial ratios predicted by the NEC model for the tangential turnstile antenna. The histogram was constructed using samples taken at 5° intervals in theta and phi over a 1 pi steradian area. From this histogram the statistical nature of the axial ratio is apparent. The histogram may be rescaled by the total number of samples taken to form a probability density function for the

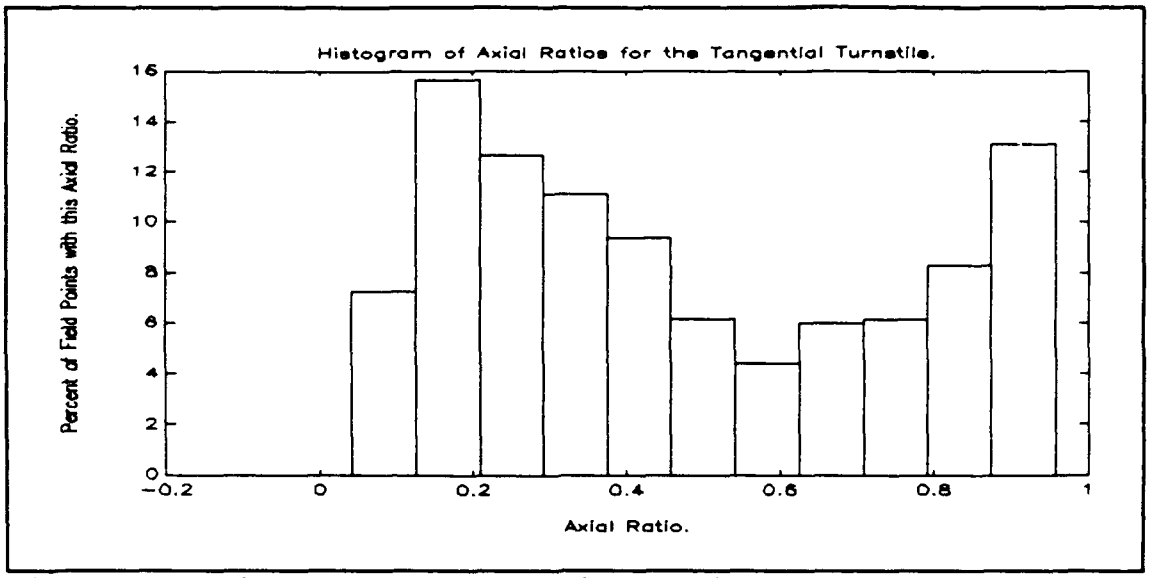

Figure 20 Histogram of the Axial Ratios.

axial ratio. This probability density function may then be integrated and smoothed to form a cumulative distribution function (CDF). This was done and the result is shown in Figure 21.

From the CDF shown in Figure 21 it is clear that 10% of the time the axial ratio is less than 0.1, 20% of the time it is less than 0.16, and so on. From this it is apparent that although the mean value of the axial ratio is 0.4666, it takes on values far below this in a significant number of cases. These low axial ratio values will correspond to high polarization losses under certain circumstances.

As the axial ratio varies with the satellite orientation, the polarization loss between the satellite and a linearly polarized antenna on the ground will also vary. The value of this polarization loss will depend not only on the

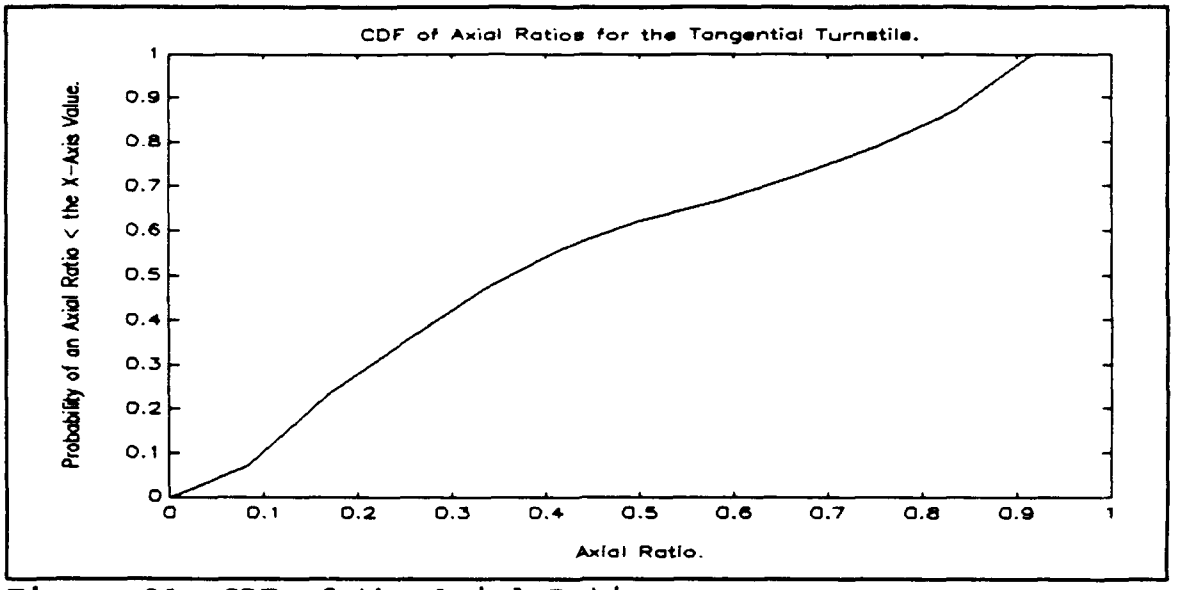

Figure 21 CDF of the Axial Ratios.

axial ratio of the elliptical polarization at that time, but also on the angle between the linear receiving antenna and the major axis of the ellipse. Calculation of an accurate value for this loss at the various satellite orientations, and prediction of the net effect on the bit error rate (BER) for the communication link, is a non-trivial task. Fortunately, an estimate of the polarization loss is sufficient here, and exact calculation may be avoided.

3. Estimation of the Average Polarization Loss

An estimate for this loss may be made through the use of loss curves[16] from an engineering reference book (Jordan, pp. 32-10, 1985). In his handbook, Jordan provides loss curves

[16] Another way of obtaining estimates for the polarization loss is through the use of polarization loss nomograms (Milligan, pp. 21, 1985). The results agree closely regardless of which approach is used.

for near circular polarization coupling with a near linear antenna for the case where the near linear antenna is aligned (0°) with the major axis of the elliptical polarization and for the case where the two are perpendicular (90°). The use of these curves may be illustrated by an example. When the antennas are aligned and the axial ratio is 0.32 (-5 dB) the loss is approximately 1.2 dB[17]. Notice that this is considerably less than the three decibel loss between a perfectly circularly polarized wave and a linear antenna. However, in the 90° case the polarization loss is approximately 6.2 dB for the same axial ratio. Since the orientation of the ground antenna with respect to the major axis of the ellipse is random and uniformly distributed, a mean value of the polarization loss for this axial ratio may be found by averaging the losses for the 0° and 90° cases. Using this approach[18] the average polarization loss for an axial ratio of 0.32 (-5 dB) is found to be 3.0 dB. Repetition of this process for several different axial ratios will show that this average polarization loss is always 3.0 dB, the same as the fixed (non-varying, non-averaged) polarization loss

---

[17] The curve does not actually show values for the case where one of the antennas is a true linear antenna, but this case may be approximated by observing how the values converge as the axial ratio approaches -55 dB on the illustrated curve.

[18] It is important to remember here that numbers in dB must be converted to real numbers, averaged, and converted back to dB. Numbers expressed in decibels cannot be averaged directly.

between a linear antenna and a perfect circularly polarized antenna.

4. General Behavior of the Polarization Loss

From the above discussion the general behavior of the polarization loss may be inferred. When a linearly polarized antenna is oriented with the major axis of an elliptically polarized wave (0°), the polarization loss approaches zero as the axial ratio approaches zero. On the other hand, when the major axis of an elliptically polarized wave and a linear antenna are perpendicular (90°), the loss approaches infinity as the axial ratio approaches zero. This may be seen clearly when it is noted that as the axial ratio approaches zero, the elliptically polarized wave collapses into a linearly polarized wave and the polarization loss behaves as it would between two linearly polarized antennas. Furthermore, if the relative angle between a linearly polarized antenna and the major axis of an elliptically polarized wave is a random variable with a uniform distribution between 0° and 90°, then the mean polarization loss will be three decibels. Regardless of the orientation of the linear antenna, when the axial ratio approaches unity, the special case of circular polarization results and the polarization loss is fixed at three decibels.

5. Polarization Loss in the PANSAT Link Budget

At this point it is clear that the polarization loss must be included in the PANSAT communication link budget in

order to provide accurate results. Since a polarization loss term was not explicitly included in the link budget developed by Stephen Paluszek (1990, pp. 19-23), the polarization loss may be considered as having been implicitly included in the specification requiring the PANSAT antenna design to have nulls no worse than -10 dBi. Therefore the polarization loss may be taken into account by modifying the original specification to read "antenna pattern nulls + polarization loss no worse than -10 dBi," rather than "antenna pattern nulls no worse than -10 dBi." When the predicted worst nulls (-3.06 dBi) for the tangential turnstile antenna are considered, the result is a new specification, "polarization loss must be no worse than -6.94 dB."

The previously used curves (Jordan, pp. 32-10, 1985) do not include the axial ratio line that would correspond to a loss of 6.94 dB; however, an estimate may be made. Extrapolating the data presented on the curves indicates that an axial ratio of about 0.25 (-6 dB) would correspond to a polarization loss of seven decibels for the 90° case. Examination of Figure 21 shows that the tangential turnstile antenna has an axial ratio less than 0.25 about 35% of the time. This means that a linear ground antenna consistently placed perpendicular to the major axis of the PANSAT antenna pattern elliptically polarized wave would experience excessive polarization loss about 35% of the time. In reality of course, the relative antenna orientations would change constantly and

the ground antenna would be perpendicular to the major axis of the incoming wave only a small fraction of the time. Nonetheless, this example illustrates that a ground communication station employing a linearly polarized antenna is likely to experience signal fades due to polarization loss at least occasionally.

C. ANTENNAS FOR PANSAT GROUND STATIONS

The preceding discussion indicates that a simple linearly polarized antenna is a poor choice for a PANSAT ground station antenna, because fading problems due to polarization loss would occur at least part of the time. On the other hand, circularly polarized ground station antennas would have even more fading problems due to polarization loss resulting from differing senses of rotation (left handed to right handed mismatch).

These problems with fading due to polarization loss can, however, be avoided without resorting to complex designs for ground station antennas by using an antenna whose radiation pattern includes E field components oriented in more than one direction. For example, a dipole antenna with a 90° bend in the center has a linearly polarized antenna pattern with both horizontal and vertical components. With this configuration the major axis of an arriving elliptically polarized wave could never be perpendicular to both the horizontal and vertical parts of the antenna simultaneously as long as the

antenna is oriented broadside to the satellite. In this way the polarization loss may be held to reasonable values on the order of a few decibels. A loop antenna oriented broadside to the satellite would work even better, because the major axis of an arriving elliptically polarized wave would always fall directly across the loop at some point. In this configuration the polarization loss would have a near constant value of about three decibels.

Using a resonant circular loop antenna with a circumference of approximately one wavelength 0.68 meters (27") would combine a low polarization loss of about three decibels with an antenna gain of about four decibels. In this configuration, the sum of the polarization loss and the antenna gain would always be less than about six decibels, well within the specification of a maximum loss of ten decibels. This configuration would also provide about two decibels more gain at the ground antenna than the configuration suggested by Stephen Paluszek (pp. 23, 1990). Therefore, the resonant circular loop is recommended as the primary ground station antenna for communicating with PANSAT.

D. BROADBAND TANGENTIAL TURNSTILE PERFORMANCE

The operational bandwidth required for the PANSAT antenna system is 960 kHz of bandwidth at 437.25 MHz. As stated earlier, any antenna system that meets the other PANSAT design criteria will easily meet this specification. However, it has

also been mentioned that PANSAT is, among other things, a proof of concept satellite for quick reaction, spread spectrum, packet radio, communication satellites. In an operational configuration such satellites would need to be switchable between various spread spectrum channels, and would require a far larger operating bandwidth than PANSAT. Therefore, if this communication concept is pursued, the question of how much bandwidth the tangential turnstile antenna design can support will quickly arise. For this reason the antenna patterns and input impedances for the PANSAT tangential turnstile antenna system were computed at 20 MHz intervals across the frequency range from 370 MHz to 490 MHz. The antenna pattern data exhibited only minor variations across this frequency range and is not presented here. The worst nulls were between approximately two and three decibels down in all cases. The antenna element input impedance varied significantly and is recorded in Table V for each frequency step. No effort is made to analyze this data here except to say that, with an appropriate impedance matching network, the tangential turnstile design should be useful over a wide range of frequencies. This data was gathered solely to provide a starting point for follow-on work and is not used for the PANSAT design in any way.

TABLE V. TANGENTIAL TURNSTILE INPUT IMPEDANCES

FREQUENCY (MHz)	ANTENNA ELEMENT INPUT IMPEDANCE (OHMS)
370.0	62.7-j46.4
390.0	67.3-j32.4
410.0	70.1-j19.1
430.0	71.5-j5.5
450.0	72.6+j9.3
470.0	74.7+j24.4
490.0	77.6+j39.6

VIII. PERFORMANCE OF THE 80386 HARDWARE & SOFTWARE

A. COMPUTER HARDWARE USED

A Northgate personal computer with an Intel 80386 central processing unit (CPU) and a single Intel 80387 math coprocessor was used for all of the design work performed for this thesis. Both the CPU and the math coprocessor were operated at a clock speed of 33 MHz. The computer was configured with 16 megabytes of random access memory and a 200 megabyte SCSI hard disk. All of the random access memory was configured as extended memory. The hard disk was formatted as a single primary DOS partition. The CPU was also supported by a high speed 64 kilobyte memory cache. MS-DOS version 4.01 was used.

B. 386 NEC SOFTWARE USE

1. Version of 386 NEC Used

The version of 386 NEC used was a full implementation of NEC-3 which had been ported to 80386 personal computers by Timothy O'Hara and further modified and debugged by James J. Wright (1990). This version of the source code was configured to handle up to 1000 unknowns and compiled with the Lahey F77L-EM/32 FORTRAN compiler. Extended memory support was provided by the Ergo OS 386 DOS Extender. This software configuration implements the full 32 bit version of NEC-3.

Output from this version of 386 NEC is identified with the header, "NUMERICAL ELECTROMAGNETICS CODE (NPG1000) VERSION - LAHEY DOUBLE W/SAVES DATE:04/02/91 TIME:17:49:29:89."

2. Summary of Use and Problems Encountered

The bulk of the design work was done using the version of 386 NEC described above. The only exception to this is that a few of the earliest models were run using NEC-81, the personal computer version of NEC which is bundled with NEEDs. The model complexity quickly grew beyond the 300 unknowns constraint imposed by NEC-81 however, thus necessitating the switch to 386 NEC.

A large number of NEC "runs" were performed before the antenna design was completed. In all, 67 NEC output files were generated which filled 24 megabytes of hard disk space. Total CPU processing time for computing the NEC output files was in excess of 150 hours. Problem complexity ranged from 9 unknowns to 940 unknowns[19]. The bulk of these runs were optimization runs made to test the effects of small changes in the design such as varying the antenna position in 5° increments across a range of theta and phi values. In retrospect, many of these runs would have been unnecessary for a more experienced modeler, because with experience the effects of minor changes in the model could be accurately predicted from consideration

[19] The number of unknowns here corresponds to the number of wire segments in the model since no patches were used.

of the basic problem physics without using NEC. Table VI lists sample CPU times for several problem sizes. Note that the last item in the table is an example of the output produced by a software bug which is discussed below.

TABLE VI. CPU TIME REQUIRED FOR 386 NEC MODELS

MODEL NAME	NUMBER OF UNKNOWNS	MATRIX FILL TIME (SECONDS)	MATRIX FACTOR TIME (SECONDS)	TOTAL RUN TIME (SECONDS)
M3BOXT1B	160	64.59	32.40	107.87
PANSATM2	492	706.45	1390.33	2236.62
PANSAT14	940	2472.31	10288.97	14309.96
PANSATN7	580	*********	2272.98	-82222.20

The heavy usage of the 386 NEC software provided ample opportunity to discover any bugs or problems that might remain in the software since it was ported to run on 386 PCs. Despite this only one software bug was discovered, and it does not critically effect usage of the software. Of course, since this design effort used only wire models in free space, problems may exist in portions of the code that were not exercised.

The software bug that was discovered involves the tracking of CPU time. Some of the models ran produced output indicating negative total CPU times. In all of the cases where a negative total CPU time was indicated, the Matrix Fill Time field was filled with asterisks, which in FORTRAN normally indicates that the computed value could not be fit in the space allowed by the corresponding format statement.

Interestingly enough, the problem does not appear in a consistent fashion. The same NEC input file can be run several times and sometimes the problem will appear and sometimes it will not. This behavior indicates that there is some possibility that the problem is not in the 386 NEC software at all, but rather in the Northgate hardware or the MS-DOS operating system software. It should be noted that the system clock kept perfect time throughout the design effort.

C. COMPARISON OF 386 NEC AND MAINFRAME PERFORMANCE

The final antenna design model was run on the Northgate personal computer using 386 NEC and on the Amdahl 5990 mainframe using NEC-3, local version number DNP61K4H. This was done in order to observe the relative performance of the two machine/software combinations, and to provide additional 386 NEC validation. The NEC input file used on both the Northgate and the mainframe is included in Appendix C. Selected portions of the 386 NEC output file are included in the same appendix. The mainframe NEC output was not identical to the 386 NEC output, but agreed to three decimal places for the antenna element input impedances and agreed exactly for all antenna pattern data.

Table VII compares the time requirements for the two computer systems. As can be seen in the table, the Amdahl mainframe produced the problem solution in 1/27th of the time required by the Northgate personal computer. This demonstrates

that the Amdahl 5990 is blazingly fast in comparison with the Northgate personal computer. Even so, the convenience of having a dedicated desktop computer and the low cost of personal computers compared with mainframes still make the personal computer approach attractive for many applications. Additionally, it should be noted that the problem turnaround time on the mainframe would be much longer under even modest system loading than the CPU times listed in the table.

TABLE VII. AMDAHL MAINFRAME CPU TIME VS. 386 CPU TIME

COMPUTER SYSTEM USED	NUMBER OF UNKNOWNS (FINAL DESIGN)	MATRIX FILL TIME (SECONDS)	MATRIX FACTOR TIME (SECONDS)	TOTAL RUN TIME (SECONDS)
Northgate	772	1684.13	5606.08	7682.59
Amdahl 5990	772	103.58	153.437	278.957

In any case, the results of this comparison are not necessarily representative of the performance of other mainframes. LCDR Howard reported in his thesis (pp. C-3, 1990), that his 386 computer, equipped with dual math coprocessors[20], consistently outperformed the IBM 3033 mainframe which was in use at that time.

[20] LCDR Howard used a 33 MHz 386 clone personal computer equipped with both an Intel 80387 and a Weitek 3167.

IX. SUMMARY AND CONCLUSIONS

A. SUMMARY OF WORK PERFORMED

In this thesis omnidirectional antenna designs for satellites were researched and examined for applicability to PANSAT. Several promising candidate designs were modeled using 386 NEC and evaluated for use on PANSAT. The tangential turnstile design was selected as the best of the candidate designs and optimized for PANSAT. The optimization process consisted of progressively modifying the design and evaluating the effect of the design changes through NEC modeling. Elementary statistical concepts and functions were used to generate performance predictions for the completed antenna system design. In particular, the problem of polarization loss between the satellite antenna and ground station antennas was examined in some detail and resolved by suggesting the use of mixed polarization ground station antenna. An antenna feed system was designed which provided a single connection point for a satellite transceiver and 90° phase progression feeds for the satellite antenna elements. Finally, the performance of the 386 NEC software on the Northgate personal computer was evaluated and compared to the performance of NEC-3 on an Amdahl 5990 mainframe by using the final NEC model of the tangential turnstile antenna design as a test problem.

B. FUTURE WORK - DESIGN VERIFICATION

After the construction of the PANSAT body has been completed, the antenna system should be tested before the satellite is launched. This should be done both to confirm that the antenna system has been constructed properly and to verify the performance predictions made from the NEC model. In order to make accurate measurements of the antenna pattern generated by the tangential turnstile antenna, it will be necessary to have all exterior panels of the satellite body in place and the satellite isolated from all conducting materials, including the ground, by several wavelengths.

The measurements will be quite sensitive to effects from other conducting objects in the area because of the omnidirectional antenna pattern. It should be kept in mind at all times that the satellite body is an integral part of the antenna and that no useful information can be gained by testing the antenna elements when they are not in place on the satellite body. A good test methodology might include suspending the assembled satellite from a nonconducting cord so that it is 12 to 15 feet away from the ground, buildings, cables, tree trunks and branches, etc. A loop or other antenna can then be used to measure the pattern generated when the satellite transmitter is activated. It is also desirable to verify the antenna element feed impedance, but this may be difficult to do accurately since the ideal measurement setup would require that the test equipment be placed inside the

satellite body in order to eliminate the effects that might result from having a conducting cable running from the inside of the satellite to the outside.

C. CONCLUSIONS

The tangential turnstile antenna system design should provide an excellent omnidirectional antenna system for PANSAT based on the results of numerical modeling performed with NEC. Nonetheless, it is advisable that the predicted antenna system performance be verified by testing the completed satellite and antenna system prior to launch. At the current level of numerical electromagnetic modeling technology, the predictions made from such models should always be verified with physical laboratory measurements unless the design is extremely low risk.

APPENDIX A - PANSAT INFORMATION

A. PANSAT DESIGN OVERVIEW

The PANSAT design has been broken down into several subsystems which relate to various functions performed by the satellite. This approach allows the satellite design to proceed simultaneously in several different areas. Later in the design process these subsystems will be integrated into the satellite and any conflicts will be resolved. Since the mission, concept, and objectives of PANSAT were covered in Chapter I, this appendix is simply a reference document that provides an overview of each satellite subsystem and updates the current status of the project.

B. PANSAT SUBSYSTEMS

1. Structure Subsystem

The PANSAT structure is composed of 20 separate parts made of 6061-T6 aluminum. These parts will be bonded together to form the satellite structure. The structure will then be covered with lightweight aluminum body plates. The bonding method for the structure components and body plates has not yet been finalized, however it will be done in a manner that provides electrical conductivity between all sections of the satellite body due to the requirements of the antenna system. Details of the structure subsystem, including diagrams for the

milling of the structure componer . parts, may be found in the NPS PANSAT Final Design Report (pp. 17-19, 1989).

2. Power Subsystem

The PANSAT power subsystem will consist of a 12 volt unregulated bus supplied by solar cells and batteries. The planned solar cell set uses 17 exposed solar cell panels attached to the rectangular satellite surfaces (except the base). Each solar cell panel will use 256 cm^2 of solar cells for energy collection. The battery assembly will consist of a sealed container housing six battery packs of lead-acid batteries with six two-volt batteries per battery pack. The total energy storage capacity of the battery assembly will be 360 watt-hours. When the satellite is in sunlight, the solar cells will provide power for operations and for recharging the batteries. When the satellite is in the dark, the batteries will provide all power requirements. Further details of the power subsystem are included in the NPS PANSAT Final Design Report (pp. 7, 1989).

3. Data Processor & Sequencer (DP&S) Subsystem

The heart of the DP&S subsystem for PANSAT will be a Harris 80C86RH microprocessor. This low-power, radiation-hardened model of the popular 8086 microprocessor will interface to the communication subsystem, the structure subsystem, the power subsystem, and the experiments aboard PANSAT. Programming for the DP&S subsystem will be done in the Ada language. Further information on this subsystem is

available in the NPS PANSAT Final Design Report (pp. 3-6, 1989).

4. Communications Subsystem

As discussed previously, the satellite communications package will implement a direct sequence spread spectrum packet communications channel with a center frequency of 437.25 MHz (Paluszek, 1990). A Binary Phase Shift Keyed (BPSK), 1200 bit-per-second signal with a bandwidth of 960 kHz will be used. Communications will be done in the half duplex mode using the AX.25 message protocol. This communications channel will perform all required Telemetry, Tracking, and Control (TT&C) functions and act as the message conduit for packet communications. A tangential turnstile antenna system will be used to provide circularly polarized, omnidirectional coverage. Further details concerning the communication subsystem may be found in Stephen Paluszek's thesis (1990).

5. Experimental Payload

At this time, the only experiment slated to fly aboard PANSAT involves the collection of in-orbit solar cell current-voltage curves for several solar cell types. In-orbit solar cell annealing through the use of forward biasing will also be tested. The data which will be gathered from this experiment will be more complete than data currently available in that the full current-voltage characteristic will be measured rather than only a section of the curve. Further details

concerning this experiment may be obtained from Professor Sherif Michael at NPS.

There is sufficient space on board PANSAT to allow one or two more small experiments to be included. Anyone desiring more details concerning this opportunity to place an experimental payload in orbit should contact Professor Rudolf Panholzer at NPS.

C. PANSAT PROJECT STATUS

At this time milling of the PANSAT structural components is nearly complete and assembly of the satellite should begin soon. The DP&S subsystem is undergoing breadboard testing and the communication subsystem is temporarily on hold until additional interested students come forward to work on it. The possibility of using off-the-shelf communication equipment is being investigated in case an in-house design cannot be completed on schedule. The target date for flight readiness is July of 1993. The PANSAT proposal was ranked 9 of 13 at the 1991 Navy Space Test Program (STP) review of satellite proposals and 30 of 36 at the 1991 Tri-Service STP review.

APPENDIX B - NEC THEORY

All versions of NEC apply the method of moments (MoM) in order to numerically solve simplified versions of the electric and magnetic field integral equations (EFIE & MFIE) in order to provide model antenna and field problems. The EFIE is used for models consisting of thin wires, while the MFIE is used for models consisting of surface patches. When a model consists of both wires and patches, both the EFIE and the MFIE are used. As an example of how NEC works, the general theory and solution approach used by NEC for problems consisting of structures involving only thin wires is summarized below.

The solution strategy is to apply the MoM to a simplified version of the EFIE. The EFIE may be developed from the boundary condition which requires that the total tangential electric field on a perfect electric conducting surface is zero. The thin wire approximation is applied to the EFIE in order to reduce it to a scaler integral equation. NEC solves the scaler integral equation numerically through application of the MoM. This solution approach is compromised of expanding the unknown current on the wire segments in a summation of basis functions with unknown amplitude coefficients and enforcing equality of weighted integrals of the fields. The weighting functions used by NEC are delta functions and hence the procedure is often referred to as "point matching." The basis functions used by NEC are B-spline functions spread over three segments with the current on each segment being

postulated to have the form of a constant plus sine and cosine terms. The number of unknown coefficients is then reduced by enforcing continuity of current at segment junctions and continuity of charge on uniform wires. After this is completed, only one unknown associated with each basis function remains to be determined. This remaining unknown is determined by solving the electromagnetic interaction equations for the currents. This problem takes the form of a large matrix representing a set of linear equations. The solution is found through the application of Gaussian elimination and LU decomposition. The bulk of the NEC computation time is spent in evaluating this matrix. Once this matrix has been solved, the currents on the wire segments are known and fields and input impedances are found through application of standard electromagnetic equations.

Problems involving models composed of patches, or wires and patches together are solved by analogous methods. Additionally NEC, has the capability of accurately modeling structures over real earth through the use of a separate program which computes Sommerfield ground data for NEC. These features of NEC were not used for this thesis and are not discussed further here. Additional information on the theory applied in NEC is available in part one of the NEC manual (Burke, 1981). The NEC manual also includes a detailed discussion of the assumptions applied in NEC and the resulting limitations of the code. Details of how these capabilities

vary between different NEC versions are also covered in the same reference except that the thesis by James Wright (1990) should be consulted for information on how the capabilities and limitations of 386 NEC differ from those of the mainframe version of NEC-3.

APPENDIX C - NEC FILES

A. TANGENTIAL TURNSTILE ANTENNA, NEC INPUT FILE

```
CM PANSAT WITH A TANGENITAL TURNSTILE ANTENNA, L=.167
CE
GW1,4,.218,0.,-.108,.218,0.,-.024,.007,
GW2,4,.218,0.,-.024,.218,0.,.06,.007,
GW3,4,.218,0.,-.024,.218,-.09,-.024,.007,
GW4,4,.218,0.,-.024,.218,.09,-.024,.007,
GW5,4,.218,.09,.06,.218,0.,.06,.007,
GW6,4,.156,.092,.127,.156,0.,.127,.007,
GW7,4,.218,-.09,.06,.218,0.,.06,.007,
GW8,4,.156,0.,.127,.156,-.092,.127,.007,
GW9,4,.218,.09,.06,.156,.092,.127,.005,
GW10,4,.218,0.,.06,.156,0.,.127,.007,
GW11,4,.218,-.09,.06,.156,-.092,.127,.005,
GW12,4,.094,.094,.194,.156,.092,.127,.005,
GW13,4,.156,0.,.127,.094,0.,.194,.007,
GW14,4,.094,-.094,.194,.156,-.092,.127,.005,
GW15,4,.218,-.09,-.108,.218,0.,-.108,.007,
GW16,4,.156,-.092,-.175,.156,0.,-.175,.007,
GW17,4,.218,.09,-.108,.218,0.,-.108,.007,
GW18,4,.156,0.,-.175,.156,.092,-.175,.007,
GW19,4,.218,-.09,-.108,.156,-.092,-.175,.005,
GW20,4,.218,0.,-.108,.156,0.,-.175,.007,
GW21,4,.218,.09,-.108,.156,.092,-.175,.005,
GW22,4,.094,-.094,-.242,.156,-.092,-.175,.005,
GW23,4,.156,0.,-.175,.094,0.,-.242,.007,
GW24,4,.094,.094,-.242,.156,.092,-.175,.005,
GW25,4,.218,.09,-.108,.218,.09,-.024,.007,
GW26,4,.154,.154,-.108,.154,.154,-.024,.007,
GW27,4,.218,.09,.06,.218,.09,-.024,.007,
GW28,4,.154,.154,-.024,.154,.154,.06,.007,
GW29,4,.218,.09,-.108,.154,.154,-.108,.005,
GW30,4,.218,.09,-.024,.154,.154,-.024,.007,
GW31,4,.218,.09,.06,.154,.154,.06,.005,
GW32,4,.09,.218,-.108,.154,.154,-.108,.005,
GW33,4,.154,.154,-.024,.09,.218,-.024,.007,
GW34,4,.09,.218,.06,.154,.154,.06,.005,
GW35,4,.218,-.09,-.108,.218,-.09,-.024,.007,
GW36,4,.154,-.154,-.108,.154,-.154,-.024,.007,
GW37,4,.218,-.09,.06,.218,-.09,-.024,.007,
GW38,4,.154,-.154,-.024,.154,-.154,.06,.007,
GW39,4,.218,-.09,-.108,.154,-.154,-.108,.005,
GW40,4,.218,-.09,-.024,.154,-.154,-.024,.007,
GW41,4,.218,-.09,.06,.154,-.154,.06,.005,
GW42,4,.09,-.218,-.108,.154,-.154,-.108,.005,
GW43,4,.154,-.154,-.024,.09,-.218,-.024,.007,
GW44,4,.09,-.218,.06,.154,-.154,.06,.005,
GW45,4,-.09,.218,-.024,0.,.218,-.024,.007,
GW46,4,.09,.218,-.024,0.,.218,-.024,.007,
GW47,4,0.,.218,-.024,0.,.218,.06,.007,
GW48,4,.09,.218,.06,.09,.218,-.024,.007,
GW49,4,0.,.218,-.024,0.,.218,-.108,.007,
GW50,4,.09,.218,-.108,.09,.218,-.024,.007,
GW51,4,-.09,.218,-.108,0.,.218,-.108,.007,
GW52,4,-.092,.156,-.175,0.,.156,-.175,.007,
GW53,4,.09,.218,-.108,0.,.218,-.108,.007,
GW54,4,0.,.156,-.175,.092,.156,-.175,.007,
GW55,4,-.09,.218,-.108,-.092,.156,-.175,.005,
GW56,4,0.,.218,-.108,0.,.156,-.175,.007,
GW57,4,.09,.218,-.108,.092,.156,-.175,.005,
GW58,4,-.094,.094,-.242,-.092,.156,-.175,.005,
GW59,4,0.,.156,-.175,0.,.094,-.242,.007,
GW60,4,.094,.094,-.242,.092,.156,-.175,.005,
GW61,4,-.09,.218,.06,0.,.218,.06,.007,
GW62,4,-.092,.156,.127,0.,.156,.127,.007,
```

```
GW63,4,.09,.218,.06,0.,.218,.06,.007,
GW64,4,0.,.156,.127,.092,.156,.127,.007,
GW65,4,-.09,.218,.06,-.092,.156,.127,.005,
GW66,4,0.,.218,.06,0.,.156,.127,.007,
GW67,4,.09,.218,.06,.092,.156,.127,.005,
GW68,4,-.094,.094,.194,-.092,.156,.127,.005,
GW69,4,0.,.156,.127,0.,.094,.194,.007,
GW70,4,.094,.094,.194,.092,.156,.127,.005,
GW71,4,-.09,.218,-.108,-.09,.218,-.024,.007,
GW72,4,-.154,.154,-.108,-.154,.154,-.024,.007,
GW73,4,-.09,.218,.06,-.09,.218,-.024,.007,
GW74,4,-.154,.154,-.024,-.154,.154,.06,.007,
GW75,4,-.09,.218,-.108,-.154,.154,-.108,.005,
GW76,4,-.09,.218,-.024,-.154,.154,-.024,.007,
GW77,4,-.09,.218,.06,-.154,.154,.06,.005,
GW78,4,-.218,.09,-.108,-.154,.154,-.108,.005,
GW79,4,-.154,.154,-.024,-.218,.09,-.024,.007,
GW80,4,-.218,.09,.06,-.154,.154,.06,.005,
GW81,4,.094,.094,-.242,0.,.094,-.242,.007,
GW82,4,.094,0.,-.242,0.,0.,-.242,.007,
GW83,4,-.094,.094,-.242,0.,.094,-.242,.007,
GW84,4,0.,0.,-.242,-.094,0.,-.242,.007,
GW85,4,.094,.094,-.242,.094,0.,-.242,.007,
GW86,4,0.,.094,-.242,0.,0.,-.242,.007,
GW87,4,.094,-.094,-.242,.094,0.,-.242,.007,
GW88,4,0.,0.,-.242,0.,-.094,-.242,.007,
GW89,4,.094,-.094,-.242,0.,-.094,-.242,.007,
GW90,4,.092,-.156,-.175,0.,-.156,-.175,.007,
GW91,4,-.094,-.094,-.242,0.,-.094,-.242,.007,
GW92,4,0.,-.156,-.175,-.092,-.156,-.175,.007,
GW93,4,.094,-.094,-.242,.092,-.156,-.175,.005,
GW94,4,0.,-.094,-.242,0.,-.156,-.175,.007,
GW95,4,-.094,-.094,-.242,-.092,-.156,-.175,.005,
GW96,4,.09,-.218,-.108,.092,-.156,-.175,.005,
GW97,4,0.,-.156,-.175,0.,-.218,-.108,.007,
GW98,4,-.09,-.218,-.108,-.092,-.156,-.175,.005,
GW99,4,-.094,-.094,-.242,-.094,0.,-.242,.007,
GW100,4,-.156,-.092,-.175,-.156,0.,-.175,.007,
GW101,4,-.094,.094,-.242,-.094,0.,-.242,.007,
GW102,4,-.156,0.,-.175,-.156,.092,-.175,.007,
GW103,4,-.094,-.094,-.242,-.156,-.092,-.175,.005,
GW104,4,-.094,0.,-.242,-.156,0.,-.175,.007,
GW105,4,-.094,.094,-.242,-.156,.092,-.175,.005,
GW106,4,-.218,-.09,-.108,-.156,-.092,-.175,.005,
GW107,4,-.156,0.,-.175,-.218,0.,-.108,.007,
GW108,4,-.218,.09,-.108,-.156,.092,-.175,.005,
GW109,4,.094,0.,.194,0.,0.,.194,.007,
GW110,4,.094,.094,.194,0.,.094,.194,.007,
GW111,4,0.,0.,.194,-.094,0.,.194,.007,
GW112,4,-.094,.094,.194,0.,.094,.194,.007,
GW113,4,.094,-.094,.194,.094,0.,.194,.007,
GW114,4,0.,0.,.194,0.,-.094,.194,.007,
GW115,4,.094,.094,.194,.094,0.,.194,.007,
GW116,4,0.,.094,.194,0.,0.,.194,.007,
GW117,4,.094,-.094,.194,.092,-.156,.127,.005,
GW118,4,0.,-.094,.194,0.,-.156,.127,.007,
GW119,4,-.094,-.094,.194,-.092,-.156,.127,.005,
GW120,4,.09,-.218,.06,.092,-.156,.127,.005,
GW121,4,0.,-.156,.127,0.,-.218,.06,.007,
GW122,4,-.09,-.218,.06,-.092,-.156,.127,.005,
GW123,4,.094,-.094,.194,0.,-.094,.194,.007,
GW124,4,.092,-.156,.127,0.,-.156,.127,.007,
GW125,4,-.094,-.094,.194,0.,-.094,.194,.007,
GW126,4,0.,-.156,.127,-.092,-.156,.127,.007,
GW127,4,.09,-.218,-.108,.09,-.218,-.024,.007,
GW128,4,0.,-.218,-.108,0.,-.218,-.024,.007,
GW129,4,.09,-.218,.06,.09,-.218,-.024,.007,
GW130,4,0.,-.218,.06,0.,-.218,-.024,.007,
GW131,4,.09,-.218,-.108,0.,-.218,-.108,.007,
```

```
GW132,4,.09,-.218,-.024,0.,-.218,-.024,.007,
GW133,4,.09,-.218,.06,0.,-.218,.06,.007,
GW134,4,-.09,-.218,-.108,0.,-.218,-.108,.007,
GW135,4,0.,-.218,-.024,-.09,-.218,-.024,.007,
GW136,4,-.09,-.218,.06,0.,-.218,.06,.007,
GW137,4,-.09,-.218,.06,-.154,-.154,.06,.005,
GW138,4,-.09,-.218,-.024,-.154,-.154,-.024,.007,
GW139,4,-.09,-.218,-.108,-.154,-.154,-.108,.005,
GW140,4,-.218,-.09,.06,-.154,-.154,.06,.005,
GW141,4,-.154,-.154,-.024,-.218,-.09,-.024,.007,
GW142,4,-.218,-.09,-.108,-.154,-.154,-.108,.005,
GW143,4,-.09,-.218,.06,-.09,-.218,-.024,.007,
GW144,4,-.154,-.154,.06,-.154,-.154,-.024,.007,
GW145,4,-.09,-.218,-.108,-.09,-.218,-.024,.007,
GW146,4,-.154,-.154,-.024,-.154,-.154,-.108,.007,
GW147,4,-.094,-.094,.194,-.094,0.,.194,.007,
GW148,4,-.156,-.092,.127,-.156,0.,.127,.007,
GW149,4,-.094,.094,.194,-.094,0.,.194,.007,
GW150,4,-.156,0.,.127,-.156,.092,.127,.007,
GW151,4,-.094,-.094,.194,-.156,-.092,.127,.005,
GW152,4,-.094,0.,.194,-.156,0.,.127,.007,
GW153,4,-.094,.094,.194,-.156,.092,.127,.005,
GW154,4,-.218,-.09,.06,-.156,-.092,.127,.007,
GW155,4,-.156,0.,.127,-.218,0.,.06,.005,
GW156,4,-.218,.09,.06,-.156,.092,.127,.005,
GW157,4,-.218,-.09,.06,-.218,0.,.06,.007,
GW158,4,-.218,-.09,-.024,-.218,0.,-.024,.007,
GW159,4,-.218,-.09,-.108,-.218,0.,-.108,.007,
GW160,4,-.218,.09,.06,-.218,0.,.06,.007,
GW161,4,-.218,.09,-.024,-.218,0.,-.024,.007,
GW162,4,-.218,.09,-.108,-.218,0.,-.108,.007,
GW163,4,-.218,-.09,.06,-.218,-.09,-.024,.007,
GW164,4,-.218,0.,.06,-.218,0.,-.024,.007,
GW165,4,-.218,.09,.06,-.218,.09,-.024,.007,
GW166,4,-.218,-.09,-.108,-.218,-.09,-.024,.007,
GW167,4,-.218,0.,-.108,-.218,0.,-.024,.007,
GW168,4,-.218,.09,-.108,-.218,.09,-.024,.007,
GW169,3,.092,-.156,.127,.124,-.123,.127,.003,
GW170,3,.156,-.092,.127,.124,-.123,.127,.003,
GW171,4,.154,-.154,.06,.124,-.123,.127,.006,
GW172,3,.156,.092,.127,.124,.124,.128,.003,
GW173,4,.154,.154,.06,.124,.124,.128,.006,
GW174,3,.092,.156,.127,.124,.124,.128,.003,
GW175,3,-.092,.156,.127,-.124,.124,.127,.003,
GW176,3,-.156,.092,.127,-.124,.124,.127,.003,
GW177,4,-.154,.154,.06,-.124,.124,.127,.006,
GW178,3,-.156,-.092,.127,-.124,-.124,.127,.003,
GW179,4,-.154,-.154,.06,-.124,-.124,.127,.006,
GW180,3,-.092,-.156,.127,-.124,-.124,.127,.003,
GW181,3,.092,-.156,-.175,.124,-.123,-.175,.003,
GW182,4,.154,-.154,-.108,.124,-.123,-.175,.006,
GW183,3,.156,-.092,-.175,.124,-.123,-.175,.003,
GW184,3,-.156,.092,-.175,-.123,.125,-.175,.003,
GW185,4,-.154,.154,-.108,-.123,.125,-.175,.006,
GW186,3,-.092,.156,-.175,-.123,.125,-.175,.003,
GW187,3,.092,.156,-.175,.122,.126,-.175,.003,
GW188,4,.154,.154,-.108,.122,.126,-.175,.006,
GW189,3,.156,.092,-.175,.122,.126,-.175,.003,
GW190,3,-.156,-.092,-.175,-.124,-.124,-.175,.003,
GW191,4,-.154,-.154,-.108,-.124,-.124,-.175,.006,
GW192,3,-.092,-.156,-.175,-.124,-.124,-.175,.003,
GW193,5,.124,-.123,.127,.242,-.123,.246,.0032,
GW194,5,.124,.124,.128,.124,.242,.247,.0032,
GW195,5,-.124,-.124,.127,-.124,-.242,.246,.0032,
GW196,5,-.124,.124,.127,-.242,.124,.246,.0032,
GE0,0,0,
FR0,1,0,0,437.25,0.,
EX0,193,2,00,1.,
EX0,194,2,00,0.,1.,
```

```
EX0,195,2,00,0.,-1.,
EX0,196,2,00,-1.,
RP0,37,19,0011,0.,0.,5.,5.,0.,0.,
EN
```

B. TANGENTIAL TURNSTILE ANTENNA, NEC OUTPUT FILE

```
**********************************************
   NUMERICAL ELECTROMAGNETICS CODE (NPG1000)
**********************************************

VERSION - LAHEY DOUBLE W/SAVES   DATE:05/04/91   TIME:13:52:15.84


        - - - - COMMENTS - - - -

PANSAT WITH A TANGENITAL TURNSTILE ANTENNA, L=.167


        - - - STRUCTURE SPECIFICATION - - -

        COORDINATES MUST BE INPUT IN
        METERS OR BE SCALED TO METERS
        BEFORE STRUCTURE INPUT IS ENDED

 WIRE                                                                NO. OF  FIRST  LAST   TAG
 NO.        X1         Y1         Z1         X2         Y2         Z2        RADIUS  SEG.   SEG.  SEG.   NO.
    1    0.21800    0.00000   -0.10800    0.21800    0.00000   -0.02400   0.00700     4      1     4      1
    2    0.21800    0.00000   -0.02400    0.21800    0.00000    0.06000   0.00700     4      5     8      2
    3    0.21800    0.00000   -0.02400    0.21800   -0.09000   -0.02400   0.00700     4      9    12      3
    .
    . (OMITTED TO SAVE SPACE)
    .
  193    0.12400   -0.12300    0.12700    0.24200   -0.12300    0.24600   0.00320     5    753   757    193
  194    0.12400    0.12400    0.12800    0.12400    0.24200    0.24700   0.00320     5    758   762    194
  195   -0.12400   -0.12400    0.12700   -0.12400   -0.24200    0.24600   0.00320     5    763   767    195
  196   -0.12400    0.12400    0.12700   -0.24200    0.12400    0.24600   0.00320     5    768   772    196

 TOTAL SEGMENTS USED=  772     NO. SEG. IN A SYMMETRIC CELL=  772     SYMMETRY FLAG=  0


      - MULTIPLE WIRE JUNCTIONS -
JUNCTION    SEGMENTS  (- FOR END 1, + FOR END 2)
    1         -1   60   68  -77
    2          4   -5   -9  -13
    3          8   20   28  -37
    .
    . (OMITTED TO SAVE SPACE)
    .
   96        725  729  732
   97        735  739  742
   98        745  749  752


        - - - - SEGMENTATION DATA - - - -

        COORDINATES IN METERS

     I+ AND I- INDICATE THE SEGMENTS BEFORE AND AFTER I
```

SEG. NO.	COORDINATES OF SEG. CENTER X	Y	Z	SEG. LENGTH	ORIENTATION ANGLES ALPHA	BETA	WIRE RADIUS	CONNECTION I-	I	I+	TAG NO.
1	0.21800	0.00000	-0.09750	0.02100	90.00000	0.00000	0.00700	60	1	2	1
2	0.21800	0.00000	-0.07650	0.02100	90.00000	0.00000	0.00700	1	2	3	1
3	0.21800	0.00000	-0.05550	0.02100	90.00000	0.00000	0.00700	2	3	4	1
.											
.	(OMITTED TO SAVE SPACE)										
.											
769	-0.15940	0.12400	0.16270	0.03352	45.24175	180.00000	0.00320	768	769	770	196
770	-0.18300	0.12400	0.18650	0.03352	45.24175	180.00000	0.00320	769	770	771	196
771	-0.20660	0.12400	0.21030	0.03352	45.24175	180.00000	0.00320	770	771	772	196
772	-0.23020	0.12400	0.23410	0.03352	45.24175	180.00000	0.00320	771	772	0	196

***** DATA CARD NO.	1	FR	0	1	0	0	0.43725E+03	0.00000E+00	0.00000E+00	0.00000E+00	0.00000E+00	0.00000E+00
***** DATA CARD NO.	2	EX	0	193	2	0	0.10000E+01	0.00000E+00	0.00000E+00	0.00000E+00	0.00000E+00	0.00000E+00
***** DATA CARD NO.	3	EX	0	194	2	0	0.00000E+00	0.10000E+01	0.00000E+00	0.00000E+00	0.00000E+00	0.00000E+00
***** DATA CARD NO.	4	EX	0	195	2	0	0.00000E+00	-0.10000E+01	0.00000E+00	0.00000E+00	0.00000E+00	0.00000E+00
***** DATA CARD NO.	5	EX	0	196	2	0	-0.10000E+01	0.00000E+00	0.00000E+00	0.00000E+00	0.00000E+00	0.00000E+00
***** DATA CARD NO.	6	RP	0	37	19	11	0.00000E+00	0.00000E+00	0.50000E+01	0.50000E+01	0.00000E+00	0.00000E+00

MATRIX FILE STORAGE - NO. BLOCKS= 14 COLUMNS PER BLOCK= 58 COLUMNS IN LAST BLOCK= 18

- - - - - - FREQUENCY - - - - - -

FREQUENCY= 0.4373E+03 MHZ
WAVELENGTH= 0.6856E+00 METERS

- - - STRUCTURE IMPEDANCE LOADING - - -

THIS STRUCTURE IS NOT LOADED

- - - ANTENNA ENVIRONMENT - - -

FREE SPACE

APPROXIMATE INTEGRATION EMPLOYED FOR SEGMENTS MORE THAN 0.686 METERS APART
CP TIME TAKEN FOR FACTORIZATION = 0.12100E+01

- - - MATRIX TIMING - - -

FILL= 1684.130 SEC., FACTOR= 5606.080 SEC.

- - - ANTENNA INPUT PARAMETERS - - -

TAG NO.	SEG. NO.	VOLTAGE (VOLTS) REAL	IMAG.	CURRENT (AMPS) REAL	IMAG.	IMPEDANCE (OHMS) REAL	IMAG.	ADMITTANCE (MHOS) REAL	IMAG.	POWER (WATTS)
193	754	0.10000E+01	0.00000E+00	0.13924E-01	0.49632E-04	0.71820E+02	-0.25601E+00	0.13924E-01	0.49632E-04	0.69618E-02
194	759	0.00000E+00	0.10000E+01	0.10136E-03	0.13747E-01	0.72738E+02	0.53631E+00	0.13747E-01	-0.10136E-03	0.68736E-02
195	764	0.00000E+00	-0.10000E+01	0.64693E-04	-0.13863E-01	0.72132E+02	-0.33661E+00	0.13863E-01	0.64693E-04	0.69316E-02

196 769-0.10000E+01 0.00000E+00-0.13757E-01 0.14889E-04 0.72688E+02 0.78667E-01 0.13757E-01-0.14889E-04 0.68787E-02

- - - CURRENTS AND LOCATION - - -

LENGTHS NORMALIZED BY WAVELENGTH (OR 2.*PI/CABS(K))

SEG. NO.	TAG NO.	COORD. OF SEG. CENTER X	Y	Z	SEG. LENGTH	- - - CURRENT (AMPS) - - - REAL	IMAG.	MAG.	PHASE
1	1	0.3179	0.0000	-0.1422	0.03063	0.1281E-03	-0.1266E-02	0.1273E-02	-84.226
2	1	0.3179	0.0000	-0.1116	0.03063	0.2565E-03	-0.1289E-02	0.1314E-02	-78.746
3	1	0.3179	0.0000	-0.0809	0.03063	0.4071E-03	-0.1284E-02	0.1347E-02	-72.409
.									
. (OMITTED TO SAVE SPACE)									
.									
770	196	-0.2669	0.1809	0.2720	0.04888	-0.1133E-01	0.7169E-03	0.1135E-01	176.378
771	196	-0.3013	0.1809	0.3067	0.04888	-0.7913E-02	0.9319E-03	0.7968E-02	173.284
772	196	-0.3357	0.1809	0.3414	0.04888	-0.3432E-02	0.5437E-03	0.3475E-02	170.997

- - - POWER BUDGET - - -

INPUT POWER = 0.2765E-01 WATTS
RADIATED POWER= 0.2765E-01 WATTS
STRUCTURE LOSS= 0.0000E+00 WATTS
NETWORK LOSS = 0.0000E+00 WATTS
EFFICIENCY = 100.00 PERCENT

- - - RADIATION PATTERNS - - -

- - ANGLES - - THETA DEGREES	PHI DEGREES	- DIRECTIVE GAINS - MAJOR DB	MINOR DB	TOTAL DB	- - - POLARIZATION - - - AXIAL RATIO	TILT DEG.	SENSE	- - - E(THETA) - - - MAGNITUDE VOLTS/M	PHASE DEGREES	- - - E(PHI) - - - MAGNITUDE VOLTS/M	PHASE DEGREES
0.00	0.00	-1.92	-1.97	1.06	0.99495	-9.33	LEFT	0.10316E+01	-9.36	0.10266E+01	80.73
5.00	0.00	-1.93	-2.02	1.03	0.98968	-30.78	LEFT	0.10278E+01	-10.10	0.10227E+01	80.42
10.00	0.00	-1.93	-2.21	0.94	0.96747	-38.85	LEFT	0.10182E+01	-12.35	0.10111E+01	79.50
15.00	0.00	-1.92	-2.53	0.80	0.93145	-40.25	LEFT	0.10036E+01	-16.03	0.99194E+00	77.98
20.00	0.00	-1.91	-2.98	0.60	0.88495	-40.38	LEFT	0.98471E+00	-21.01	0.96566E+00	75.89
25.00	0.00	-1.93	-3.54	0.35	0.83114	-40.13	LEFT	0.96202E+00	-27.14	0.93270E+00	73.25
30.00	0.00	-1.99	-4.23	0.04	0.77265	-39.77	LEFT	0.93552E+00	-34.29	0.89360E+00	70.09
35.00	0.00	-2.10	-5.06	-0.32	0.71106	-39.41	LEFT	0.90481E+00	-42.38	0.84893E+00	66.45
40.00	0.00	-2.26	-6.05	-0.75	0.64661	-39.08	LEFT	0.86973E+00	-51.43	0.79934E+00	62.34
45.00	0.00	-2.49	-7.25	-1.24	0.57816	-38.73	LEFT	0.83121E+00	-61.55	0.74553E+00	57.78
50.00	0.00	-2.76	-8.71	-1.77	0.50373	-38.20	LEFT	0.79237E+00	-73.00	0.68830E+00	52.75
55.00	0.00	-3.03	-10.53	-2.32	0.42172	-37.24	LEFT	0.75943E+00	-86.01	0.62861E+00	47.20
60.00	0.00	-3.25	-12.79	-2.79	0.33326	-35.47	LEFT	0.74172E+00	-100.59	0.56767E+00	40.99
65.00	0.00	-3.31	-15.53	-3.06	0.24507	-32.59	LEFT	0.74972E+00	-116.21	0.50707E+00	33.91
70.00	0.00	-3.14	-18.53	-3.02	0.17003	-28.56	LEFT	0.79068E+00	-131.76	0.44899E+00	25.60
75.00	0.00	-2.69	-21.02	-2.63	0.12125	-23.89	LEFT	0.86466E+00	-146.03	0.39650E+00	15.59
80.00	0.00	-2.01	-21.77	-1.96	0.10271	-19.42	LEFT	0.96433E+00	-158.32	0.35396E+00	3.37
85.00	0.00	-1.21	-20.54	-1.16	0.10803	-15.83	LEFT	0.10781E+01	-168.61	0.32698E+00	-11.22
90.00	0.00	-0.43	-18.29	-0.36	0.12791	-13.34	LEFT	0.11931E+01	-177.21	0.32121E+00	-27.29
95.00	0.00	0.25	-15.90	0.35	0.15587	-11.89	LEFT	0.12966E+01	175.46	0.33950E+00	-42.93
100.00	0.00	0.75	-13.72	0.90	0.18896	-11.40	LEFT	0.13770E+01	168.99	0.38020E+00	-56.34
105.00	0.00	1.05	-11.85	1.27	0.22652	-11.84	LEFT	0.14240E+01	163.05	0.43895E+00	-66.90
110.00	0.00	1.13	-10.28	1.43	0.26877	-13.33	LEFT	0.14295E+01	157.33	0.51120E+00	-74.91
115.00	0.00	0.97	-9.06	1.38	0.31526	-16.24	LEFT	0.13878E+01	151.53	0.59324E+00	-80.98
120.00	0.00	0.59	-8.24	1.13	0.36155	-21.25	LEFT	0.12972E+01	145.27	0.68213E+00	-85.64
125.00	0.00	0.08	-8.06	0.70	0.39156	-29.29	LEFT	0.11603E+01	138.00	0.77530E+00	-89.30
130.00	0.00	-0.37	-9.01	0.19	0.36965	-40.28	LEFT	0.98646E+00	128.72	0.87035E+00	-92.24
135.00	0.00	-0.55	-12.14	-0.25	0.26317	-51.34	LEFT	0.79523E+00	115.45	0.96486E+00	-94.65
140.00	0.00	-0.44	-21.76	-0.41	0.08594	-59.56	LEFT	0.62663E+00	94.56	0.10565E+01	-96.65
145.00	0.00	-0.18	-18.44	-0.12	0.12221	-64.86	RIGHT	0.55329E+00	63.79	0.11430E+01	-98.33
150.00	0.00	0.12	-9.49	0.57	0.33100	-68.19	RIGHT	0.62913E+00	33.13	0.12221E+01	-99.72

155.00	0.00	0.41	-5.22	1.46	0.52324	-70.28	RIGHT	0.80553E+00	12.92	0.12922E+01	-100.88
160.00	0.00	0.66	-2.57	2.35	0.68931	-71.50	RIGHT	0.10090E+01	1.10	0.13514E+01	-101.80
165.00	0.00	0.86	-0.83	3.10	0.82337	-71.96	RIGHT	0.11961E+01	-5.94	0.13986E+01	-102.51
170.00	0.00	1.00	0.29	3.67	0.92160	-71.17	RIGHT	0.13431E+01	-10.14	0.14327E+01	-103.00
175.00	0.00	1.08	0.92	4.01	0.98096	-63.97	RIGHT	0.14359E+01	-12.42	0.14530E+01	-103.29
180.00	0.00	1.14	1.08	4.12	0.99363	-16.62	RIGHT	0.14670E+01	-13.17	0.14592E+01	-103.37
0.00	5.00	-1.92	-1.97	1.06	0.99495	-14.33	LEFT	0.10314E+01	-4.38	0.10268E+01	85.76
5.00	5.00	-1.93	-2.03	1.03	0.98826	-30.56	LEFT	0.10282E+01	-5.14	0.10224E+01	85.46
10.00	5.00	-1.91	-2.23	0.94	0.96409	-36.31	LEFT	0.10202E+01	-7.42	0.10092E+01	84.58
15.00	5.00	-1.89	-2.57	0.80	0.92505	-37.29	LEFT	0.10081E+01	-11.17	0.98744E+00	83.13
20.00	5.00	-1.87	-3.04	0.60	0.87429	-37.27	LEFT	0.99233E+00	-16.25	0.95762E+00	81.15
25.00	5.00	-1.87	-3.65	0.34	0.81497	-36.93	LEFT	0.97336E+00	-22.52	0.92022E+00	78.68
30.00	5.00	-1.90	-4.40	0.04	0.74973	-36.48	LEFT	0.95099E+00	-29.86	0.87581E+00	75.74
35.00	5.00	-1.98	-5.33	-0.33	0.68023	-36.00	LEFT	0.92474E+00	-38.18	0.82509E+00	72.40
40.00	5.00	-2.12	-6.46	-0.76	0.60684	-35.51	LEFT	0.89442E+00	-47.51	0.76879E+00	68.70
45.00	5.00	-2.32	-7.86	-1.25	0.52872	-34.95	LEFT	0.86097E+00	-57.95	0.70770E+00	64.66
50.00	5.00	-2.57	-9.62	-1.79	0.44432	-34.16	LEFT	0.82758E+00	-69.70	0.64274E+00	60.31
55.00	5.00	-2.83	-11.88	-2.32	0.35275	-32.89	LEFT	0.80044E+00	-82.93	0.57494E+00	55.61
60.00	5.00	-3.04	-14.86	-2.76	0.25627	-30.78	LEFT	0.78864E+00	-97.60	0.50554E+00	50.44
65.00	5.00	-3.10	-18.84	-2.99	0.16328	-27.50	LEFT	0.80203E+00	-113.14	0.43602E+00	44.59
70.00	5.00	-2.92	-23.98	-2.88	0.08850	-23.07	LEFT	0.84708E+00	-128.52	0.36826E+00	37.59
75.00	5.00	-2.45	-29.32	-2.44	0.04532	-18.12	LEFT	0.92329E+00	-142.65	0.30493E+00	28.61
80.00	5.00	-1.75	-30.81	-1.74	0.03523	-13.61	LEFT	0.10232E+01	-154.95	0.25027E+00	16.28
85.00	5.00	-0.95	-27.21	-0.94	0.04868	-10.19	LEFT	0.11354E+01	-165.36	0.21151E+00	-1.01
90.00	5.00	-0.19	-22.71	-0.17	0.07487	-8.01	LEFT	0.12468E+01	-174.16	0.19863E+00	-22.79
95.00	5.00	0.44	-18.95	0.49	0.10728	-6.90	LEFT	0.13449E+01	178.28	0.21747E+00	-44.03
100.00	5.00	0.90	-15.96	0.99	0.14348	-6.73	LEFT	0.14184E+01	171.58	0.26338E+00	-59.97
105.00	5.00	1.15	-13.59	1.29	0.18336	-7.44	LEFT	0.14574E+01	165.42	0.32791E+00	-70.51
110.00	5.00	1.16	-11.69	1.38	0.22771	-9.14	LEFT	0.14544E+01	159.50	0.40524E+00	-77.36
115.00	5.00	0.94	-10.22	1.26	0.27670	-12.18	LEFT	0.14048E+01	153.49	0.49214E+00	-81.97
120.00	5.00	0.49	-9.23	0.93	0.32674	-17.25	LEFT	0.13077E+01	146.99	0.58643E+00	-85.26
125.00	5.00	-0.10	-8.91	0.43	0.36262	-25.35	LEFT	0.11668E+01	139.43	0.68613E+00	-87.74
130.00	5.00	-0.63	-9.82	-0.13	0.34719	-36.65	LEFT	0.99258E+00	129.76	0.78908E+00	-89.74
135.00	5.00	-0.84	-13.14	-0.59	0.24271	-48.29	LEFT	0.80610E+00	116.03	0.89283E+00	-91.41
140.00	5.00	-0.72	-24.78	-0.70	0.06269	-57.01	LEFT	0.64834E+00	94.99	0.99476E+00	-92.85
145.00	5.00	-0.42	-17.01	-0.33	0.14811	-62.60	RIGHT	0.58699E+00	65.54	0.10921E+01	-94.12
150.00	5.00	-0.07	-9.02	0.45	0.35661	-66.10	RIGHT	0.66424E+00	36.97	0.11824E+01	-95.22
155.00	5.00	0.27	-4.99	1.40	0.54551	-68.29	RIGHT	0.83353E+00	17.70	0.12629E+01	-96.17
160.00	5.00	0.57	-2.45	2.32	0.70623	-69.57	RIGHT	0.10283E+01	6.11	0.13317E+01	-96.96
165.00	5.00	0.80	-0.77	3.10	0.83430	-70.04	RIGHT	0.12078E+01	-0.91	0.13869E+01	-97.58
170.00	5.00	0.97	0.32	3.67	0.92718	-69.19	RIGHT	0.13488E+01	-5.14	0.14271E+01	-98.02
175.00	5.00	1.07	0.92	4.01	0.98284	-61.33	RIGHT	0.14378E+01	-7.44	0.14513E+01	-98.28
180.00	5.00	1.14	1.08	4.12	0.99363	-11.62	RIGHT	0.14674E+01	-8.20	0.14588E+01	-98.35
0.00	10.00	-1.92	-1.97	1.06	0.99495	-19.33	LEFT	0.10311E+01	0.60	0.10271E+01	90.78
5.00	10.00	-1.92	-2.04	1.03	0.98679	-31.33	LEFT	0.10285E+01	-0.18	0.10222E+01	90.50
10.00	10.00	-1.89	-2.25	0.94	0.95972	-35.21	LEFT	0.10217E+01	-2.53	0.10078E+01	89.69
15.00	10.00	-1.85	-2.61	0.80	0.91627	-35.82	LEFT	0.10115E+01	-6.38	0.98410E+00	88.37
20.00	10.00	-1.81	-3.12	0.60	0.85965	-35.73	LEFT	0.99824E+00	-11.62	0.95167E+00	86.57
25.00	10.00	-1.77	-3.79	0.35	0.79318	-35.39	LEFT	0.98213E+00	-18.10	0.91110E+00	84.35
30.00	10.00	-1.77	-4.63	0.04	0.71967	-34.97	LEFT	0.96290E+00	-25.69	0.86312E+00	81.77
35.00	10.00	-1.82	-5.69	-0.33	0.64087	-34.51	LEFT	0.94003E+00	-34.32	0.80854E+00	78.91
40.00	10.00	-1.93	-7.00	-0.75	0.55728	-34.02	LEFT	0.91335E+00	-44.01	0.74825E+00	75.84
45.00	10.00	-2.09	-8.68	-1.23	0.46820	-33.41	LEFT	0.88395E+00	-54.84	0.68322E+00	72.63
50.00	10.00	-2.31	-10.89	-1.75	0.37243	-32.53	LEFT	0.85518E+00	-66.98	0.61449E+00	69.38
55.00	10.00	-2.55	-13.93	-2.24	0.26970	-31.08	LEFT	0.83334E+00	-80.54	0.54322E+00	66.12
60.00	10.00	-2.74	-18.47	-2.62	0.16339	-28.69	LEFT	0.82731E+00	-95.39	0.47066E+00	62.88
65.00	10.00	-2.79	-26.71	-2.78	0.06372	-25.00	LEFT	0.84621E+00	-110.92	0.39811E+00	59.59
70.00	10.00	-2.61	-40.70	-2.61	0.01246	-20.04	RIGHT	0.89542E+00	-126.17	0.32687E+00	56.05
75.00	10.00	-2.14	-27.98	-2.13	0.05105	-14.59	RIGHT	0.97358E+00	-140.16	0.25823E+00	51.70
80.00	10.00	-1.46	-26.99	-1.44	0.05291	-9.79	RIGHT	0.10729E+01	-152.39	0.19366E+00	45.18
85.00	10.00	-0.69	-30.88	-0.69	0.03094	-6.33	RIGHT	0.11817E+01	-162.82	0.13615E+00	32.96
90.00	10.00	0.02	-52.74	0.02	0.00230	-4.25	LEFT	0.12873E+01	-171.69	0.95768E-01	6.53
95.00	10.00	0.60	-27.35	0.61	0.04002	-3.32	LEFT	0.13777E+01	-179.37	0.97137E-01	-34.08
100.00	10.00	1.00	-20.93	1.03	0.08009	-3.34	LEFT	0.14419E+01	173.82	0.14285E+00	-60.39
105.00	10.00	1.18	-17.03	1.25	0.12284	-4.22	LEFT	0.14709E+01	167.54	0.21076E+00	-71.99
110.00	10.00	1.13	-14.29	1.25	0.16949	-6.06	LEFT	0.14582E+01	161.48	0.29154E+00	-77.50
115.00	10.00	0.83	-12.29	1.04	0.22074	-9.17	LEFT	0.14001E+01	155.33	0.38262E+00	-80.53
120.00	10.00	0.31	-10.94	0.62	0.27381	-14.22	LEFT	0.12966E+01	148.67	0.48261E+00	-82.51
125.00	10.00	-0.36	-10.41	0.05	0.31457	-22.24	LEFT	0.11526E+01	140.85	0.58984E+00	-84.05

130.00	10.00	-0.96	-11.26	-0.57	0.30564	-33.60	LEFT	0.97962E+00	130.79	0.70206E+00	-85.39
135.00	10.00	-1.21	-14.98	-1.03	0.20496	-45.63	LEFT	0.80012E+00	116.53	0.81651E+00	-86.65
140.00	10.00	-1.07	-33.29	-1.07	0.02449	-54.81	LEFT	0.65609E+00	95.13	0.93008E+00	-87.85
145.00	10.00	-0.72	-15.30	-0.57	0.18654	-60.74	RIGHT	0.61052E+00	66.63	0.10395E+01	-88.99
150.00	10.00	-0.30	-8.43	0.32	0.39213	-64.45	RIGHT	0.69377E+00	39.97	0.11416E+01	-90.05
155.00	10.00	0.10	-4.70	1.34	0.57503	-66.77	RIGHT	0.85918E+00	21.87	0.12333E+01	-91.00
160.00	10.00	0.46	-2.30	2.30	0.72797	-68.13	RIGHT	0.10468E+01	10.76	0.13119E+01	-91.82
165.00	10.00	0.74	-0.69	3.09	0.84803	-68.63	RIGHT	0.12191E+01	3.93	0.13753E+01	-92.48
170.00	10.00	0.94	0.35	3.67	0.93409	-67.71	RIGHT	0.13543E+01	-0.22	0.14216E+01	-92.96
175.00	10.00	1.06	0.93	4.01	0.98512	-58.96	RIGHT	0.14395E+01	-2.48	0.14496E+01	-93.24
180.00	10.00	1.14	1.08	4.12	0.99363	-6.62	RIGHT	0.14676E+01	-3.23	0.14585E+01	-93.32
0.00	15.00	-1.92	-1.97	1.06	0.99495	-24.33	LEFT	0.10308E+01	5.58	0.10274E+01	95.80
5.00	15.00	-1.91	-2.04	1.03	0.98535	-32.84	LEFT	0.10285E+01	4.78	0.10222E+01	95.55
10.00	15.00	-1.87	-2.27	0.94	0.95506	-35.32	LEFT	0.10226E+01	2.34	0.10071E+01	94.83
15.00	15.00	-1.81	-2.66	0.80	0.90669	-35.67	LEFT	0.10135E+01	-1.65	0.98234E+00	93.66
20.00	15.00	-1.73	-3.21	0.60	0.84377	-35.55	LEFT	0.10018E+01	-7.08	0.94858E+00	92.10
25.00	15.00	-1.67	-3.94	0.35	0.76995	-35.27	LEFT	0.98736E+00	-13.80	0.90659E+00	90.20
30.00	15.00	-1.64	-4.88	0.05	0.68827	-34.94	LEFT	0.96999E+00	-21.69	0.85730E+00	88.06
35.00	15.00	-1.65	-6.08	-0.31	0.60061	-34.58	LEFT	0.94913E+00	-30.67	0.80174E+00	85.77
40.00	15.00	-1.72	-7.61	-0.72	0.50752	-34.17	LEFT	0.92471E+00	-40.75	0.74105E+00	83.45
45.00	15.00	-1.85	-9.63	-1.18	0.40834	-33.63	LEFT	0.89804E+00	-52.02	0.67643E+00	81.24
50.00	15.00	-2.03	-12.43	-1.65	0.30204	-32.77	LEFT	0.87276E+00	-64.60	0.60921E+00	79.26
55.00	15.00	-2.24	-16.73	-2.09	0.18870	-31.29	LEFT	0.85536E+00	-78.55	0.54080E+00	77.66
60.00	15.00	-2.42	-25.23	-2.40	0.07237	-28.76	LEFT	0.85454E+00	-93.64	0.47266E+00	76.58
65.00	15.00	-2.48	-31.49	-2.48	0.03546	-24.75	RIGHT	0.87860E+00	-109.23	0.40622E+00	76.11
70.00	15.00	-2.32	-21.04	-2.26	0.11584	-19.26	RIGHT	0.93168E+00	-124.38	0.34262E+00	76.29
75.00	15.00	-1.87	-18.17	-1.77	0.15309	-13.16	RIGHT	0.10113E+01	-138.22	0.28250E+00	77.04
80.00	15.00	-1.22	-17.73	-1.12	0.14934	-7.87	RIGHT	0.11090E+01	-150.32	0.22566E+00	78.06
85.00	15.00	-0.49	-18.87	-0.43	0.12057	-4.17	RIGHT	0.12132E+01	-160.69	0.17093E+00	78.65
90.00	15.00	0.17	-21.63	0.19	0.08131	-2.03	RIGHT	0.13115E+01	-169.55	0.11636E+00	77.03
95.00	15.00	0.68	-27.52	0.69	0.03890	-1.15	RIGHT	0.13924E+01	-177.24	0.60935E-01	65.56
100.00	15.00	1.01	-45.74	1.01	0.00460	-1.25	LEFT	0.14459E+01	175.92	0.32346E-01	-15.95
105.00	15.00	1.12	-24.94	1.13	0.04978	-2.24	LEFT	0.14639E+01	169.60	0.92677E-01	-62.34
110.00	15.00	1.00	-19.16	1.04	0.09817	-4.17	LEFT	0.14408E+01	163.51	0.17618E+00	-70.29
115.00	15.00	0.64	-15.79	0.73	0.15084	-7.34	LEFT	0.13741E+01	157.30	0.27245E+00	-73.33
120.00	15.00	0.04	-13.70	0.22	0.20563	-12.36	LEFT	0.12649E+01	150.52	0.37976E+00	-75.23
125.00	15.00	-0.70	-12.76	-0.44	0.24943	-20.25	LEFT	0.11189E+01	142.50	0.49614E+00	-76.83
130.00	15.00	-1.37	-13.56	-1.11	0.24566	-31.48	LEFT	0.94859E+00	132.06	0.61890E+00	-78.36
135.00	15.00	-1.65	-18.14	-1.55	0.14972	-43.70	LEFT	0.77779E+00	117.17	0.74481E+00	-79.88
140.00	15.00	-1.48	-32.38	-1.48	0.02851	-53.28	RIGHT	0.64957E+00	95.22	0.87024E+00	-81.37
145.00	15.00	-1.06	-13.58	-0.83	0.23658	-59.54	RIGHT	0.62241E+00	67.35	0.99144E+00	-82.81
150.00	15.00	-0.57	-7.77	0.19	0.43611	-63.50	RIGHT	0.71509E+00	42.41	0.11047E+01	-84.15
155.00	15.00	-0.09	-4.38	1.29	0.61023	-65.99	RIGHT	0.87980E+00	25.56	0.12067E+01	-85.36
160.00	15.00	0.33	-2.13	2.28	0.75318	-67.46	RIGHT	0.10624E+01	15.10	0.12943E+01	-86.39
165.00	15.00	0.67	-0.61	3.09	0.86367	-68.02	RIGHT	0.12288E+01	8.60	0.13651E+01	-87.23
170.00	15.00	0.91	0.39	3.66	0.94189	-67.05	RIGHT	0.13591E+01	4.63	0.14168E+01	-87.83
175.00	15.00	1.05	0.95	4.01	0.98774	-57.15	RIGHT	0.14409E+01	2.46	0.14482E+01	-88.19
180.00	15.00	1.14	1.08	4.12	0.99363	-1.62	RIGHT	0.14678E+01	1.74	0.14584E+01	-88.28
0.00	20.00	-1.92	-1.97	1.06	0.99495	-29.33	LEFT	0.10305E+01	10.56	0.10278E+01	100.81
5.00	20.00	-1.91	-2.05	1.03	0.98405	-34.87	LEFT	0.10283E+01	9.73	0.10225E+01	100.60
10.00	20.00	-1.85	-2.29	0.94	0.95060	-36.33	LEFT	0.10226E+01	7.20	0.10073E+01	99.97
15.00	20.00	-1.77	-2.70	0.80	0.89750	-36.50	LEFT	0.10139E+01	3.06	0.98243E+00	98.97
20.00	20.00	-1.67	-3.30	0.60	0.82869	-36.38	LEFT	0.10025E+01	-2.57	0.94878E+00	97.66
25.00	20.00	-1.57	-4.09	0.36	0.74822	-36.18	LEFT	0.98849E+00	-9.55	0.90732E+00	96.11
30.00	20.00	-1.50	-5.12	0.06	0.65942	-35.96	LEFT	0.97152E+00	-17.75	0.85922E+00	94.41
35.00	20.00	-1.48	-6.45	-0.28	0.56428	-35.73	LEFT	0.95112E+00	-27.09	0.80580E+00	92.71
40.00	20.00	-1.52	-8.20	-0.67	0.46332	-35.47	LEFT	0.92739E+00	-37.58	0.74846E+00	91.12
45.00	20.00	-1.61	-10.59	-1.10	0.35590	-35.07	LEFT	0.90194E+00	-49.29	0.68873E+00	89.80
50.00	20.00	-1.77	-14.13	-1.52	0.24096	-34.34	LEFT	0.87876E+00	-62.33	0.62819E+00	88.89
55.00	20.00	-1.96	-20.47	-1.90	0.11864	-32.97	LEFT	0.86465E+00	-76.69	0.56846E+00	88.54
60.00	20.00	-2.13	-45.32	-2.13	0.00692	-30.48	RIGHT	0.86811E+00	-92.07	0.51107E+00	88.83
65.00	20.00	-2.20	-20.34	-2.14	0.12395	-26.37	RIGHT	0.89660E+00	-107.78	0.45726E+00	89.78
70.00	20.00	-2.08	-15.55	-1.88	0.21202	-20.46	RIGHT	0.95289E+00	-122.86	0.40763E+00	91.27
75.00	20.00	-1.68	-13.62	-1.41	0.25274	-13.68	RIGHT	0.10332E+01	-136.55	0.36182E+00	93.06
80.00	20.00	-1.07	-13.20	-0.81	0.24754	-7.72	RIGHT	0.11286E+01	-148.50	0.31833E+00	94.72
85.00	20.00	-0.40	-13.76	-0.20	0.21479	-3.60	RIGHT	0.12272E+01	-158.73	0.27461E+00	95.73
90.00	20.00	0.20	-15.12	0.33	0.17134	-1.27	RIGHT	0.13173E+01	-167.50	0.22757E+00	95.37
95.00	20.00	0.65	-17.37	0.72	0.12550	-0.33	RIGHT	0.13879E+01	-175.11	0.17437E+00	92.28
100.00	20.00	0.91	-21.08	0.94	0.07950	-0.47	RIGHT	0.14300E+01	178.11	0.11429E+00	82.24

105.00	20.00	0.96	-28.76	0.96	0.03267	-1.53	RIGHT	0.14367E+01	171.85	0.60653E-01	42.61
110.00	20.00	0.77	-34.79	0.77	0.01668	-3.55	LEFT	0.14036E+01	165.81	0.90204E-01	-29.28
115.00	20.00	0.34	-22.78	0.36	0.06985	-6.79	LEFT	0.13290E+01	159.63	0.18352E+00	-51.23
120.00	20.00	-0.32	-18.38	-0.25	0.12504	-11.84	LEFT	0.12150E+01	152.81	0.29642E+00	-59.51
125.00	20.00	-1.12	-16.51	-1.00	0.17003	-19.61	LEFT	0.10682E+01	144.63	0.42099E+00	-64.34
130.00	20.00	-1.83	-17.24	-1.71	0.16962	-30.66	LEFT	0.90165E+00	133.82	0.55310E+00	-67.89
135.00	20.00	-2.12	-24.18	-2.10	0.07893	-42.90	LEFT	0.74054E+00	118.23	0.68882E+00	-70.82
140.00	20.00	-1.92	-22.46	-1.88	0.09398	-52.78	RIGHT	0.62920E+00	95.50	0.82407E+00	-73.36
145.00	20.00	-1.42	-12.02	-1.06	0.29523	-59.39	RIGHT	0.62195E+00	67.97	0.95475E+00	-75.61
150.00	20.00	-0.84	-7.12	0.08	0.48528	-63.62	RIGHT	0.72651E+00	44.51	0.10769E+01	-77.59
155.00	20.00	-0.28	-4.05	1.24	0.64811	-66.32	RIGHT	0.89336E+00	28.93	0.11868E+01	-79.29
160.00	20.00	0.20	-1.96	2.27	0.77956	-67.95	RIGHT	0.10734E+01	19.22	0.12812E+01	-80.71
165.00	20.00	0.59	-0.52	3.08	0.87975	-68.61	RIGHT	0.12359E+01	13.15	0.13574E+01	-81.84
170.00	20.00	0.87	0.42	3.66	0.94989	-67.71	RIGHT	0.13625E+01	9.43	0.14133E+01	-82.64
175.00	20.00	1.04	0.96	4.01	0.99058	-56.58	RIGHT	0.14419E+01	7.38	0.14473E+01	-83.12
180.00	20.00	1.14	1.08	4.12	0.99363	3.38	RIGHT	0.14677E+01	6.70	0.14584E+01	-83.25
0.00	25.00	-1.92	-1.97	1.06	0.99495	-34.33	LEFT	0.10301E+01	15.55	0.10282E+01	105.82
5.00	25.00	-1.90	-2.05	1.03	0.98296	-37.27	LEFT	0.10278E+01	14.69	0.10231E+01	105.64
10.00	25.00	-1.83	-2.31	0.95	0.94673	-37.96	LEFT	0.10218E+01	12.07	0.10083E+01	105.11
15.00	25.00	-1.73	-2.75	0.80	0.88953	-38.00	LEFT	0.10125E+01	7.78	0.98438E+00	104.27
20.00	25.00	-1.61	-3.37	0.61	0.81575	-37.91	LEFT	0.10004E+01	1.95	0.95228E+00	103.19
25.00	25.00	-1.48	-4.22	0.37	0.72988	-37.79	LEFT	0.98540E+00	-5.28	0.91323E+00	101.95
30.00	25.00	-1.39	-5.33	0.08	0.63548	-37.69	LEFT	0.96733E+00	-13.77	0.86866E+00	100.65
35.00	25.00	-1.34	-6.77	-0.24	0.53463	-37.62	LEFT	0.94579E+00	-23.45	0.82014E+00	99.41
40.00	25.00	-1.34	-8.71	-0.61	0.42786	-37.53	LEFT	0.92109E+00	-34.32	0.76935E+00	98.37
45.00	25.00	-1.41	-11.46	-1.00	0.31442	-37.32	LEFT	0.89518E+00	-46.46	0.71797E+00	97.64
50.00	25.00	-1.54	-15.82	-1.38	0.19321	-36.82	LEFT	0.87253E+00	-59.96	0.66765E+00	97.34
55.00	25.00	-1.70	-25.55	-1.69	0.06425	-35.70	LEFT	0.86022E+00	-74.76	0.61985E+00	97.49
60.00	25.00	-1.87	-25.12	-1.85	0.06881	-33.48	RIGHT	0.86669E+00	-90.47	0.57566E+00	98.08
65.00	25.00	-1.97	-16.16	-1.80	0.19502	-29.55	RIGHT	0.89855E+00	-106.32	0.53552E+00	98.97
70.00	25.00	-1.89	-12.52	-1.53	0.29398	-23.54	RIGHT	0.95718E+00	-121.38	0.49895E+00	99.94
75.00	25.00	-1.57	-10.83	-1.08	0.34411	-16.16	RIGHT	0.10375E+01	-134.92	0.46451E+00	100.67
80.00	25.00	-1.03	-10.32	-0.55	0.34313	-9.41	RIGHT	0.11298E+01	-146.68	0.42982E+00	100.80
85.00	25.00	-0.42	-10.59	-0.03	0.31021	-4.68	RIGHT	0.12224E+01	-156.72	0.39204E+00	99.96
90.00	25.00	0.11	-11.42	0.41	0.26489	-2.02	RIGHT	0.13039E+01	-165.32	0.34841E+00	97.63
95.00	25.00	0.50	-12.76	0.70	0.21707	-0.96	RIGHT	0.13642E+01	-172.77	0.29699E+00	93.02
100.00	25.00	0.70	-14.72	0.82	0.16953	-1.10	RIGHT	0.13953E+01	-179.39	0.23805E+00	84.34
105.00	25.00	0.68	-17.61	0.75	0.12172	-2.24	RIGHT	0.13915E+01	174.52	0.17788E+00	67.00
110.00	25.00	0.43	-22.43	0.46	0.07191	-4.38	RIGHT	0.13494E+01	168.63	0.14175E+00	32.14
115.00	25.00	-0.05	-34.61	-0.05	0.01871	-7.75	RIGHT	0.12683E+01	162.57	0.17431E+00	-9.46
120.00	25.00	-0.75	-29.56	-0.75	0.03627	-12.89	LEFT	0.11510E+01	155.82	0.26670E+00	-33.66
125.00	25.00	-1.58	-23.37	-1.56	0.08140	-20.64	LEFT	0.10044E+01	147.57	0.38696E+00	-46.38
130.00	25.00	-2.31	-23.90	-2.28	0.08330	-31.52	LEFT	0.84227E+00	136.42	0.52053E+00	-54.24
135.00	25.00	-2.59	-60.77	-2.59	0.00123	-43.69	RIGHT	0.69080E+00	120.04	0.65999E+00	-59.82
140.00	25.00	-2.33	-17.97	-2.22	0.16521	-53.78	RIGHT	0.59615E+00	96.25	0.79987E+00	-64.14
145.00	25.00	-1.76	-10.74	-1.24	0.35557	-60.71	RIGHT	0.60917E+00	68.71	0.93537E+00	-67.64
150.00	25.00	-1.09	-6.55	0.00	0.53325	-65.24	RIGHT	0.72715E+00	46.50	0.10621E+01	-70.54
155.00	25.00	-0.45	-3.76	1.21	0.68348	-68.19	RIGHT	0.89860E+00	32.12	0.11762E+01	-72.93
160.00	25.00	0.09	-1.81	2.26	0.80340	-70.03	RIGHT	0.10786E+01	23.20	0.12743E+01	-74.86
165.00	25.00	0.53	-0.45	3.08	0.89400	-70.90	RIGHT	0.12395E+01	17.62	0.13534E+01	-76.35
170.00	25.00	0.84	0.46	3.66	0.95701	-70.32	RIGHT	0.13643E+01	14.18	0.14115E+01	-77.41
175.00	25.00	1.03	0.97	4.01	0.99343	-59.05	RIGHT	0.14424E+01	12.30	0.14468E+01	-78.04
180.00	25.00	1.14	1.08	4.12	0.99363	8.38	RIGHT	0.14676E+01	11.67	0.14586E+01	-78.22
0.00	30.00	-1.92	-1.97	1.06	0.99495	-39.33	LEFT	0.10296E+01	20.55	0.10286E+01	110.83
5.00	30.00	-1.90	-2.06	1.03	0.98211	-39.93	LEFT	0.10271E+01	19.66	0.10239E+01	110.67
10.00	30.00	-1.82	-2.32	0.95	0.94372	-40.00	LEFT	0.10203E+01	16.96	0.10101E+01	110.23
15.00	30.00	-1.70	-2.78	0.81	0.88334	-39.95	LEFT	0.10096E+01	12.54	0.98800E+00	109.52
20.00	30.00	-1.56	-3.43	0.62	0.80585	-39.88	LEFT	0.99561E+00	6.54	0.95868E+00	108.62
25.00	30.00	-1.42	-4.32	0.38	0.71608	-39.85	LEFT	0.97842E+00	-0.89	0.92358E+00	107.61
30.00	30.00	-1.30	-5.48	0.11	0.61781	-39.87	LEFT	0.95783E+00	-9.63	0.88433E+00	106.59
35.00	30.00	-1.22	-7.01	-0.20	0.51320	-39.96	LEFT	0.93361E+00	-19.60	0.84271E+00	105.65
40.00	30.00	-1.20	-9.10	-0.54	0.40274	-40.07	LEFT	0.90631E+00	-30.81	0.80047E+00	104.89
45.00	30.00	-1.24	-12.12	-0.90	0.28565	-40.10	LEFT	0.87824E+00	-43.34	0.75926E+00	104.39
50.00	30.00	-1.34	-17.21	-1.23	0.16080	-39.88	LEFT	0.85434E+00	-57.28	0.72049E+00	104.17
55.00	30.00	-1.48	-32.53	-1.48	0.02802	-39.12	LEFT	0.84213E+00	-72.52	0.68512E+00	104.20
60.00	30.00	-1.64	-20.84	-1.59	0.10970	-37.36	RIGHT	0.85004E+00	-88.59	0.65345E+00	104.37
65.00	30.00	-1.76	-14.04	-1.51	0.24318	-33.98	RIGHT	0.88392E+00	-104.64	0.62502E+00	104.50
70.00	30.00	-1.74	-10.76	-1.23	0.35410	-28.36	RIGHT	0.94383E+00	-119.71	0.59850E+00	104.38
75.00	30.00	-1.52	-9.07	-0.81	0.41921	-20.80	RIGHT	0.10234E+01	-133.11	0.57181E+00	103.75

80.00	30.00	-1.08	-8.42	-0.34	0.42970	-13.27	RIGHT	0.11123E+01	-144.66	0.54248E+00	102.37
85.00	30.00	-0.55	-8.47	0.10	0.40190	-7.76	RIGHT	0.11988E+01	-154.46	0.50797E+00	99.95
90.00	30.00	-0.08	-9.01	0.44	0.35771	-4.62	RIGHT	0.12720E+01	-162.79	0.46628E+00	96.14
95.00	30.00	0.25	-9.94	0.65	0.30945	-3.35	RIGHT	0.13229E+01	-169.98	0.41655E+00	90.34
100.00	30.00	0.39	-11.28	0.68	0.26102	-3.47	RIGHT	0.13444E+01	-176.34	0.36018E+00	81.51
105.00	30.00	0.32	-13.14	0.51	0.21226	-4.70	RIGHT	0.13318E+01	177.84	0.30310E+00	67.67
110.00	30.00	0.03	-15.80	0.14	0.16154	-7.01	RIGHT	0.12828E+01	172.22	0.26037E+00	46.08
115.00	30.00	-0.48	-19.85	-0.43	0.10751	-10.58	RIGHT	0.11974E+01	166.41	0.25807E+00	17.48
120.00	30.00	-1.20	-26.91	-1.19	0.05182	-15.90	RIGHT	0.10785E+01	159.86	0.31214E+00	-8.98
125.00	30.00	-2.03	-46.88	-2.03	0.00572	-23.71	RIGHT	0.93317E+00	151.67	0.40984E+00	-27.44
130.00	30.00	-2.73	-65.31	-2.73	0.00074	-34.45	RIGHT	0.77536E+00	140.26	0.53197E+00	-39.65
135.00	30.00	-2.96	-25.22	-2.94	0.07709	-46.50	RIGHT	0.63220E+00	123.01	0.66570E+00	-48.16
140.00	30.00	-2.64	-15.46	-2.42	0.2285	-56.68	RIGHT	0.55238E+00	97.81	0.80270E+00	-54.48
145.00	30.00	-1.99	-9.84	-1.33	0.40509	-63.85	RIGHT	0.58479E+00	69.83	0.93675E+00	-59.39
150.00	30.00	-1.26	-6.15	-0.04	0.56967	-68.63	RIGHT	0.71693E+00	48.60	0.10628E+01	-63.31
155.00	30.00	-0.57	-3.56	1.20	0.70861	-71.80	RIGHT	0.89506E+00	35.31	0.11765E+01	-66.46
160.00	30.00	0.02	-1.71	2.25	0.81948	-73.88	RIGHT	0.10776E+01	27.15	0.12744E+01	-68.95
165.00	30.00	0.49	-0.40	3.08	0.90331	-75.09	RIGHT	0.12393E+01	22.06	0.13535E+01	-70.84
170.00	30.00	0.82	0.48	3.66	0.96165	-75.30	RIGHT	0.13643E+01	18.93	0.14115E+01	-72.17
175.00	30.00	1.02	0.98	4.01	0.99566	-69.71	RIGHT	0.14422E+01	17.21	0.14470E+01	-72.95
180.00	30.00	1.14	1.08	4.12	0.99363	13.38	RIGHT	0.14673E+01	16.64	0.14589E+01	-73.19
0.00	35.00	-1.92	-1.97	1.06	0.99495	-44.33	LEFT	0.10292E+01	25.54	0.10291E+01	115.83
5.00	35.00	-1.90	-2.06	1.03	0.98156	-42.77	LEFT	0.10263E+01	24.63	0.10248E+01	115.70
10.00	35.00	-1.81	-2.33	0.95	0.94172	-42.31	LEFT	0.10182E+01	21.88	0.10125E+01	115.30
15.00	35.00	-1.68	-2.80	0.81	0.87930	-42.17	LEFT	0.10055E+01	17.37	0.99286E+00	114.69
20.00	35.00	-1.52	-3.47	0.62	0.79952	-42.13	LEFT	0.98874E+00	11.25	0.96720E+00	113.91
25.00	35.00	-1.37	-4.37	0.40	0.70749	-42.17	LEFT	0.96830E+00	3.67	0.93704E+00	113.03
30.00	35.00	-1.23	-5.57	0.13	0.60716	-42.32	LEFT	0.94401E+00	-5.24	0.90416E+00	112.13
35.00	35.00	-1.14	-7.14	-0.16	0.50074	-42.57	LEFT	0.91580E+00	-15.42	0.87036E+00	111.28
40.00	35.00	-1.09	-9.30	-0.48	0.38870	-42.88	LEFT	0.88441E+00	-26.89	0.83732E+00	110.55
45.00	35.00	-1.11	-12.47	-0.80	0.27030	-43.16	LEFT	0.85251E+00	-39.75	0.80647E+00	109.95
50.00	35.00	-1.19	-17.99	-1.10	0.14444	-43.26	LEFT	0.82556E+00	-54.07	0.77876E+00	109.46
55.00	35.00	-1.30	-40.53	-1.30	0.01093	-42.91	LEFT	0.81156E+00	-69.75	0.75450E+00	109.00
60.00	35.00	-1.44	-19.31	-1.37	0.12781	-41.73	RIGHT	0.81907E+00	-86.22	0.73331E+00	108.44
65.00	35.00	-1.56	-13.11	-1.27	0.26450	-39.14	RIGHT	0.85341E+00	-102.52	0.71402E+00	107.63
70.00	35.00	-1.60	-9.90	-1.00	0.38438	-34.47	RIGHT	0.91344E+00	-117.63	0.69481E+00	106.40
75.00	35.00	-1.47	-8.10	-0.62	0.46609	-27.51	RIGHT	0.99165E+00	-130.91	0.67348E+00	104.56
80.00	35.00	-1.16	-7.27	-0.21	0.49480	-19.70	RIGHT	0.10770E+01	-142.21	0.64773E+00	101.95
85.00	35.00	-0.74	-7.13	0.16	0.47894	-13.42	RIGHT	0.11579E+01	-151.70	0.61558E+00	98.34
90.00	35.00	-0 34	-7.47	0.43	0.43996	-9.66	RIGHT	0.12241E+01	-159.69	0.57581E+00	93.44
95.00	35.00	-0.06	-8.18	0.56	0.39289	-8.07	RIGHT	0.12673E+01	-166.52	0.52853E+00	86.82
100.00	35.00	0.04	-9.24	0.52	0.34351	-8.11	RIGHT	0.12816E+01	-172.49	0.47604E+00	77.78
105.00	35.00	-0.06	-10.74	0.30	0.29249	-9.42	RIGHT	0.12631E+01	-177.91	0.42429E+00	65.29
110.00	35.00	-0.36	-12.81	-0.12	0.23863	-11.90	RIGHT	0.12102E+01	176.87	0.38475E+00	48.31
115.00	35.00	-0.87	-15.72	-0.73	0.18088	-15.66	RIGHT	0.11232E+01	171.46	0.37426E+00	27.19
120.00	35.00	-1.56	-19.88	-1.49	0.12126	-21.13	RIGHT	0.10049E+01	165.26	0.40650E+00	5.37
125.00	35.00	-2.33	-25.28	-2.31	0.07119	-28.96	RIGHT	0.86198E+00	157.31	0.48055E+00	-13.10
130.00	35.00	-2.96	-27.29	-2.94	0.06070	-39.50	RIGHT	0.70773E+00	145.82	0.58429E+00	-27.10
135.00	35.00	-3.12	-21.05	-3.05	0.12685	-51.24	RIGHT	0.56991E+00	127.72	0.70481E+00	-37.48
140.00	35.00	-2.74	-14.30	-2.45	0.26442	-61.29	RIGHT	0.50091E+00	100.65	0.83211E+00	-45.34
145.00	35.00	-2.05	-9.43	-1.32	0.42803	-68.47	RIGHT	0.55033E+00	71.64	0.95871E+00	-51.44
150.00	35.00	-1.29	-5.98	-0.02	0.58294	-73.31	RIGHT	0.69660E+00	51.03	0.10788E+01	-56.27
155.00	35.00	-0.59	-3.49	1.21	0.71556	-76.58	RIGHT	0.88306E+00	38.65	0.11877E+01	-60.10
160.00	35.00	0.01	-1.68	2.26	0.82278	-78.81	RIGHT	0.10704E+01	31.18	0.12816E+01	-63.10
165.00	35.00	0.48	-0.39	3.08	0.90476	-80.37	RIGHT	0.12353E+01	26.53	0.13576E+01	-65.36
170.00	35.00	0.82	0.48	3.66	0.96224	-81.70	RIGHT	0.13623E+01	23.69	0.14135E+01	-66.94
175.00	35.00	1.02	0.98	4.01	0.99570	89.93	RIGHT	0.14415E+01	22.13	0.14477E+01	-67.87
180.00	35.00	1.14	1.08	4.12	0.99363	18.38	RIGHT	0.14668E+01	21.62	0.14593E+01	-68.16
0.00	40.00	-1.92	-1.97	1.06	0.99495	-49.33	LEFT	0.10287E+01	30.54	0.10295E+01	120.83
5.00	40.00	-1.89	-2.06	1.04	0.98133	-45.70	LEFT	0.10254E+01	29.63	0.10258E+01	120.71
10.00	40.00	-1.80	-2.33	0.95	0.94085	-44.75	LEFT	0.10157E+01	26.85	0.10152E+01	120.34
15.00	40.00	-1.67	-2.80	0.81	0.87761	-44.53	LEFT	0.10005E+01	22.30	0.99842E+00	119.76
20.00	40.00	-1.51	-3.48	0.63	0.79704	-44.51	LEFT	0.98056E+00	16.12	0.97682E+00	119.01
25.00	40.00	-1.34	-4.39	0.41	0.70444	-44.62	LEFT	0.95617E+00	8.47	0.95197E+00	118.14
30.00	40.00	-1.20	-5.58	0.15	0.60385	-44.88	LEFT	0.92739E+00	-0.53	0.92563E+00	117.22
35.00	40.00	-1.09	-7.15	-0.13	0.49751	-45.28	LEFT	0.89423E+00	-10.81	0.89953E+00	116.29
40.00	40.00	-1.03	-9.30	-0.43	0.38590	-45.78	LEFT	0.85759E+00	-22.42	0.87515E+00	115.37
45.00	40.00	-1.03	-12.46	-0.73	0.26834	-46.31	LEFT	0.82045E+00	-35.49	0.85354E+00	114.44
50.00	40.00	-1.08	-17.92	-0.99	0.14391	-46.71	LEFT	0.78872E+00	-50.12	0.83519E+00	113.47

55.00	40.00	-1.17	-39.19	-1.17	0.01256	-46.76	LEFT	0.77096E+00	-66.20	0.81988E+00	112.36
60.00	40.00	-1.28	-19.45	-1.21	0.12353	-46.14	RIGHT	0.77611E+00	-83.09	0.80668E+00	111.01
65.00	40.00	-1.39	-13.14	-1.10	0.25838	-44.38	RIGHT	0.80919E+00	-99.70	0.79405E+00	109.28
70.00	40.00	-1.44	-9.83	-0.85	0.38061	-40.90	RIGHT	0.86814E+00	-114.90	0.78000E+00	107.07
75.00	40.00	-1.39	-7.89	-0.51	0.47325	-35.29	RIGHT	0.94443E+00	-128.06	0.76242E+00	104.22
80.00	40.00	-1.19	-6.87	-0.15	0.52035	-28.24	RIGHT	0.10265E+01	-139.09	0.73935E+00	100.62
85.00	40.00	-0.88	-6.54	0.16	0.52130	-21.79	RIGHT	0.11030E+01	-148.21	0.70939E+00	96.07
90.00	40.00	-0.57	-6.73	0.37	0.49168	-17.51	RIGHT	0.11641E+01	-155.78	0.67203E+00	90.35
95.00	40.00	-0.34	-7.33	0.46	0.44724	-15.51	RIGHT	0.12026E+01	-162.14	0.62819E+00	83.11
100.00	40.00	-0.25	-8.30	0.38	0.39597	-15.33	RIGHT	0.12132E+01	-167.61	0.58085E+00	73.89
105.00	40.00	-0.34	-9.71	0.13	0.34011	-16.54	RIGHT	0.11927E+01	-172.51	0.53589E+00	62.12
110.00	40.00	-0.61	-11.68	-0.29	0.27951	-18.97	RIGHT	0.11399E+01	-177.18	0.50272E+00	47.42
115.00	40.00	-1.07	-14.45	-0.87	0.21414	-22.68	RIGHT	0.10549E+01	177.95	0.49329E+00	30.20
120.00	40.00	-1.68	-18.32	-1.58	0.14713	-28.02	RIGHT	0.93983E+00	172.28	0.51724E+00	12.22
125.00	40.00	-2.35	-23.19	-2.32	0.09077	-35.59	RIGHT	0.80027E+00	164.80	0.57611E+00	-4.26
130.00	40.00	-2.87	-25.45	-2.85	0.07431	-45.66	RIGHT	0.64824E+00	153.54	0.66313E+00	-17.96
135.00	40.00	-2.97	-20.56	-2.89	0.13193	-56.79	RIGHT	0.51115E+00	134.81	0.76833E+00	-28.86
140.00	40.00	-2.58	-14.30	-2.29	0.25940	-66.35	RIGHT	0.44614E+00	105.42	0.88231E+00	-37.45
145.00	40.00	-1.91	-9.53	-1.21	0.41588	-73.23	RIGHT	0.50824E+00	74.51	0.99743E+00	-44.27
150.00	40.00	-1.18	-6.09	0.04	0.56824	-77.89	RIGHT	0.66778E+00	54.03	0.11076E+01	-49.70
155.00	40.00	-0.50	-3.57	1.24	0.70191	-81.06	RIGHT	0.86369E+00	42.30	0.12080E+01	-54.03
160.00	40.00	0.07	-1.74	2.27	0.81220	-83.29	RIGHT	0.10579E+01	35.37	0.12949E+01	-57.42
165.00	40.00	0.52	-0.42	3.08	0.89787	-85.04	RIGHT	0.12279E+01	31.10	0.13653E+01	-59.97
170.00	40.00	0.83	0.47	3.66	0.95857	-87.20	RIGHT	0.13587E+01	28.48	0.14172E+01	-61.75
175.00	40.00	1.03	0.97	4.01	0.99348	78.92	RIGHT	0.14402E+01	27.05	0.14490E+01	-62.81
180.00	40.00	1.14	1.08	4.12	0.99363	23.38	RIGHT	0.14663E+01	26.59	0.14599E+01	-63.14
0.00	45.00	-1.92	-1.97	1.06	0.99495	-54.33	LEFT	0.10283E+01	35.55	0.10299E+01	125.83
5.00	45.00	-1.89	-2.06	1.04	0.98143	-48.69	LEFT	0.10244E+01	34.63	0.10269E+01	125.70
10.00	45.00	-1.81	-2.33	0.95	0.94116	-47.23	LEFT	0.10132E+01	31.86	0.10180E+01	125.32
15.00	45.00	-1.67	-2.80	0.81	0.87835	-46.92	LEFT	0.99543E+00	27.32	0.10041E+01	124.72
20.00	45.00	-1.51	-3.46	0.63	0.79852	-46.91	LEFT	0.97200E+00	21.16	0.98641E+00	123.92
25.00	45.00	-1.34	-4.36	0.42	0.70703	-47.08	LEFT	0.94346E+00	13.54	0.96657E+00	122.97
30.00	45.00	-1.20	-5.52	0.17	0.60793	-47.44	LEFT	0.90988E+00	4.57	0.94618E+00	121.89
35.00	45.00	-1.09	-7.05	-0.10	0.50345	-47.97	LEFT	0.87134E+00	-5.68	0.92677E+00	120.73
40.00	45.00	-1.02	-9.11	-0.39	0.39411	-48.64	LEFT	0.82883E+00	-17.29	0.90953E+00	119.46
45.00	45.00	-1.00	-12.08	-0.68	0.27931	-49.37	LEFT	0.78549E+00	-30.41	0.89520E+00	118.08
50.00	45.00	-1.03	-17.04	-0.92	0.15834	-50.02	LEFT	0.74757E+00	-45.21	0.88384E+00	116.53
55.00	45.00	-1.09	-31.15	-1.09	0.03141	-50.39	LEFT	0.72423E+00	-61.60	0.87487E+00	114.74
60.00	45.00	-1.17	-21.24	-1.13	0.09919	-50.20	RIGHT	0.72499E+00	-78.91	0.86708E+00	112.61
65.00	45.00	-1.25	-14.09	-1.03	0.22809	-49.08	RIGHT	0.75502E+00	-95.87	0.85877E+00	110.06
70.00	45.00	-1.29	-10.51	-0.80	0.34601	-46.59	RIGHT	0.81173E+00	-111.23	0.84801E+00	106.99
75.00	45.00	-1.26	-8.40	-0.50	0.43978	-42.39	RIGHT	0.88582E+00	-124.30	0.83291E+00	103.30
80.00	45.00	-1.13	-7.22	-0.18	0.49600	-36.77	RIGHT	0.96541E+00	-135.04	0.81194E+00	98.87
85.00	45.00	-0.91	-6.76	0.10	0.50980	-31.08	RIGHT	0.10393E+01	-143.74	0.78420E+00	93.56
90.00	45.00	-0.65	-6.86	0.28	0.48940	-26.80	RIGHT	0.10983E+01	-150.81	0.74987E+00	87.17
95.00	45.00	-0.45	-7.43	0.35	0.44772	-24.47	RIGHT	0.11358E+01	-156.61	0.71049E+00	79.44
100.00	45.00	-0.35	-8.45	0.27	0.39376	-23.87	RIGHT	0.11472E+01	-161.50	0.66949E+00	70.05
105.00	45.00	-0.40	-9.99	0.05	0.33171	-24.66	RIGHT	0.11297E+01	-165.79	0.63256E+00	58.71
110.00	45.00	-0.61	-12.20	-0.32	0.26329	-26.64	RIGHT	0.10816E+01	-169.85	0.60758E+00	45.36
115.00	45.00	-0.98	-15.40	-0.83	0.19016	-29.88	RIGHT	0.10026E+01	-174.09	0.60327E+00	30.46
120.00	45.00	-1.50	-20.13	-1.44	0.11702	-34.73	RIGHT	0.89359E+00	-179.11	0.62615E+00	15.11
125.00	45.00	-2.06	-26.90	-2.05	0.05729	-41.74	RIGHT	0.75850E+00	174.09	0.67737E+00	0.69
130.00	45.00	-2.49	-30.58	-2.49	0.03943	-51.12	RIGHT	0.60727E+00	163.46	0.75252E+00	-11.92
135.00	45.00	-2.55	-23.03	-2.51	0.09467	-61.46	RIGHT	0.46544E+00	144.73	0.84419E+00	-22.45
140.00	45.00	-2.20	-15.38	-1.99	0.21908	-70.35	RIGHT	0.39454E+00	112.92	0.94457E+00	-31.08
145.00	45.00	-1.60	-10.10	-1.02	0.37557	-76.76	RIGHT	0.46214E+00	78.92	0.10467E+01	-38.10
150.00	45.00	-0.94	-6.42	0.14	0.53218	-81.09	RIGHT	0.63300E+00	57.84	0.11450E+01	-43.80
155.00	45.00	-0.34	-3.78	1.28	0.67302	84.05	RIGHT	0.83886E+00	46.41	0.12348E+01	-48.38
160.00	45.00	0.17	-1.86	2.29	0.79158	-86.17	RIGHT	0.10412E+01	39.82	0.13125E+01	-51.98
165.00	45.00	0.58	-0.48	3.09	0.88508	-87.94	RIGHT	0.12179E+01	35.79	0.13756E+01	-54.71
170.00	45.00	0.86	0.44	3.67	0.95201	89.60	RIGHT	0.13539E+01	33.34	0.14221E+01	-56.62
175.00	45.00	1.04	0.96	4.01	0.99061	76.32	RIGHT	0.14385E+01	32.00	0.14506E+01	-57.75
180.00	45.00	1.14	1.08	4.12	0.99363	28.38	RIGHT	0.14657E+01	31.57	0.14605E+01	-58.12
0.00	50.00	-1.92	-1.97	1.06	0.99495	-59.33	LEFT	0.10279E+01	40.56	0.10304E+01	130.82
5.00	50.00	-1.90	-2.05	1.04	0.98185	-51.66	LEFT	0.10235E+01	39.66	0.10278E+01	130.68
10.00	50.00	-1.81	-2.32	0.95	0.94263	-49.64	LEFT	0.10108E+01	36.92	0.10205E+01	130.26
15.00	50.00	-1.68	-2.78	0.82	0.88148	-49.22	LEFT	0.99071E+00	32.45	0.10091E+01	129.58
20.00	50.00	-1.53	-3.42	0.64	0.80389	-49.20	LEFT	0.96411E+00	26.38	0.99490E+00	128.66
25.00	50.00	-1.37	-4.28	0.42	0.71512	-49.42	LEFT	0.93169E+00	18.87	0.97920E+00	127.52

30.00	50.00	-1.23	-5.40	0.18	0.61918	-49.85	LEFT	0.89361E+00	10.06	0.96349E+00	126.20
35.00	50.00	-1.12	-6.83	-0.09	0.51824	-50.49	LEFT	0.84993E+00	-0.02	0.94907E+00	124.69
40.00	50.00	-1.06	-8.74	-0.38	0.41281	-51.30	LEFT	0.80165E+00	-11.44	0.93687E+00	123.00
45.00	50.00	-1.04	-11.42	-0.66	0.30239	-52.19	LEFT	0.75188E+00	-24.41	0.92731E+00	121.10
50.00	50.00	-1.05	-15.64	-0.90	0.18641	-53.02	LEFT	0.70701E+00	-39.17	0.92021E+00	118.94
55.00	50.00	-1.09	-24.78	-1.07	0.06540	-53.58	LEFT	0.67667E+00	-55.70	0.91478E+00	116.47
60.00	50.00	-1.14	-25.85	-1.13	0.05816	-53.64	RIGHT	0.67118E+00	-73.35	0.90974E+00	113.62
65.00	50.00	-1.19	-16.13	-1.05	0.17901	-52.87	RIGHT	0.69642E+00	-90.69	0.90345E+00	110.33
70.00	50.00	-1.20	-11.99	-0.85	0.28880	-50.94	RIGHT	0.74982E+00	-106.26	0.89418E+00	106.52
75.00	50.00	-1.16	-9.64	-0.58	0.37654	-47.63	RIGHT	0.82174E+00	-119.29	0.88035E+00	102.10
80.00	50.00	-1.03	-8.33	-0.29	0.43132	-43.14	RIGHT	0.90007E+00	-129.76	0.86086E+00	96.96
85.00	50.00	-0.82	-7.80	-0.03	0.44804	-38.39	RIGHT	0.97382E+00	-138.04	0.83538E+00	90.99
90.00	50.00	-0.59	-7.90	0.15	0.43107	-34.50	RIGHT	0.10344E+01	-144.58	0.80460E+00	84.02
95.00	50.00	-0.38	-8.55	0.24	0.39014	-32.04	RIGHT	0.10756E+01	-149.81	0.77061E+00	75.85
100.00	50.00	-0.25	-9.78	0.21	0.33391	-31.02	RIGHT	0.10931E+01	-154.11	0.73707E+00	66.29
105.00	50.00	-0.25	-11.69	0.05	0.26783	-31.24	RIGHT	0.10837E+01	-157.82	0.70933E+00	55.23
110.00	50.00	-0.39	-14.58	-0.23	0.19522	-32.62	RIGHT	0.10452E+01	-161.31	0.69391E+00	42.77
115.00	50.00	-0.68	-19.15	-0.62	0.11917	-35.26	RIGHT	0.97581E+00	-164.98	0.69714E+00	29.40
120.00	50.00	-1.10	-27.92	-1.09	0.04559	-39.54	RIGHT	0.87524E+00	-169.39	0.72307E+00	15.92
125.00	50.00	-1.58	-40.37	-1.58	0.01150	-46.00	LEFT	0.74546E+00	-175.48	0.77184E+00	3.21
130.00	50.00	-1.95	-34.09	-1.95	0.02471	-54.74	LEFT	0.59400E+00	174.86	0.83985E+00	-8.14
135.00	50.00	-2.01	-31.34	-2.00	0.03417	-64.37	RIGHT	0.44302E+00	157.08	0.92129E+00	-17.91
140.00	50.00	-1.72	-17.58	-1.60	0.16101	-72.63	RIGHT	0.35490E+00	123.76	0.10098E+01	-26.13
145.00	50.00	-1.21	-11.06	-0.79	0.32195	-78.57	RIGHT	0.41714E+00	85.42	0.10997E+01	-32.97
150.00	50.00	-0.66	-6.92	0.26	0.48632	-82.60	RIGHT	0.59574E+00	62.73	0.11858E+01	-38.61
155.00	50.00	-0.14	-4.05	1.34	0.63720	-85.34	RIGHT	0.81115E+00	51.12	0.12644E+01	-43.20
160.00	50.00	0.30	-2.01	2.31	0.76639	-87.32	RIGHT	0.10223E+01	44.60	0.13323E+01	-46.84
165.00	50.00	0.65	-0.56	3.09	0.86963	-89.04	RIGHT	0.12065E+01	40.66	0.13873E+01	-49.61
170.00	50.00	0.90	0.40	3.67	0.94425	88.50	RIGHT	0.13482E+01	38.26	0.14277E+01	-51.57
175.00	50.00	1.05	0.95	4.01	0.98771	76.84	RIGHT	0.14366E+01	36.96	0.14526E+01	-52.72
180.00	50.00	1.14	1.08	4.12	0.99363	33.38	RIGHT	0.14649E+01	36.56	0.14612E+01	-53.11
0.00	55.00	-1.92	-1.97	1.06	0.99495	-64.33	LEFT	0.10275E+01	45.57	0.10307E+01	135.80
5.00	55.00	-1.90	-2.05	1.04	0.98260	-54.56	LEFT	0.10228E+01	44.69	0.10287E+01	135.64
10.00	55.00	-1.82	-2.31	0.95	0.94519	-51.89	LEFT	0.10090E+01	42.02	0.10226E+01	135.16
15.00	55.00	-1.70	-2.75	0.82	0.88686	-51.32	LEFT	0.98695E+00	37.66	0.10131E+01	134.36
20.00	55.00	-1.56	-3.36	0.64	0.81289	-51.27	LEFT	0.95784E+00	31.75	0.10013E+01	133.26
25.00	55.00	-1.42	-4.18	0.42	0.72836	-51.51	LEFT	0.92235E+00	24.45	0.98846E+00	131.88
30.00	55.00	-1.30	-5.22	0.18	0.63714	-51.99	LEFT	0.88067E+00	15.89	0.97572E+00	130.23
35.00	55.00	-1.21	-6.54	-0.09	0.54129	-52.71	LEFT	0.83284E+00	6.14	0.96418E+00	128.33
40.00	55.00	-1.15	-8.26	-0.38	0.44126	-53.61	LEFT	0.77973E+00	-4.92	0.95452E+00	126.16
45.00	55.00	-1.13	-10.59	-0.67	0.33655	-54.60	LEFT	0.72425E+00	-17.50	0.94697E+00	123.71
50.00	55.00	-1.15	-14.04	-0.93	0.22669	-55.52	LEFT	0.67266E+00	-31.94	0.94122E+00	120.95
55.00	55.00	-1.18	-20.17	-1.12	0.11236	-56.16	LEFT	0.63474E+00	-48.34	0.93648E+00	117.83
60.00	55.00	-1.21	-49.80	-1.21	0.00372	-56.28	RIGHT	0.62168E+00	-66.14	0.93152E+00	114.32
65.00	55.00	-1.23	-19.92	-1.17	0.11620	-55.59	RIGHT	0.64063E+00	-83.83	0.92493E+00	110.35
70.00	55.00	-1.21	-14.48	-1.01	0.21700	-53.81	RIGHT	0.68988E+00	-99.67	0.91529E+00	105.87
75.00	55.00	-1.13	-11.70	-0.76	0.29608	-50.82	RIGHT	0.75994E+00	-112.74	0.90143E+00	100.79
80.00	55.00	-0.97	-10.24	-0.48	0.34411	-46.86	RIGHT	0.83872E+00	-123.02	0.88273E+00	95.02
85.00	55.00	-0.74	-9.69	-0.22	0.35695	-42.66	RIGHT	0.91543E+00	-130.94	0.85937E+00	88.44
90.00	55.00	-0.47	-9.89	0.00	0.33821	-39.07	RIGHT	0.98173E+00	-137.04	0.83254E+00	80.93
95.00	55.00	-0.23	-10.80	0.14	0.29615	-36.57	RIGHT	0.10315E+01	-141.81	0.80469E+00	72.34
100.00	55.00	-0.05	-12.49	0.19	0.23888	-35.25	RIGHT	0.10599E+01	-145.67	0.77960E+00	62.59
105.00	55.00	0.01	-15.27	0.14	0.17222	-35.04	RIGHT	0.10632E+01	-148.99	0.76210E+00	51.70
110.00	55.00	-0.06	-20.05	-0.02	0.10014	-35.94	RIGHT	0.10376E+01	-152.13	0.75742E+00	39.88
115.00	55.00	-0.28	-31.86	-0.28	0.02638	-38.14	RIGHT	0.98018E+00	-155.49	0.76987E+00	27.62
120.00	55.00	-0.64	-28.04	-0.63	0.04268	-42.03	LEFT	0.88896E+00	-159.54	0.80152E+00	15.55
125.00	55.00	-1.06	-21.71	-1.02	0.09283	-48.14	LEFT	0.76436E+00	-165.09	0.85144E+00	4.24
130.00	55.00	-1.39	-21.59	-1.35	0.09779	-56.49	LEFT	0.61198E+00	-173.81	0.91617E+00	-5.91
135.00	55.00	-1.46	-31.36	-1.46	0.03200	-65.61	LEFT	0.45025E+00	170.10	0.99085E+00	-14.77
140.00	55.00	-1.24	-21.24	-1.19	0.10000	-73.37	RIGHT	0.33694E+00	137.43	0.10703E+01	-22.35
145.00	55.00	-0.83	-12.30	-0.53	0.26702	-78.94	RIGHT	0.37992E+00	94.46	0.11498E+01	-28.75
150.00	55.00	-0.37	-7.51	0.39	0.43987	-82.71	RIGHT	0.56037E+00	68.90	0.12252E+01	-34.10
155.00	55.00	0.06	-4.36	1.40	0.60105	-85.28	RIGHT	0.78371E+00	56.50	0.12934E+01	-38.48
160.00	55.00	0.43	-2.18	2.33	0.74100	-87.15	RIGHT	0.10033E+01	49.74	0.13519E+01	-41.99
165.00	55.00	0.72	-0.65	3.10	0.85406	-88.78	RIGHT	0.11950E+01	45.70	0.13989E+01	-44.68
170.00	55.00	0.93	0.36	3.67	0.93649	88.85	RIGHT	0.13425E+01	43.27	0.14334E+01	-46.58
175.00	55.00	1.07	0.93	4.01	0.98502	78.62	RIGHT	0.14345E+01	41.95	0.14546E+01	-47.72
180.00	55.00	1.14	1.08	4.12	0.99363	38.38	RIGHT	0.14642E+01	41.55	0.14620E+01	-48.10
0.00	60.00	-1.92	-1.97	1.06	0.99495	-69.33	LEFT	0.10272E+01	50.59	0.10311E+01	140.78

5.00	60.00	-1.90	-2.05	1.04	0.98363	-57.33	LEFT	0.10222E+01	49.74	0.10293E+01	140.60
10.00	60.00	-1.84	-2.29	0.95	0.94872	-53.83	LEFT	0.10077E+01	47.15	0.10239E+01	140.02
15.00	60.00	-1.73	-2.71	0.82	0.89420	-53.07	LEFT	0.98460E+00	42.93	0.10156E+01	139.08
20.00	60.00	-1.62	-3.29	0.64	0.82505	-52.96	LEFT	0.95398E+00	37.22	0.10050E+01	137.76
25.00	60.00	-1.50	-4.04	0.42	0.74611	-53.18	LEFT	0.91664E+00	30.19	0.99339E+00	136.10
30.00	60.00	-1.40	-5.00	0.17	0.66100	-53.68	LEFT	0.87281E+00	21.98	0.98165E+00	134.10
35.00	60.00	-1.33	-6.19	-0.10	0.57164	-54.44	LEFT	0.82246E+00	12.64	0.97064E+00	131.77
40.00	60.00	-1.30	-7.70	-0.40	0.47835	-55.38	LEFT	0.76628E+00	2.11	0.96089E+00	129.11
45.00	60.00	-1.30	-9.69	-0.71	0.33052	-56.41	LEFT	0.70686E+00	-9.89	0.95254E+00	126.12
50.00	60.00	-1.32	-12.46	-1.00	0.27762	-57.35	LEFT	0.64999E+00	-23.72	0.94526E+00	122.77
55.00	60.00	-1.36	-16.74	-1.24	0.17032	-57.96	LEFT	0.60523E+00	-39.65	0.93837E+00	119.05
60.00	60.00	-1.39	-25.62	-1.37	0.06146	-57.99	LEFT	0.58436E+00	-57.28	0.93088E+00	114.91
65.00	60.00	-1.39	-28.64	-1.39	0.04340	-57.15	RIGHT	0.59618E+00	-75.14	0.92169E+00	110.31
70.00	60.00	-1.35	-18.67	-1.27	0.13603	-55.23	RIGHT	0.64076E+00	-91.28	0.90980E+00	105.20
75.00	60.00	-1.22	-14.92	-1.04	0.20663	-52.18	RIGHT	0.70952E+00	-104.53	0.89453E+00	99.49
80.00	60.00	-1.02	-13.17	-0.76	0.24682	-48.31	RIGHT	0.79061E+00	-114.78	0.87578E+00	93.11
85.00	60.00	-0.73	-12.64	-0.46	0.25375	-44.28	RIGHT	0.87327E+00	-122.55	0.85423E+00	85.94
90.00	60.00	-0.40	-13.11	-0.18	0.23160	-40.80	RIGHT	0.94899E+00	-128.44	0.83154E+00	77.88
95.00	60.00	-0.10	-14.59	0.06	0.18838	-38.24	RIGHT	0.10111E+01	-133.01	0.81043E+00	68.87
100.00	60.00	0.14	-17.46	0.22	0.13180	-36.73	RIGHT	0.10539E+01	-136.73	0.79459E+00	58.90
105.00	60.00	0.27	-23.15	0.29	0.06748	-36.24	RIGHT	0.10721E+01	-139.99	0.78823E+00	48.10
110.00	60.00	0.25	-63.01	0.25	0.00069	-36.86	LEFT	0.10606E+01	-143.14	0.79523E+00	36.78
115.00	60.00	0.09	-23.13	0.11	0.06901	-38.81	LEFT	0.10149E+01	-146.52	0.81814E+00	25.40
120.00	60.00	-0.22	-17.87	-0.14	0.13107	-42.53	LEFT	0.93187E+00	-150.55	0.85733E+00	14.46
125.00	60.00	-0.60	-15.85	-0.47	0.17266	-48.53	LEFT	0.81097E+00	-155.91	0.91093E+00	4.36
130.00	60.00	-0.91	-16.39	-0.79	0.16826	-56.73	LEFT	0.65677E+00	-164.01	0.97543E+00	-4.69
135.00	60.00	-0.99	-21.50	-0.95	0.09430	-65.57	LEFT	0.48508E+00	-178.43	0.10465E+01	-12.61
140.00	60.00	-0.82	-27.95	-0.81	0.04400	-72.98	RIGHT	0.34627E+00	151.62	0.11199E+01	-19.43
145.00	60.00	-0.50	-13.75	-0.30	0.21742	-78.27	RIGHT	0.35792E+00	105.86	0.11917E+01	-25.24
150.00	60.00	-0.12	-8.12	0.52	0.39821	-81.84	RIGHT	0.53185E+00	76.41	0.12586E+01	-30.13
155.00	60.00	0.23	-4.67	1.45	0.56864	-84.27	RIGHT	0.75997E+00	62.57	0.13183E+01	-34.16
160.00	60.00	0.54	-2.33	2.35	0.71818	-86.05	RIGHT	0.98643E+00	55.24	0.13689E+01	-37.41
165.00	60.00	0.79	-0.73	3.11	0.84004	-87.62	RIGHT	0.11846E+01	50.93	0.14092E+01	-39.90
170.00	60.00	0.96	0.33	3.67	0.92950	-89.87	RIGHT	0.13372E+01	48.35	0.14386E+01	-41.67
175.00	60.00	1.08	0.92	4.01	0.98264	80.99	RIGHT	0.14325E+01	46.96	0.14565E+01	-42.73
180.00	60.00	1.14	1.08	4.12	0.99363	43.38	RIGHT	0.14634E+01	46.54	0.14628E+01	-43.09
0.00	65.00	-1.92	-1.97	1.06	0.99495	-74.33	LEFT	0.10269E+01	55.61	0.10313E+01	145.76
5.00	65.00	-1.91	-2.04	1.04	0.98492	-59.87	LEFT	0.10219E+01	54.79	0.10297E+01	145.54
10.00	65.00	-1.85	-2.27	0.95	0.95302	-55.30	LEFT	0.10073E+01	52.30	0.10245E+01	144.88
15.00	65.00	-1.77	-2.66	0.82	0.90303	-54.26	LEFT	0.98394E+00	48.24	0.10162E+01	143.77
20.00	65.00	-1.68	-3.20	0.64	0.83964	-54.04	LEFT	0.95302E+00	42.75	0.10056E+01	142.23
25.00	65.00	-1.59	-3.89	0.42	0.76732	-54.21	LEFT	0.91533E+00	36.01	0.99352E+00	140.28
30.00	65.00	-1.53	-4.76	0.16	0.68945	-54.69	LEFT	0.87111E+00	28.17	0.98071E+00	137.92
35.00	65.00	-1.49	-5.82	-0.13	0.60775	-55.43	LEFT	0.82030E+00	19.30	0.96790E+00	135.17
40.00	65.00	-1.49	-7.13	-0.45	0.52237	-56.37	LEFT	0.76338E+00	9.34	0.95551E+00	132.03
45.00	65.00	-1.53	-8.81	-0.78	0.43247	-57.38	LEFT	0.70254E+00	-1.97	0.94365E+00	128.52
50.00	65.00	-1.58	-11.02	-1.12	0.33724	-58.26	LEFT	0.64294E+00	-15.00	0.93212E+00	124.62
55.00	65.00	-1.64	-14.14	-1.40	0.23716	-58.75	LEFT	0.59354E+00	-30.15	0.92044E+00	120.32
60.00	65.00	-1.69	-19.08	-1.61	0.13503	-58.58	LEFT	0.56619E+00	-47.24	0.90794E+00	115.59
65.00	65.00	-1.69	-30.41	-1.68	0.03665	-57.46	LEFT	0.57126E+00	-64.99	0.89396E+00	110.38
70.00	65.00	-1.62	-27.76	-1.61	0.04929	-55.21	RIGHT	0.61125E+00	-81.37	0.87799E+00	104.65
75.00	65.00	-1.45	-20.41	-1.40	0.11281	-51.87	RIGHT	0.67934E+00	-94.92	0.85991E+00	98.32
80.00	65.00	-1.18	-17.88	-1.09	0.14616	-47.83	RIGHT	0.76423E+00	-105.41	0.84017E+00	91.30
85.00	65.00	-0.82	-17.42	-0.72	0.14790	-43.75	RIGHT	0.85489E+00	-113.33	0.81998E+00	83.51
90.00	65.00	-0.41	-18.60	-0.35	0.12326	-40.24	RIGHT	0.94213E+00	-119.37	0.80143E+00	74.88
95.00	65.00	-0.03	-21.92	0.00	0.08042	-37.62	RIGHT	0.10182E+01	-124.11	0.78742E+00	65.39
100.00	65.00	0.28	-31.20	0.28	0.02667	-35.98	RIGHT	0.10759E+01	-128.06	0.78142E+00	55.15
105.00	65.00	0.47	-29.17	0.47	0.03297	-35.34	LEFT	0.11086E+01	-131.60	0.78681E+00	44.40
110.00	65.00	0.51	-19.92	0.55	0.09517	-35.83	LEFT	0.11095E+01	-135.06	0.80612E+00	33.50
115.00	65.00	0.39	-15.71	0.49	0.15666	-37.70	LEFT	0.10731E+01	-138.75	0.84023E+00	22.88
120.00	65.00	0.12	-13.39	0.31	0.21119	-41.43	LEFT	0.99545E+00	-143.05	0.88813E+00	12.94
125.00	65.00	-0.23	-12.47	0.02	0.24446	-47.53	LEFT	0.87582E+00	-148.53	0.94719E+00	3.90
130.00	65.00	-0.53	-13.26	-0.31	0.23108	-55.81	LEFT	0.71860E+00	-156.40	0.10138E+01	-4.10
135.00	65.00	-0.63	-17.18	-0.54	0.14874	-64.58	LEFT	0.53853E+00	-169.67	0.10841E+01	-11.09
140.00	65.00	-0.50	-49.45	-0.50	0.00357	-71.79	LEFT	0.37977E+00	163.58	0.11543E+01	-17.11
145.00	65.00	-0.24	-15.31	-0.10	0.17623	-76.88	RIGHT	0.35659E+00	118.31	0.12214E+01	-22.24
150.00	65.00	0.08	-8.70	0.62	0.36404	-80.30	RIGHT	0.51485E+00	85.02	0.12827E+01	-26.57
155.00	65.00	0.38	-4.94	1.49	0.54221	-82.65	RIGHT	0.74313E+00	69.24	0.13366E+01	-30.14
160.00	65.00	0.63	-2.47	2.36	0.69958	-84.36	RIGHT	0.97379E+00	61.06	0.13816E+01	-33.03

165.00	65.00	0.84	-0.79	3.11	0.82858	-85.88	RIGHT	0.11765E+01	56.31	0.14171E+01	-35.24
170.00	65.00	0.99	0.30	3.67	0.92374	-88.04	RIGHT	0.13329E+01	53.49	0.14427E+01	-36.82
175.00	65.00	1.08	0.91	4.01	0.98065	83.62	RIGHT	0.14307E+01	51.99	0.14582E+01	-37.76
180.00	65.00	1.14	1.08	4.12	0.99363	48.38	RIGHT	0.14625E+01	51.54	0.14636E+01	-38.09
0.00	70.00	-1.92	-1 97	1.06	0.99495	-79.33	LEFT	0.10267E+01	60.64	0.10315E+01	150.74
5.00	70.00	-1.91	-2.03	1.04	0.98642	-62.08	LEFT	0.10219E+01	59.84	0.10298E+01	150.49
10.00	70.00	-1.87	-2.25	0.95	0.95780	-56.05	LEFT	0.10077E+01	57.44	0.10242E+01	149.73
15.00	70.00	-1.81	-2.61	0.82	0.91268	-54.62	LEFT	0.98505E+00	53.54	0.10151E+01	148.47
20.00	70.00	-1.75	-3.11	0.63	0.85547	-54.23	LEFT	0.95508E+00	48.26	0.10031E+01	146.72
25.00	70.00	-1.70	-3.74	0.41	0.79030	-54.29	LEFT	0.91858E+00	41.80	0.98887E+00	144.49
30.00	70.00	-1.67	-4.52	0.15	0.72029	-54.67	LEFT	0.87581E+00	34.31	0.97308E+00	141.80
35.00	70.00	-1.68	-5.46	-0.16	0.64698	-55.33	LEFT	0.82665E+00	25.86	0.95630E+00	138.66
40.00	70.00	-1.72	-6.60	-0.50	0.57032	-56.20	LEFT	0.77141E+00	16.42	0.93894E+00	135.10
45.00	70.00	-1.81	-8.02	-0.87	0.48915	-57.13	LEFT	0.71190E+00	5.77	0.92119E+00	131.11
50.00	70.00	-1.91	-9.82	-1.26	0.40223	-57.89	LEFT	0.65262E+00	-6.48	0.90300E+00	126.70
55.00	70.00	-2.01	-12.19	-1.61	0.30955	-58.20	LEFT	0.60173E+00	-20.74	0.88418E+00	121.86
60.00	70.00	-2.08	-15.49	-1.89	0.21367	-57.75	LEFT	0.57070E+00	-37.05	0.86448E+00	116.57
65.00	70.00	-2.10	-20.47	-2.03	0.12057	-56.26	LEFT	0.57088E+00	-54.39	0.84373E+00	110.77
70.00	70.00	-2.01	-30.06	-2.01	0.03959	-53.57	LEFT	0.60724E+00	-70.84	0.82198E+00	104.42
75.00	70.00	-1.80	-36.32	-1.80	0.01880	-49.83	RIGHT	0.67526E+00	-84.76	0.79971E+00	97.42
80.00	70.00	-1.45	-27.94	-1.44	0.04735	-45.50	RIGHT	0.76447E+00	-95.72	0.77800E+00	89.71
85.00	70.00	-0.99	-27.73	-0.99	0.04604	-41.28	RIGHT	0.86350E+00	-104.11	0.75861E+00	81.20
90.00	70.00	-0.50	-33.96	0.49	0.02122	-37.71	RIGHT	0.96208E+00	-110.62	0.74403E+00	71.89
95.00	70.00	-0.03	-34.52	0.02	0.01885	-35.04	LEFT	0.10510E+01	-115.85	0.73726E+00	61.86
100.00	70.00	0.36	-23.05	0.38	0.06758	-33.35	LEFT	0.11216E+01	-120.29	0.74136E+00	51.30
105.00	70.00	0.61	-17.75	0.67	0.12084	-32.68	LEFT	0.11656E+01	-124.34	0.75875E+00	40.56
110.00	70.00	0.70	-14.39	0.83	0.17610	-33.17	LEFT	0.11754E+01	-128.30	0.79052E+00	30.06
115.00	70.00	0.61	-12.13	0.83	0.23068	-35.11	LEFT	0.11445E+01	-132.46	0.83605E+00	20.17
120.00	70.00	0.36	-10.74	0.68	0.27854	-39.01	LEFT	0.10689E+01	-137.15	0.89320E+00	11.15
125.00	70.00	0.01	-10.30	0.40	0.30504	-45.39	LEFT	0.94804E+00	-142.93	0.95881E+00	3.14
130.00	70.00	-0.28	-11.21	0.05	0.28406	-53.98	LEFT	0.78681E+00	-150.86	0.10293E+01	-3.87
135.00	70.00	-0.39	-14.65	-0.23	0.19370	-62.88	LEFT	0.60002E+00	-163.56	0.11010E+01	-9.94
140.00	70.00	-0.29	-27.95	-0.28	0.04138	-70.03	LEFT	0.42822E+00	172.23	0.11709E+01	-15.13
145.00	70.00	-0.06	-16.85	0.03	0.14474	-75.01	RIGHT	0.37608E+00	129.84	0.12364E+01	-19.55
150.00	70.00	0.21	-9.19	0.68	0.33868	-78.34	RIGHT	0.51243E+00	94.10	0.12953E+01	-23.25
155.00	70.00	0.47	-5.16	1.52	0.52297	-80.63	RIGHT	0.73560E+00	76.27	0.13463E+01	-26.31
160.00	70.00	0.70	-2.57	2.37	0.68617	-82.30	RIGHT	0.96697E+00	67.07	0.13886E+01	-28.77
165.00	70.00	0.88	-0.84	3.11	0.82032	-83.79	RIGHT	0.11717E+01	61.79	0.14216E+01	-30.66
170.00	70.00	1.01	0.28	3.67	0.91951	-85.89	RIGHT	0.13301E+01	58.68	0.14453E+01	-32.00
175.00	70.00	1.09	0.91	4.01	0.97909	86.37	RIGHT	0.14292E+01	57.03	0.14595E+01	-32.81
180.00	70.00	1.14	1.08	4.12	0.99363	53.38	RIGHT	0.14617E+01	56.55	0.14644E+01	-33.10
0.00	75.00	-1.92	-1.97	1.06	0.99495	-84.33	LEFT	0.10266E+01	65.66	0.10317E+01	155.72
5.00	75.00	-1.92	-2.03	1.04	0.98805	-63.76	LEFT	0.10221E+01	64.89	0.10296E+01	155.44
10.00	75.00	-1.89	-2.23	0.95	0.96263	-55.76	LEFT	0.10089E+01	62.57	0.10231E+01	154.60
15.00	75.00	-1.86	-2.56	0.82	0.92216	-53.82	LEFT	0.98779E+00	58.79	0.10123E+01	153.21
20.00	75.00	-1.82	-3.02	0.63	0.87080	-53.17	LEFT	0.95988E+00	53.70	0.99775E+00	151.28
25.00	75.00	-1.80	-3.60	0.40	0.81242	-53.03	LEFT	0.92596E+00	47.46	0.97999E+00	148.83
30.00	75.00	-1.81	-4.31	0.13	0.74991	-53.23	LEFT	0.88622E+00	40.23	0.95957E+00	145.86
35.00	75.00	-1.87	-5.16	-0.20	0.68474	-53.71	LEFT	0.84053E+00	32.10	0.93705E+00	142.41
40.00	75.00	-1.96	-6.16	-0.56	0.61671	-54.40	LEFT	0.78902E+00	23.05	0.91283E+00	138.48
45.00	75.00	-2.10	-7.38	-0.97	0.54436	-55.16	LEFT	0.73318E+00	12.88	0.88722E+00	134.10
50.00	75.00	-2.26	-8.90	-1.41	0.46588	-55.73	LEFT	0.67693E+00	1.23	0.86042E+00	129.26
55.00	75.00	-2.42	-10.81	-1.83	0.38054	-55.81	LEFT	0.62769E+00	-12.30	0.83256E+00	123.95
60.00	75.00	-2.54	-13.28	-2.19	0.29032	-55.04	LEFT	0.59631E+00	-27.84	0.80385E+00	118.13
65.00	75.00	-2.57	-16.50	-2.40	0.20123	-53.15	LEFT	0.59448E+00	-44.63	0.77463E+00	111.76
70.00	75.00	-2.48	-20.66	-2.41	0.12331	-50.00	LEFT	0.62898E+00	-60.98	0.74558E+00	104.76
75.00	75.00	-2.21	-25.59	-2.19	0.06776	-45.83	LEFT	0.69749E+00	-75.21	0.71785E+00	97.03
80.00	75.00	-1.77	-29.42	-1.76	0.04145	-41.23	LEFT	0.79065E+00	-86.71	0.69316E+00	88.51
85.00	75.00	-1.21	-28.52	-1.20	0.04309	-36.89	LEFT	0.89674E+00	-95.72	0.67389E+00	79.14
90.00	75.00	-0.60	-24.29	-0.59	0.06544	-33.32	LEFT	0.10044E+01	-102.87	0.66292E+00	68.98
95.00	75.00	-0.05	-20.00	0.00	0.10054	-30.71	LEFT	0.11030E+01	-108.73	0.66326E+00	58.25
100.00	75.00	0.41	-16.50	0.49	0.14276	-29.10	LEFT	0.11826E+01	-113.78	0.67739E+00	47.29
105.00	75.00	0.71	-13.76	0.86	0.18902	-28.54	LEFT	0.12336E+01	-118.40	0.70654E+00	36.56
110.00	75.00	0.83	-11.65	1.07	0.23764	-29.16	LEFT	0.12479E+01	-122.89	0.75035E+00	26.49
115.00	75.00	0.76	-10.10	1.10	0.28649	-31.30	LEFT	0.12186E+01	-127.54	0.80688E+00	17.35
120.00	75.00	0.51	-9.13	0.96	0.32972	-35.49	LEFT	0.11420E+01	-132.68	0.87319E+00	9.28
125.00	75.00	0.16	-8.91	0.66	0.35205	-42.30	LEFT	0.10180E+01	-138.82	0.94585E+00	2.27
130.00	75.00	-0.15	-9.90	0.28	0.32575	-51.40	LEFT	0.85237E+00	-146.99	0.10214E+01	-3.76
135.00	75.00	-0.27	-13.10	-0.05	0.22830	-60.62	LEFT	0.66069E+00	-159.50	0.10966E+01	-8.90

140.00	75.00	-0.18	-23.43	-0.16	0.06876	-67.86	LEFT	0.48200E+00	177.92	0.11687E+01	-13.27
145.00	75.00	0.03	-18.13	0.10	0.12358	-72.82	RIGHT	0.41106E+00	139.07	0.12355E+01	-16.95
150.00	75.00	0.28	-9.54	0.71	0.32278	-76.12	RIGHT	0.52486E+00	102.85	0.12952E+01	-20.03
155.00	75.00	0.52	-5.30	1.53	0.51153	-78.38	RIGHT	0.73843E+00	83.35	0.13467E+01	-22.55
160.00	75.00	0.73	-2.64	2.38	0.67847	-80.04	RIGHT	0.96679E+00	73.15	0.13892E+01	-24.57
165.00	75.00	0.90	-0.87	3.11	0.81559	-81.51	RIGHT	0.11707E+01	67.32	0.14224E+01	-26.11
170.00	75.00	1.02	0.27	3.67	0.91698	-83.57	RIGHT	0.13290E+01	63.90	0.14461E+01	-27.21
175.00	75.00	1.09	0.90	4.01	0.97799	89.11	RIGHT	0.14282E+01	62.09	0.14604E+01	-27.87
180.00	75.00	1.14	1.08	4.12	0.99363	58.38	RIGHT	0.14610E+01	61.56	0.14652E+01	-28.11
0.00	80.00	-1.92	-1.97	1.06	0.99495	-89.33	LEFT	0.10265E+01	70.69	0.10317E+01	160.69
5.00	80.00	-1.93	-2.02	1.04	0.98975	-64.65	LEFT	0.10226E+01	69.94	0.10293E+01	160.40
10.00	80.00	-1.91	-2.20	0.95	0.96694	-54.07	LEFT	0.10107E+01	67.67	0.10214E+01	159.50
15.00	80.00	-1.89	-2.52	0.82	0.93006	-51.55	LEFT	0.99181E+00	63.98	0.10082E+01	158.02
20.00	80.00	-1.88	-2.96	0.63	0.88314	-50.58	LEFT	0.96683E+00	59.00	0.99024E+00	155.97
25.00	80.00	-1.88	-3.50	0.39	0.82981	-50.15	LEFT	0.93649E+00	52.90	0.96788E+00	153.36
30.00	80.00	-1.93	-4.17	0.11	0.77286	-50.05	LEFT	0.90093E+00	45.82	0.94168E+00	150.21
35.00	80.00	-2.02	-4.95	-0.23	0.71374	-50.22	LEFT	0.85994E+00	37.87	0.91215E+00	146.54
40.00	80.00	-2.16	-5.87	-0.62	0.65229	-50.59	LEFT	0.81351E+00	29.01	0.87977E+00	142.38
45.00	80.00	-2.35	-6.98	-1.07	0.58691	-51.03	LEFT	0.76286E+00	19.08	0.84498E+00	137.72
50.00	80.00	-2.58	-8.33	-1.55	0.51532	-51.31	LEFT	0.71149E+00	7.76	0.80823E+00	132.58
55.00	80.00	-2.79	-10.00	-2.04	0.43597	-51.10	LEFT	0.66624E+00	-5.33	0.77001E+00	126.91
60.00	80.00	-2.96	-12.08	-2.46	0.35003	-50.01	LEFT	0.63736E+00	-20.31	0.73093E+00	120.68
65.00	80.00	-3.02	-14.61	-2.73	0.26330	-47.75	LEFT	0.63642E+00	-36.60	0.69191E+00	113.79
70.00	80.00	-2.91	-17.49	-2.76	0.18656	-44.22	LEFT	0.67112E+00	-52.72	0.65423E+00	106.14
75.00	80.00	-2.57	-20.17	-2.50	0.13191	-39.74	LEFT	0.74075E+00	-67.13	0.61975E+00	97.60
80.00	80.00	-2.03	-21.53	-1.98	0.10592	-34.99	LEFT	0.83695E+00	-79.07	0.59094E+00	88.08
85.00	80.00	-1.36	-20.85	-1.32	0.10613	-30.71	LEFT	0.94789E+00	-88.68	0.57088E+00	77.58
90.00	80.00	-0.67	-18.75	-0.60	0.12476	-27.32	LEFT	0.10613E+01	-96.45	0.56292E+00	66.29
95.00	80.00	-0.04	-16.26	0.07	0.15443	-24.95	LEFT	0.11655E+01	-102.92	0.56995E+00	54.61
100.00	80.00	0.47	-13.93	0.62	0.19052	-23.61	LEFT	0.12494E+01	-108.54	0.59362E+00	43.14
105.00	80.00	0.80	-11.93	1.03	0.23092	-23.31	LEFT	0.13030E+01	-113.70	0.63378E+00	32.43
110.00	80.00	0.93	-10.29	1.25	0.27464	-24.19	LEFT	0.13176E+01	-118.67	0.68857E+00	22.86
115.00	80.00	0.86	-9.04	1.28	0.32005	-26.61	LEFT	0.12865E+01	-123.76	0.75507E+00	14.55
120.00	80.00	0.58	-8.25	1.12	0.36151	-31.14	LEFT	0.12064E+01	-129.31	0.82988E+00	7.48
125.00	80.00	0.20	-8.14	0.79	0.38306	-38.46	LEFT	0.10782E+01	-135.83	0.90961E+00	1.50
130.00	80.00	-0.14	-9.15	0.38	0.35452	-48.21	LEFT	0.90844E+00	-144.31	0.99104E+00	-3.53
135.00	80.00	-0.27	-12.25	0.00	0.25154	-57.95	LEFT	0.71402E+00	-156.91	0.10713E+01	-7.75
140.00	80.00	-0.18	-21.58	-0.15	0.08508	-65.42	LEFT	0.53373E+00	-178.54	0.11480E+01	-11.30
145.00	80.00	0.03	-18.89	0.09	0.11321	-70.45	RIGHT	0.45405E+00	145.75	0.12189E+01	-14.27
150.00	80.00	0.28	-9.70	0.70	0.31670	-73.76	RIGHT	0.54949E+00	110.61	0.12826E+01	-16.72
155.00	80.00	0.52	-5.35	1.52	0.50822	-76.03	RIGHT	0.75097E+00	90.14	0.13377E+01	-18.73
160.00	80.00	0.73	-2.66	2.37	0.67673	-77.70	RIGHT	0.97312E+00	79.14	0.13836E+01	-20.33
165.00	80.00	0.90	-0.88	3.11	0.81457	-79.18	RIGHT	0.11735E+01	72.81	0.14195E+01	-21.54
170.00	80.00	1.02	0.26	3.67	0.91621	-81.23	RIGHT	0.13296E+01	69.10	0.14453E+01	-22.41
175.00	80.00	1.10	0.90	4.01	0.97734	-88.24	RIGHT	0.14277E+01	67.15	0.14608E+01	-22.93
180.00	80.00	1.14	1.08	4.12	0.99363	63.38	RIGHT	0.14603E+01	66.58	0.14659E+01	-23.13
0.00	85.00	-1.92	-1.97	1.06	0.99495	85.67	LEFT	0.10265E+01	75.71	0.10317E+01	165.67
5.00	85.00	-1.93	-2.01	1.04	0.99139	-64.35	LEFT	0.10232E+01	74.97	0.10287E+01	165.36
10.00	85.00	-1.93	-2.19	0.95	0.97000	-50.82	LEFT	0.10130E+01	72.73	0.10192E+01	164.44
15.00	85.00	-1.91	-2.50	0.82	0.93474	-47.85	LEFT	0.99663E+00	69.08	0.10033E+01	162.92
20.00	85.00	-1.91	-2.92	0.62	0.88962	-46.60	LEFT	0.97506E+00	64.14	0.98143E+00	160.81
25.00	85.00	-1.93	-3.46	0.38	0.83805	-45.88	LEFT	0.94883E+00	58.08	0.95395E+00	158.14
30.00	85.00	-1.99	-4.11	0.09	0.78275	-45.44	LEFT	0.91801E+00	51.03	0.92140E+00	154.93
35.00	85.00	-2.10	-4.89	-0.26	0.72523	-45.21	LEFT	0.88227E+00	43.09	0.88432E+00	151.19
40.00	85.00	-2.27	-5.80	-0.67	0.66549	-45.16	LEFT	0.84148E+00	34.24	0.84325E+00	146.96
45.00	85.00	-2.49	-6.90	-1.15	0.60208	-45.16	LEFT	0.79667E+00	24.33	0.79878E+00	142.22
50.00	85.00	-2.75	-8.22	-1.67	0.53261	-45.03	LEFT	0.75107E+00	13.06	0.75158E+00	136.98
55.00	85.00	-3.02	-9.85	-2.20	0.45510	-44.46	LEFT	0.71113E+00	0.13	0.70241E+00	131.18
60.00	85.00	-3.22	-11.86	-2.67	0.37016	-43.06	LEFT	0.68665E+00	-14.56	0.65228E+00	124.75
65.00	85.00	-3.30	-14.25	-2.96	0.28357	-40.50	LEFT	0.68883E+00	-30.49	0.60255E+00	117.53
70.00	85.00	-3.16	-16.84	-2.98	0.20696	-36.72	LEFT	0.72554E+00	-46.37	0.55507E+00	109.35
75.00	85.00	-2.77	-19.06	-2.66	0.15328	-32.11	LEFT	0.79686E+00	-60.80	0.51241E+00	99.98
80.00	85.00	-2.14	-19.96	-2.07	0.12852	-27.45	LEFT	0.89510E+00	-73.04	0.47791E+00	89.25
85.00	85.00	-1.39	-19.19	-1.31	0.12879	-23.45	LEFT	0.10085E+01	-83.09	0.45560E+00	77.18
90.00	85.00	-0.63	-17.35	-0.53	0.14573	-20.45	LEFT	0.11242E+01	-91.35	0.44950E+00	64.19
95.00	85.00	0.05	-15.22	0.18	0.17243	-18.51	LEFT	0.12298E+01	-98.32	0.46238E+00	51.13
100.00	85.00	0.57	-13.19	0.75	0.20515	-17.57	LEFT	0.13137E+01	-104.42	0.49468E+00	38.93
105.00	85.00	0.90	-11.40	1.15	0.24250	-17.64	LEFT	0.13656E+01	-110.01	0.54453E+00	28.26
110.00	85.00	1.02	-9.91	1.36	0.28411	-18.85	LEFT	0.13769E+01	-115.38	0.60870E+00	19.31

115.00	85.00	0.91	-8.75	1.36	0.32886	-21.55	LEFT	0.13413E+01	-120.84	0.68362E+00	11.98
120.00	85.00	0.60	-8.00	1.16	0.37151	-26.40	LEFT	0.12561E+01	-126.74	0.76590E+00	6.00
125.00	85.00	0.16	-7.89	0.79	0.39572	-34.18	LEFT	0.11232E+01	-133.61	0.85243E+00	1.11
130.00	85.00	-0.23	-8.90	0.33	0.36846	-44.61	LEFT	0.95028E+00	-142.45	0.94038E+00	-2.90
135.00	85.00	-0.37	-12.00	-0.08	0.26213	-54.99	LEFT	0.75555E+00	-155.31	0.10272E+01	-6.23
140.00	85.00	-0.28	-21.24	-0.24	0.08955	-62.82	LEFT	0.57827E+00	-176.47	0.11105E+01	-8.99
145.00	85.00	-0.05	-18.90	0.01	0.11409	-68.00	RIGHT	0.49830E+00	150.30	0.11883E+01	-11.29
150.00	85.00	0.22	-9.66	0.64	0.32070	-71.40	RIGHT	0.58185E+00	117.04	0.12587E+01	-13.18
155.00	85.00	0.48	-5.32	1.49	0.51314	-73.71	RIGHT	0.77113E+00	96.40	0.13204E+01	-14.73
160.00	85.00	0.70	-2.63	2.36	0.68095	-75.42	RIGHT	0.98494E+00	84.90	0.13722E+01	-15.97
165.00	85.00	0.88	-0.87	3.11	0.81722	-76.92	RIGHT	0.11796E+01	78.21	0.14132E+01	-16.91
170.00	85.00	1.01	0.26	3.67	0.91717	-78.98	RIGHT	0.13318E+01	74.28	0.14428E+01	-17.58
175.00	85.00	1.10	0.90	4.01	0.97714	-85.75	RIGHT	0.14276E+01	72.20	0.14607E+01	-17.99
180.00	85.00	1.14	1.08	4.12	0.99363	68.38	RIGHT	0.14597E+01	71.60	0.14665E+01	-18.15
0.00	90.00	-1.92	-1.97	1.06	0.99495	80.67	LEFT	0.10266E+01	80.73	0.10316E+01	170.64
5.00	90.00	-1.94	-2.00	1.04	0.99284	-62.29	LEFT	0.10239E+01	80.00	0.10281E+01	170.34
10.00	90.00	-1.93	-2.18	0.95	0.97114	-46.48	LEFT	0.10154E+01	77.75	0.10169E+01	169.42
15.00	90.00	-1.91	-2.50	0.82	0.93499	-43.53	LEFT	0.10017E+01	74.08	0.99822E+00	167.92
20.00	90.00	-1.90	-2.93	0.62	0.88834	-42.21	LEFT	0.98357E+00	69.11	0.97239E+00	165.84
25.00	90.00	-1.92	-3.49	0.38	0.83448	-41.35	LEFT	0.96150E+00	62.99	0.93984E+00	163.22
30.00	90.00	-1.97	-4.17	0.08	0.77603	-40.68	LEFT	0.93537E+00	55.86	0.90112E+00	160.07
35.00	90.00	-2.08	-4.99	-0.28	0.71460	-40.16	LEFT	0.90476E+00	47.79	0.85678E+00	156.44
40.00	90.00	-2.24	-5.98	-0.71	0.65036	-39.76	LEFT	0.86946E+00	38.78	0.80747E+00	152.35
45.00	90.00	-2.47	-7.17	-1.20	0.58214	-39.37	LEFT	0.83038E+00	28.69	0.75390E+00	147.81
50.00	90.00	-2.74	-8.62	-1.74	0.50787	-38.85	LEFT	0.79066E+00	17.27	0.69685E+00	142.79
55.00	90.00	-3.01	-10.43	-2.29	0.42583	-37.91	LEFT	0.75655E+00	4.27	0.63730E+00	137.25
60.00	90.00	-3.24	-12.68	-2.77	0.33701	-36.17	LEFT	0.73750E+00	-10.35	0.57647E+00	131.06
65.00	90.00	-3.32	-15.43	-3.06	0.24796	-33.31	LEFT	0.74421E+00	-26.06	0.51595E+00	124.02
70.00	90.00	-3.16	-18.47	-3.03	0.17159	-29.29	LEFT	0.78417E+00	-41.72	0.45790E+00	115.78
75.00	90.00	-2.72	-21.04	-2.65	0.12136	-24.59	LEFT	0.85750E+00	-56.08	0.40537E+00	105.89
80.00	90.00	-2.04	-21.89	-2.00	0.10174	-20.07	LEFT	0.95681E+00	-68.45	0.36262E+00	93.86
85.00	90.00	-1.25	-20.70	-1.20	0.10648	-16.41	LEFT	0.10704E+01	-78.77	0.33512E+00	79.56
90.00	90.00	-0.47	-18.45	-0.40	0.12616	-13.87	LEFT	0.11852E+01	-87.39	0.32843E+00	63.76
95.00	90.00	0.21	-16.04	0.31	0.15408	-12.39	LEFT	0.12885E+01	-94.72	0.34550E+00	48.30
100.00	90.00	0.71	-13.84	0.86	0.18718	-11.87	LEFT	0.13686E+01	-101.16	0.38499E+00	34.91
105.00	90.00	1.01	-11.95	1.23	0.22473	-12.31	LEFT	0.14153E+01	-107.08	0.44276E+00	24.27
110.00	90.00	1.09	-10.38	1.39	0.26691	-13.81	LEFT	0.14204E+01	-112.75	0.51430E+00	16.14
115.00	90.00	0.93	-9.15	1.34	0.31320	-16.74	LEFT	0.13782E+01	-118.50	0.59589E+00	9.96
120.00	90.00	0.55	-8.34	1.08	0.35910	-21.79	LEFT	0.12871E+01	-124.69	0.68453E+00	5.20
125.00	90.00	0.04	-8.17	0.65	0.38842	-29.86	LEFT	0.11496E+01	-131.89	0.77763E+00	1.46
130.00	90.00	-0.40	-9.14	0.14	0.36562	-40.85	LEFT	0.97486E+00	-141.09	0.87274E+00	-1.56
135.00	90.00	-0.58	-12.33	-0.30	0.25852	-51.92	LEFT	0.78236E+00	-154.32	0.96746E+00	-4.03
140.00	90.00	-0.47	-22.28	-0.44	0.08116	-60.20	LEFT	0.61221E+00	-175.36	0.10594E+01	-6.08
145.00	90.00	-0.21	-18.15	-0.14	0.12673	-65.62	RIGHT	0.53863E+00	153.29	0.11463E+01	-7.81
150.00	90.00	0.09	-9.41	0.56	0.33490	-69.14	RIGHT	0.61698E+00	122.17	0.12260E+01	-9.25
155.00	90.00	0.39	-5.19	1.45	0.52618	-71.53	RIGHT	0.79586E+00	101.99	0.12966E+01	-10.45
160.00	90.00	0.65	-2.57	2.34	0.69093	-73.30	RIGHT	0.10005E+01	90.3[illegible]	0.13565E+01	-11.41
165.00	90.00	0.85	-0.84	3.10	0.82337	-74.86	RIGHT	0.11881E+01	83.47	0.14044E+01	-12.16
170.00	90.00	1.00	0.28	3.66	0.91975	-76.95	RIGHT	0.13351E+01	79.40	0.14392E+01	-12.71
175.00	90.00	1.10	0.90	4.01	0.97733	-83.50	RIGHT	0.14279E+01	77.25	0.14602E+01	-13.04
180.00	90.00	1.14	1.08	4.12	0.99363	73.38	RIGHT	0.14592E+01	76.63	0.14670E+01	-13.17

AVERAGE POWER GAIN= 0.96142E+00 SOLID ANGLE USED IN AVERAGING=(1.0000)*PI [illegible]ERADIANS.

***** DATA CARD NO. 7 EN 0 0 0 0 0.00000E+00 0.00000E+00 0.00000E+00 0.00000E+00 0.00000E+00 0.00000E+00
RUN TIME = 7682.590

APPENDIX D - PANSAT CONSTRUCTION

A. ANTENNA SYSTEM DESIGN SUMMARY

The PANSAT antenna system consists of four identical antenna elements mounted as shown in Figure D-1. Each element is a 16.8 cm (6.6") length of 1/2" Stanley tape. The orientation of the flat surface of the Stanley tape is not critical and may be considered arbitrary. Mounting hardware

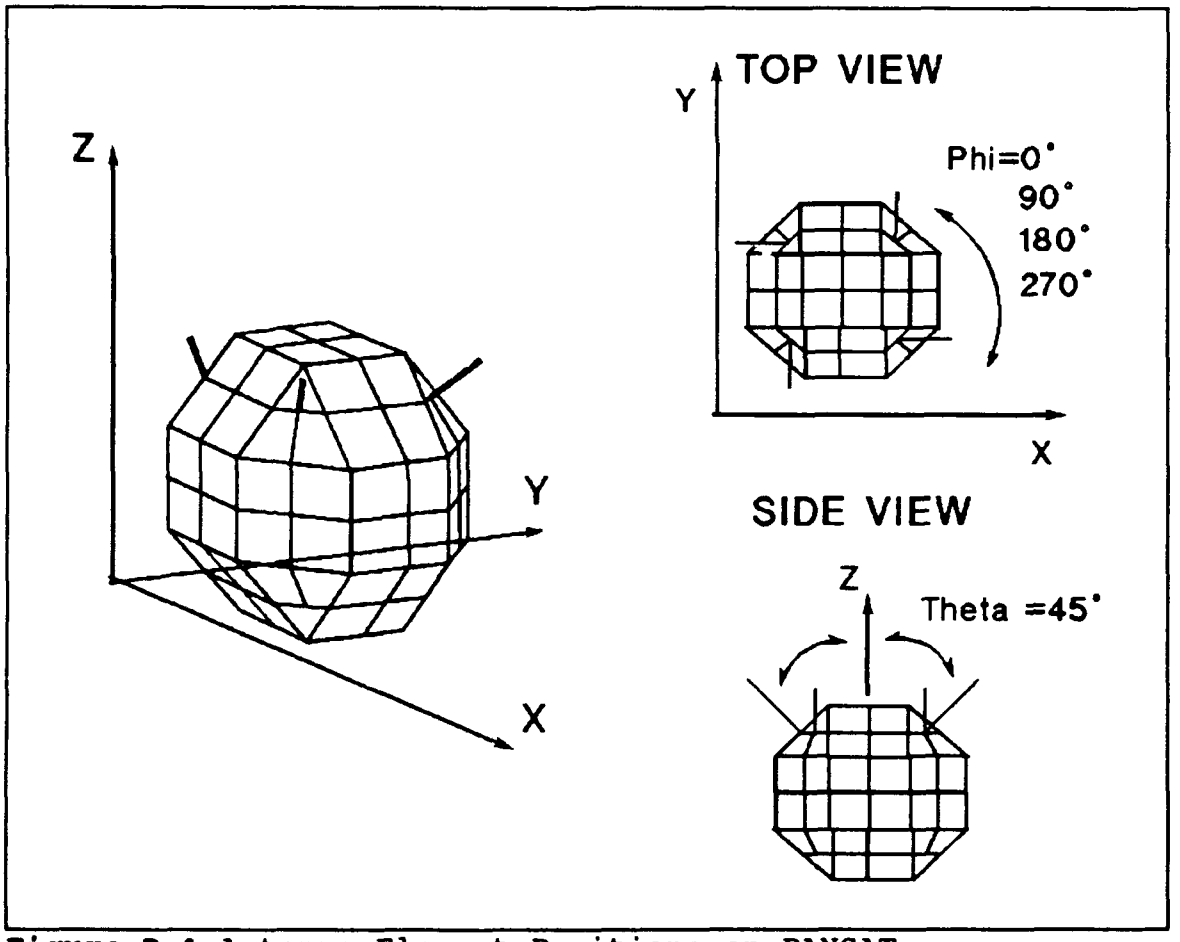

Figure D-1 Antenna Element Positions on PANSAT

should be chosen that allows the antenna elements to be fed through the satellite skin from the center conductor of a coaxial cable inside the satellite. The coaxial cable shielding should be well grounded to the satellite skin in a radially symmetric fashion.

B. ANTENNA FEED SYSTEM DESIGN SUMMARY

Figure D-2 is a schematic representation of the antenna feed system. When the antenna elements are mounted, the feeds must be in 90° phase progression as seen from above. It does not matter whether the phase progression proceeds in a clockwise or counter-clockwise direction. Note the use of 75Ω impedance coaxial cable vice the more common 50Ω cable.

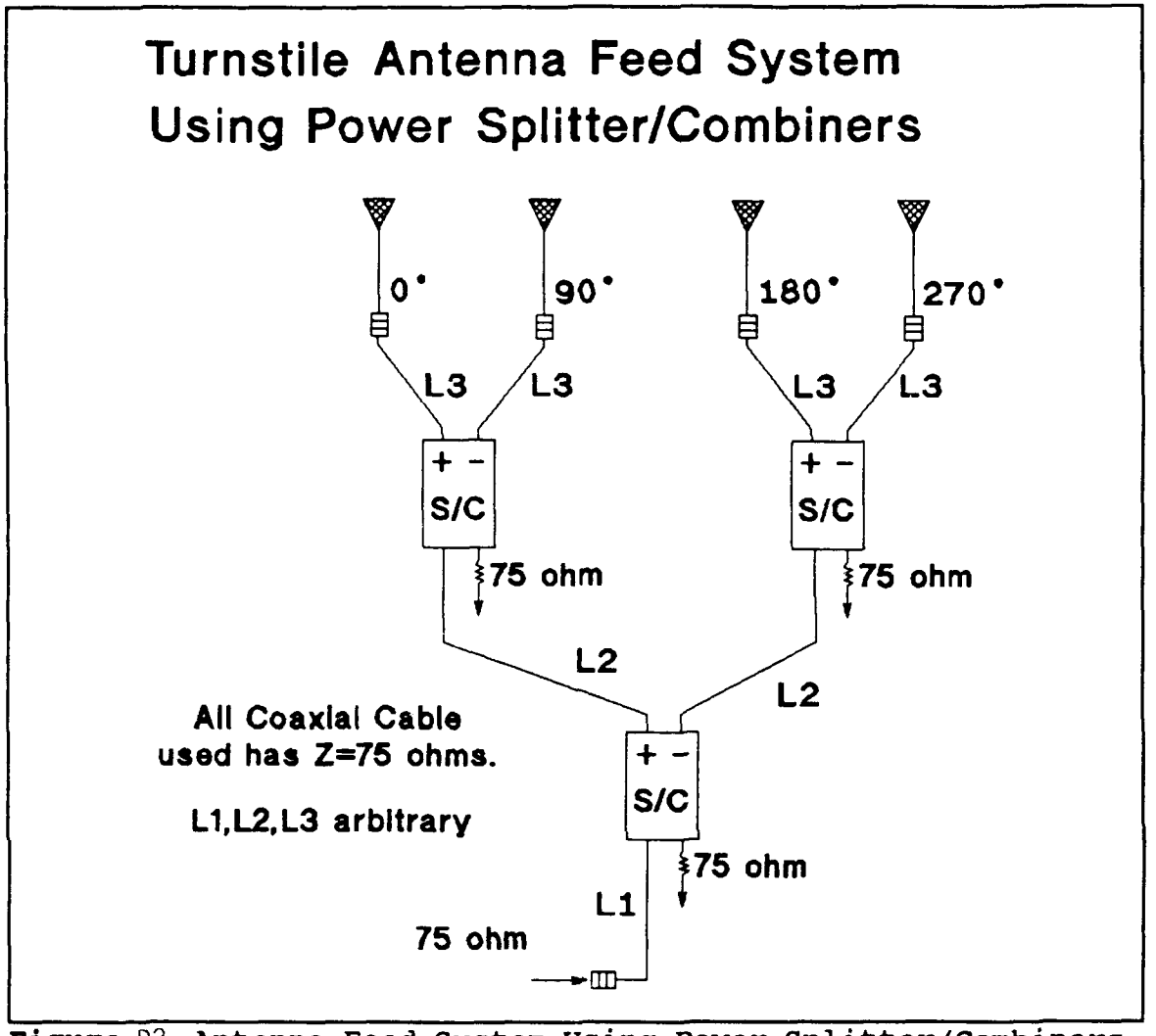

Figure D2 Antenna Feed System Using Power Splitter/Combiners.

LIST OF REFERENCES

Adler, R. W., Notes for EC3650 (Computational Electromagnetic Modeling Techniques), Naval Postgraduate School, Monterey, California, Spring 1990.

Batson, D.D., and others, "VHF Unfurlable Turnstile Antennas," paper prepared for the Nineteenth Annual Symposium USAF Antenna Research and Development Program, Monticello, Illinois, 14-16 October 1969.

Burke, G. J. and Poggio, A. J., Naval Ocean Systems Center Technical Document 116, Numerical Electromagnetics Code (NEC) - Method of Moments, San Diego, California, January 1981.

Burton, Robert W. and King, Ronald W. P., "Theoretical Considerations and Experimental Results for the Hula-Hoop Antenna," The Microwave Journal, pp. 89-90, November,1963.

Gregorwich, W. S., "A Novel VHF Turnstile Antenna for the SMS Satellite," paper presented at the IEEE National Telecommunications Conference, 1972.

Howard, Andrew J., LCDR, USN, Numerical Analysis of the Complex Airborne Pod Mounted Band 2/3 Antenna System Using the Numerical Electromagnetics Code - Method of Moments Version III (NEC-3) on a Personal Computer, Master's Thesis, Naval Postgraduate School, Monterey, California, December, 1990.

Jackson, R. B., "The Canted Turnstile as an Omnidirectional Spacecraft Antenna System," Report N67-37172, NASA Goddard Space Flight Center, September 1967.

Jakstys, Jack, "Omni-Directional Antennas for Small Satellites," informal paper provided to the author directly from Mr. Jakstys of Space Systems/LORAL, 4 March 1991.

Jordan, Edward C., Reference Data for Engineers: Radio, Electronics, Computer, and Communications Seventh Edition, Howard W. Sams & Company, 1985.

Kilgus, C. C., "Multielement, Fractional Turn Helices," IEEE Transactions on Antennas and Propagation, v. AP-16, pp. 499-500, July 1968.

Milligan, Thomas A., Modern Antenna Design, McGraw-Hill Book Company, 1985.

Naval Postgraduate School, Space Systems Academic Group, Final Design Report, Naval Postgraduate School Petite Amateur Navy Satellite (PANSAT), Summer 1989.

Naval Research Laboratory, Report NRL-6907, Satellite Turnstile Antennas, by S. Nichols, 6 August 1969.

Paluszek, Stephen E., LTCMDR, USN, Spread Spectrum Communications for the Petite Amateur Navy Satellite (PANSAT), Master's Thesis, Naval Postgraduate School, Monterey, California, June 1990.

Philco-Ford Corporation, Space and Re-Entry Systems Division, TP-DA0652, vol. TECH I-E.

Sakoda, Daniel, "Naval Postgraduate School Petite Navy Satellite (PANSAT)," paper presented at the 3rd Annual AIAA/Utah State University Conference on Small Satellites, 26-28 September 1989.

Schleher, D. Curtis, Introduction to Electronic Warfare, Artech House Inc.,1986.

Wright, James J., LT, USN, The Porting of a Mainframe Dependent Antenna Modeling Program (NEC-3) to a 32-Bit Personal Computer, Master's Thesis, Naval Postgraduate School, Monterey, California, June 1990.